THE
PHYSICAL REVIEW
A Journal of Experimental and Theoretical Physics Established by E. L. Nichols in 1893
VOL. 50, NO. 5 SEPTEMBER 1, 1936 SECOND SERIES

A Search for Protons in the Primary Cosmic-Ray Beam[1]

C. G. MONTGOMERY, D. D. MONTGOMERY, W. E. RAMSEY AND W. F. G. SWANN, *Bartol Research Foundation of the Franklin Institute, Swarthmore, Pa.*

(Received July 1, 1936)

It has been suggested that a large proportion of the cosmic rays found at sea level are protons. Now a charged particle is characterized by the fact that its ionization increases enormously towards the end of its range, so that, in the case of protons and alpha-particles large and measurable spurts of ionization should be produced in relatively short distances by those rays which are ending their journeys. If r is the distance from the end of the range to the point where the ionization per centimeter of path is σ, then, the fraction of the rays which, passing through a length l of a vessel containing gas at pressure p, produce therein spurts of ions greater in number than $lp\sigma$, is $(1-e^{-\mu r})$, or approximately, μr, where μ is the absorption coefficient of the radiation concerned. The assignment of a lower limit to the spurts which can be measured determines σ, and so r, through the aid of Bethe's theory; and, it becomes possible to calculate how many such spurts should be observed if the rays are protons. In an experiment based upon the foregoing principles spurts above an assigned size (7.2×10^4 ion pairs in one experiment, and 3.9×10^4 ion pairs in another experiment) produced in a small ionization chamber were measured. To eliminate alpha-particles the chamber was divided into two halves by horizontal partition, and only spurts occurring simultaneously in both halves were counted. Spurts produced by "showers" were recognized and eliminated by suitably arranged Geiger counters. A conservative interpretation of the results gives an upper limit for the number of protons present as five percent of the total number of cosmic rays at sea level, or 12 percent of the intensity of the hard component if Compton's estimate of the absorption coefficient and intensity of the hard component be used. If Millikan's values are adopted our estimate of the upper limit is six percent.

IT has been suggested[2] that a large proportion of the cosmic-ray ionization observed at sea level and below is produced by protons of high energy which have penetrated the earth's atmosphere. This conclusion has been reached as a result of studies of the variation of the intensity of the cosmic radiation over the earth's surface. To reach the earth's surface at a given point, the particles must have both sufficient energy not to be deflected away by the earth's magnetic field and sufficient penetrating power to traverse the earth's atmosphere. It is observed at sea level, that the cosmic radiation in the northern hemisphere increases in intensity with increasing geomagnetic latitude up to a latitude of about 50°. From there northward, it remains quite constant. A natural interpretation of these observations is that at 50° the particles with just enough energy to penetrate the earth's magnetic field have a range of just one atmosphere, and at higher latitudes, the particles of lower energy which are not excluded by the field can no longer reach the earth's surface because they are stopped within the atmosphere. Thus, we know the energy and the range of a particle which just reaches sea level at a latitude of 50° and we may apply the theo-

[1] Presented at the Washington meeting of the American Physical Society, May, 1936.

[2] A. H. Compton and H. Bethe, Nature **134**, 734 (1934); A. H. Compton, Rev. Sci. Inst. **7**, 71 (1936); A. H. Compton, Proc. Phys. Soc. **47**, 747 (1935); J. Clay, Physica **3**, 332 (1936).

retical formulae of Bethe[3] and learn with what kind of particle we are dealing. The assumption that these particles are protons gives the closest agreement with observations. Such considerations, taken together with the observations on the east-west effect,[4] which show that at least some of the primary cosmic rays are positively charged, constitute a strong body of evidence in favor of protons as a constituent of cosmic radiation.

A proton of sufficiently high energy to function as a primary cosmic ray would in all regions where it possessed that energy function as regards ionization in a manner indistinguishable from an electron. Only near the end of its range would its ionization characteristics serve to differentiate it from a particle of equal charge but smaller mass. It has been pointed out by one of us,[5] however, that if protons function as cosmic rays the number of them which while passing through an ionization chamber of relatively small size were sufficiently near the end of their range to produce measurable spurts of ionization would be appreciable for experiments of reasonable duration. A measurement of this number provides information on the extent to which protons figure in the total observed cosmic radiation.

Suppose we consider spurts of ionization in the chamber which are greater than S ions per spurt. A spurt S may be considered as produced by a particle traveling a distance l in the ionization chamber with specific ionization σ, where l and σ are such that S equals $l\sigma$. By employing Bethe's formula[3] for the energy loss of protons, we can determine the range, r, that such protons will have after they pass through the chamber. Then, if n be the number of protons which traverse the chamber with path lengths l or greater, the number which will produce spurts of ionization greater than S is $n\mu r$, where μ is the coefficient of absorption of the proton beam.

For μ and n, various estimates have been made. For example, Compton,[2] invoking Eckart's[6] analysis of the variation of the cosmic-ray ionization with elevation quotes, for μ, 0.08 per meter of water, and an intensity of the proton beam equal to 40 percent of the total cosmic-ray intensity. Millikan and his collaborators[7] give for the hard component of the radiation a value, among others, of $\mu = 0.078$ per meter of water and an 81 percent intensity. Other estimates[8] do not differ greatly from these.

Experimental Procedure. Experiments to detect the spurts of ionization caused by protons were carried out in a thin-walled, cylindrical brass chamber 15.4 cm high and 6.7 cm in diameter, filled with nitrogen to a pressure of 14.7 atm. In order to eliminate the effects of alpha-particles, the chamber was divided in half by a thin copper diaphragm, placed horizontally, and only those spurts of ionization were measured which occurred simultaneously in both halves of the chamber. Each half of the chamber was furnished with an electrode to collect the ions and two FP–54 vacuum tube electrometers with photographic recording were employed. To minimize the statistical fluctuations in the ionization a potential of 450 volts was applied to the chamber. The presence of showers of electrons which passed through both halves of the chamber was recognized and the effect eliminated by the use of a system of Geiger-Müller counters whose discharges were recorded on the same photographic paper as the electrometer records. The arrangement of the counters and the chamber is represented diagrammatically to scale in Fig. 1. A group, B, of four counters, 10 cm long, were connected in parallel and placed as close as possible to the ionization chamber A. These counters acted as a master counter for the groups C and D. Groups C and D each consisted of seven counters, 20 cm long, and were arranged to record independently when any two or more counters in a group were discharged. Thus, a mark was made upon the photographic paper when at least one counter of group B and at least two counters of group C were simultaneously discharged, and similarly for group D. To increase the probability that a shower of rays be recorded, under each of the groups C and D were placed 0.6 cm of Pb which could scatter the shower radiation backward. It is intended to describe in detail the electrical circuits used for these purposes in a separate publication by one of us (W. E. R.).

[3] H. Bethe, Zeits. f. Physik **76**, 293 (1932).
[4] T. H. Johnson, Phys. Rev. **48**, 287 (1935).
[5] W. F. G. Swann, Phys. Rev. **49**, 478 (1936).
[6] C. Eckart, Phys. Rev. **45**, 851 (1934).
[7] I. S. Bowen, R. A. Millikan and V. Neher, Phys. Rev. **44**, 246 (1933).
[8] Cf., e.g., T. H. Johnson, Rev. Sci. Inst. **4**, 639 (1933).

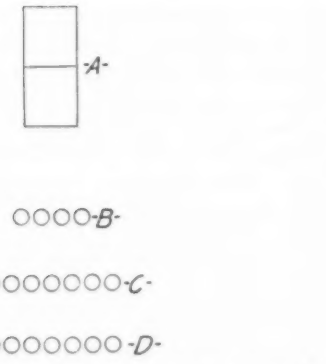

FIG. 1. Arrangement of ionization chamber and counters.

The observations were divided into two series. In the first, extending over a period of 175 hours, only those spurts of ionization of more than 7.2×10^4 ion pairs in each half of the chamber were counted. This limit corresponds to a specific ionization of the proton of 678 ion pairs per cm at atmospheric pressure after applying a small correction of the order of ten percent for lack of saturation.[9] The residual range of such a proton is 1010 cm, or 1010 cm − 309 cm = 701 cm after it has passed through the chamber, and the proton would have an energy of 4.5×10^7 electron volts. The total number of cosmic rays which traverse the chamber and have path lengths in each half greater than half the length of the chamber is 300 per hour.[10] Hence we would expect to find during the 175 hours of observation 15 spurts of ionization, if Compton's estimate of μ and of the fraction of the rays which are protons is taken, or 30 spurts on Millikan's estimate. Actually we observed only twelve spurts of ionization of these sizes, of which ten were accompanied by discharges of the counters, leaving only two possible protons. This is considerably smaller than the expected number and we must conclude that such protons are not present to an appreciable extent. We also note that the counter arrangement used here is quite efficient for the detection of showers of rays which produce these amounts of ionization. However, it is reasonable to suppose that even the two spurts unaccompanied by counts were showers which the counters did not record.

[9] E. F. Cox, Phys. Rev. **45**, 503 (1934).
[10] J. C. Street and E. H. Woodward, Phys. Rev. **46**, 1029 (1934).

While the foregoing results present, in the opinion of the writers, conclusive evidence, it was felt of interest to make an independent estimate of the possible number of protons based upon spurts of smaller size. The chief interest of such an estimate arises from the possibility of a proton disappearing by some nuclear collision act before its energy had become reduced to a value corresponding to production of spurts of ionization of the size assigned. Such a failure of the protons to die a natural death will of course invalidate the arguments above presented. The smaller the sizes of the spurts upon which the arguments are based, the more into the high energy region do we drive any proposed assumption as to disappearance of protons by nuclear encounters. Unfortunately when dealing with spurts of small size certain complicated considerations become involved which prevent the conclusion reached from depending upon considerations as clear-cut and definite, as those applicable to the experiments already cited. However, even for these spurts of smaller size the final evidence seems conclusive.

In the second series of experiments measurements were made of the number of spurts greater than 3.9×10^4 ion pairs occurring in 92.4 hours. This limit corresponds to 360 ions/cm at atmospheric pressure and would be produced by a proton of range 5100 cm and energy 1.0×10^8 electron volts. The expected number of spurts greater than this limit would be 55, using Compton's values, and 108, using those of Millikan. The number of spurts of this size observed was 62, of which 25 were accompanied by discharges of the counters. However, we must examine this result in more detail before we may draw a proper conclusion. First, the smaller spurts of ionization which we are now considering occur with a sufficient frequency that we begin to measure purely accidental coincidences between the two halves of the vessel. Of the 62 spurts counted, we estimate that 14 of them are accidental and should be disregarded. Secondly, the probability that a shower will be recorded by the counters will be lower than in the first series of observations, since the numbers of rays involved are smaller, and we should apply a correction to the number of bursts which are accompanied by counts.

In Fig. 2 are shown the frequency distributions

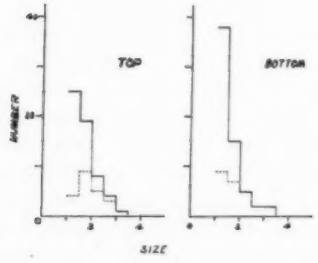

FIG. 2. Distribution in size of spurts of ionization occurring simultaneously in both halves of the chamber. Full line, all spurts; dashed lines, those spurts which were accompanied by counts.

of the bursts of ionization in each half of the chamber, together with those of the bursts which were accompanied by counter discharges. The similarity of these distribution curves to those obtained in a large double ionization chamber[11] is striking, and suggests that here we are dealing with the same phenomenon, and therefore that the spurts observed in the small ionization chamber are really caused by sprays of the electron type and not by protons. Particularly noteworthy is the fact that on the average the ionization produced in the top half of the chamber is larger than in the lower half, a circumstance which is easily explained as caused by the spreading out of a bundle of rays. A proton passing through the vessel would be expected to give a slightly larger ionization in the bottom half.

We may attempt to estimate the probability that the counters will record a shower, in the following way. Let the probability that group B be discharged be P_B, and let us assume P_C and P_D similarly for groups C and D. Then the probability that groups B and C are discharged and group D is not is $P_BP_C(1-P_D)$. Similarly for groups B and D and not C we have $P_BP_D\,(1-P_C)$, and finally, for all three, $P_BP_CP_D$. The ratio of the number of bursts of a given size recorded as accompanied by group C to the number of bursts accompanied by both groups C and D is then $(1-P_D)/P_D$. Thus we can calculate from the data P_C and P_D. The probability π, that a burst will be accompanied by some counter discharge will then be

$$\pi=P_B(P_C+P_D-P_CP_D). \qquad (1)$$

[11] C. G. and D. D. Montgomery, Phys. Rev. **49**, 705 (1936).

Table I shows the results of such a computation. Although the data are rather meager, it is evident that P_C and P_D are not low even for the smaller sizes of spurt.

To find the probability π, it is necessary to obtain also P_B. We may distinguish two extreme cases. First, it may be supposed that the spreading of the shower is negligible, so that it is sufficient, for the calculation of P_B, to assume that all the rays of the shower travel along the same line. Secondly, it may be supposed that the spread of the shower is large enough so that the shower always covers the entire area of the lower half of the chamber. We may expect the correct value of P_B to lie between the extreme values calculated from these two assumptions. Now, the solid angle subtended by the counter group B at a point within the top of the ionization chamber is about one-fourth of the solid angle subtended by the bottom of the ionization chamber. Therefore, for the first case cited above, P_B would be $\frac{1}{4}$. For the second case, P_B would be given by the expression:

$$P_B=1-(1-\tfrac{1}{4})^n, \qquad (2)$$

where n is the number of rays in the shower.[12] For the first group of sizes of spurts in Table I—that is, those spurts with sizes in the lower half of the chamber, between 3.9×10^4 and 5.8×10^4 ion pairs—the mean value of n is about 7, and P_B would be 0.86, from Eq. (2). Thus, we can set the limits of P_B, for the group of smallest spurts, corresponding to our two extreme assumptions as

$$0.25<P_B<0.86.$$

By Eq. (1), using the values of P_C and P_D found in Table I, we then estimate that

$$0.21<\pi<0.76.$$

We should expect the correct value of π to be closer to the lower limit than the upper, since the cloud chamber observations of Stevenson and Street[13] on the angular spread of showers of the order of seven rays show that more than 70 percent of the shower electrons lie within a cone of vertical angle 10°. A value of π equal to 9/27 would mean that all of the spurts observed, in the group of smallest sizes, were showers of electrons.

[12] C. G. and D. D. Montgomery, Phys. Rev. **48**, 786 (1935).

[13] E. C. Stevenson and J. C. Street, Phys. Rev. **49**, 425 (1936).

Such a value of π is in every way reasonable. For the groups of larger sizes, π would be larger as is observed. Thus there is no evidence for the occurrence of any spurts of ionization other than those produced by "showers."

Hence in conclusion, as already stated, the experiments with larger spurts would require, in the 175 hours of observation, 15 spurts of a size greater than or equal to that assigned if Compton's estimate of μ and of the fraction of the rays which are protons is taken, or 30 spurts on Millikan's estimate. Only two spurts possibly explicable by protons were observed in these experiments. While the experiments with spurts of smaller size are not as conclusive, they are in every way consistent with the conclusions reached from the spurts of larger size. It is concluded that the observations here described place upon the number of protons which can be present in the cosmic radiation at sea level a much lower limit than that which has been assigned for them. We may set a conservative upper limit to the number present as 5 percent of the total number of cosmic rays at sea level, or 12 percent of the intensity of the hard component if Compton's estimate of the absorption coefficient and intensity of the hard component be used. If Millikan's values are adopted our estimate of the upper limit is 6 percent. These experiments do not, however, exclude protons as being the initiators of what is observed as the hard component of the cosmic radiation provided that the actual number of protons present is considerably less than the number of rays measured by counters as representative of the hard component. To utilize this loop hole of escape it would be necessary to assume that the protons act chiefly through the agency of secondaries produced along their paths in a manner such as has been proposed by one of us as representative of the mechanism of the corpuscular theory of cosmic rays.[14]

TABLE I. *Distribution in size, in the lower half, of spurts occurring in both halves of the chamber.*

Size in units of 3.9×10^4 ion pairs	No. of spurts, observed	No. of accidentals, estimated	No. of spurts accompanied by counts			P_C	P_D
			Groups B and C only	Groups B and D only	Groups B, C and D		
1–1.5	38	11	2	4	3	3/7	3/4
1.5–2.0	15	3	1	1	5	5/6	5/6
2.0–2.5	5	0	0	1	4	4/5	1
2.5–3.0	2	0	0	0	2	1	1
3.0–3.5	2	0	0	0	2	1	1
Total	62	14	3	6	16		

[14] W. F. G. Swann, Phys. Rev. **48**, 641 (1935).

Anisotropy in the Atomic Vibrations of Zinc Crystals

I. Evidence from X-Ray Scattering

G. E. M. JAUNCEY* AND W. A. BRUCE, *Wayman Crow Hall of Physics, Washington University, St. Louis*

(Received June 25, 1936)

The results of Brindley's recent experiments on the intensity of the various reflections of Cu $K\alpha$ x-rays from powdered zinc crystals are compared with the results of the measurements made by the authors on the diffuse scattering of x-rays from single zinc crystals. When the method of diffuse scattering is used it is possible to obtain S values for various orientations of the crystal for a given value of $(\sin \frac{1}{2}\phi)/\lambda$. The form of Zener's formula for M for hexagonal crystals is confirmed by our experimental results. We find the root-mean-square thermal displacements of the atoms to be 0.172 and 0.093A, respectively, along and perpendicular to the c axis. These are greater than Brindley's values. They nearly explain the large difference between the F values for the (0002) and (10$\bar{1}$0) reflections. These two reflections possibly give some evidence of asymmetry in the electron structure of the zinc atoms, the structure being more diffuse in the direction of the c axis than normal to this direction.

1. Powdered Crystal Method

IN November 1935 Brindley and Spiers[1] reported some very interesting results for the scattering of Cu $K\alpha$ x-rays ($\lambda = 1.54$A) from powdered zinc. Since the Cu $K\alpha$ line is on the long wave-length side of the zinc K absorption edge ($\lambda = 1.28$A), the zinc K fluorescence radiation is not excited. However, the wave-length 1.54A is sufficiently close to 1.28A to necessitate correction for dispersion. From their experimental results, Brindley and Spiers first calculated the F values[2] and from these they in turn calculated the f values[2] from the relation

$$f = Fe^{M}, \qquad (1)$$

where e^{M} is the Debye-Waller temperature factor. Assuming a single characteristic temperature and using Waller's formula[3] for M, they obtained f values respectively for the (20$\bar{2}$1) and the (10$\bar{1}$5)+(11$\bar{2}$4) reflections[4] which do not fall upon a smooth curve. The importance of this fact was recognized by Brindley and Spiers. Brindley[5] has since obtained other reflections showing a similar peculiarity. Brindley and Spiers' experimental F values are shown as black circles in Fig. 1 and Brindley's later experimental F values are shown as crosses in the same figure.

2. Theory

In January 1936 Zener[6] published the results of a theoretical investigation of the thermal vibrations of the atoms of an anisotropic crystal. Zener found that for hexagonal crystals the Debye-Waller M should be of the form

$$M = (a \cos^2 \psi + b \sin^2 \psi) \cdot (\sin^2 \theta/\lambda^2), \qquad (2)$$

where ψ is the angle between the c axis of a crystal and the normal to a reflecting plane of atoms in the crystal. The values for a and b were calculated for room temperature from the known elastic constants, the simple Debye model of a solid being used. These values are shown in the first row of Table I. Independently Brindley[7] has pointed out that according to Grüneisen and Goens two "characteristic temperatures" must be recognized for zinc—one for vibrations along the c axis and the other for vibrations normal to this axis. These different characteristic temperatures are accompanied by different M's in the two directions. Brindley[5] returns to this matter in a later paper and, using Zener's formula (2), gives the values for a and b shown in the second row of Table I.

The angle ψ is related to the Miller indices $(h, k, -h-k, l)$ by[5]

* The senior author was aided in part by a grant from the Rockefeller Foundation to Washington University for research in science.

[1] G. W. Brindley and F. W. Spiers, Phil. Mag. **20**, 865 (1935).

[2] Throughout this and subsequent articles we shall use F to indicate the atomic structure factor as modified by the thermal vibrations of the atom, and f to indicate the atomic structure factor for an atom at rest.

[3] I. Waller, Zeits. f. Physik **51**, 213 (1923). See also C. Zener and G. E. M. Jauncey, Phys. Rev. **49**, 17 (1936).

[4] Zinc is a hexagonal crystal and four Miller indices are used, the third index being the negative sum of the first two. The fourth index refers to the long or c axis.

[5] G. W. Brindley, Phil. Mag. **21**, 760 (1936).

[6] C. Zener, Phys. Rev. **49**, 122 (1936).

[7] G. W. Brindley, Nature **137**, 315 (1936).

$$\cos\psi=(l/C)\{4(h^2+hk+l^2)/3+(l/C)^2\}^{-1}, \quad (3)$$

where C is the axial ratio 1.856. From (1), (2) and (3), the f values for zinc can be calculated from Brindley's experimental F values. Brindley's F values for the $(20\bar{2}3)$, $(10\bar{1}5)+(11\bar{2}4)$, $(21\bar{3}1)$, and the $(0006)+(21\bar{3}2)$ reflections are most interesting since they give a zig-zag in Fig. 1. Unless $a>b$ in (2) the corresponding f values show a similar zig-zag. Brindley finds that the values of a and b shown in the second row of Fig. 1 smooth out the zig-zag better than do Zener's values shown in the first row. Now $(a-b)$ may be taken as a measure of the anisotropy of the atomic vibrations. Brindley's experimental results and also his theory based upon Grüneisen and Goens' idea of two "characteristic temperatures" thus indicate a much greater anisotropy $(a-b=0.785)$ than does Zener's original theory $(a-b=0.33)$. Accordingly, Zener[8] has looked into the theory again and has used a modified Debye model of a solid in which the discrete structure of the solid is taken into account. Zener's new values of a and b are shown in the third row of Table I. Although Zener's value of b agrees fairly well with Brindley's value, Zener's anisotropy $(a-b=0.465)$ is still too small to agree with experiment.

Now, although Brindley's f values for the reflections mentioned in the previous paragraph fall fairly well on a smooth curve, his f values for other reflections do not fall so well on this curve.[9] But more important still are what Brindley calls the anomalous f values for the (0002) and $(10\bar{1}0)$ reflections. The points representing these values distinctly depart from a smooth curve. Brindley suggests that the high F value for the $(10\bar{1}0)$ reflection may be due to an impurity. However, Brindley[10] finds the same kind of anomalous F values for these same reflections from cadmium. Hence the present authors infer that the F values for the (0002) and the $(10\bar{1}0)$ reflections indicate a much greater anisotropy than does Brindley's value, $a-b=0.785$. Evidence in support of this inference is given in the next section.

TABLE I. *Anisotropy of atomic vibrations. Zinc at 298°K.*

	a	b
Simple Debye Model	$0.75A^2$	$0.42A^2$
Brindley	1.295	0.51
Modified Debye Model	1.06	0.595
Jauncey and Bruce	2.34	0.68

[8] C. Zener, letter appearing in this issue of Phys. Rev.
[9] The reader is referred to the original paper.
[10] G. W. Brindley, Proc. Leeds Phil. Soc. **3**, 200 (1936).

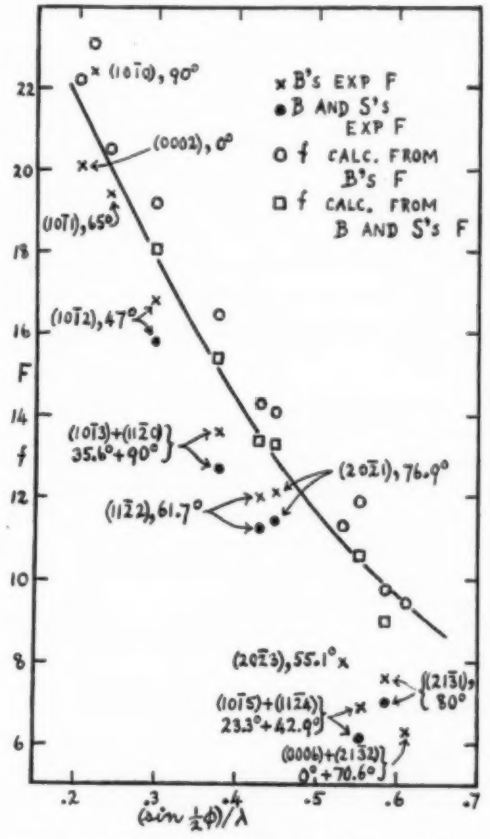

FIG. 1. Brindley's and Brindley and Spiers' experimental F values for zinc. Also these same values corrected for thermal vibration of the atoms, our values of a and b being used.

3. DIFFUSE SCATTERING FROM SINGLE CRYSTALS

The theory of diffuse scattering of x-rays[11] from a crystal gives

$$S=S_{\text{coh}}+S_{\text{inc}}/(1+\alpha \text{ vers } \phi)^2, \quad (4)$$

where

$$S_{\text{coh}}=(f^2-F^2)/Z \quad (5)$$

and where, the extra negative term being

[11] See G. E. M. Jauncey and J. H. Deming, Phys. Rev. **48**, 577 (1935) for previous references.

neglected since its values are unknown but small for zinc,

$$S_{\text{inc}}=1-(1/Z)\Sigma E_r^2. \quad (6)$$

Now imagine an atom removed from the crystal lattice without changing the structure of the electron atmosphere surrounding the nucleus. The scattering from such an atom is given by (4) but with (5) replaced by

$$S_{\text{coh}}=f^2/Z. \quad (7)$$

Let S_{cryst} refer to S for a crystal and S_{atom} to an atom removed from the crystal. Then, from (4), (5) and (7),

$$S_{\text{atom}}=S_{\text{cryst}}+F^2/Z. \quad (8)$$

This is an interesting variation of the relation between S_{gas} and S_{cryst} announced by Jauncey and Harvey[12] several years ago. The two terms on the right of (8) may be considered as experimental quantities. The method of measurement of S_{cryst} has been described in various papers by Jauncey[11] and the measurement of F^2/Z for zinc crystals has been described by Brindley. For anisotropic crystals, both S_{cryst} and F^2/Z are functions of $(\sin\frac{1}{2}\phi)/\lambda$, where ϕ is the angle of scattering, and of ψ. Hence experimental values of S_{atom} for zinc can be found if, in addition to the powdered crystal measurements made on zinc, measurements of the diffuse scattering from single zinc crystals are also made. The S_{atom} values obtained from (8) will be a function of $(\sin\frac{1}{2}\phi)/\lambda$ and possibly of ψ. If they are a function of ψ, asymmetry in the electron structure of the zinc atoms will be indicated. *Eq. (8) brings out very forcibly the value of measurements on the diffuse scattering in problems such as that under discussion.*

For (8) to be directly applicable it would be necessary to use monochromatic rays in the diffuse scattering experiments. Although experiments are now being made in this laboratory with Mo $K\alpha$ rays scattered from rocksalt, yet the intensity of the diffusely scattered rays is very weak. To attempt to use Mo $K\alpha$ rays with zinc crystals was out of the question on account of the high absorption coefficient of zinc. We therefore used the general radiation from a tungsten tube. By the method of integration over the wave-lengths present in the spectrum as described by Jauncey and Claus[13] it is possible to compare theory with experiment provided that the theoretical values are known. However, it is a matter of experience that one can use an average wave-length as obtained from half-value absorption of the primary rays in aluminum and obtain reasonably correct S values. For the present we shall use this average wave-length as if it were the wave-length of monochromatic rays. In our experiments this wave-length was 0.435A. This excites the K fluorescence rays from zinc and it was necessary to place a sufficient thickness of aluminum before the ionization chamber window in order to reduce the fluorescence rays to a negligible intensity. Owing to the high absorption in zinc we could not use the method of transmission through a thin crystal. Instead we used the method of scattering from the front surface of the crystal specimens.

It is important to note that in diffuse scattering a new definition of the angle ψ is needed. It is the angle that the line bisecting the angle between the forward direction of the scattered rays and the backward direction of the primary rays makes with the c axis of the specimen. In diffuse scattering numerous values of ψ can be obtained for the same value of $(\sin\frac{1}{2}\phi)/\lambda$. As we shall describe the experimental details in a later paper, we now proceed to the results.

Having grown several single crystals of zinc, we were able to obtain the diffuse scattering at $\phi=30°$ for various values of ψ ranging from 0° to 90°. The S values are shown as crosses in Fig. 2. These are all for $(\sin\frac{1}{2}\phi)/\lambda=0.6$. We note the high S values for all values of ψ and the large difference between the S value for $\psi=0°$ and that for $\psi=90°$.

If there is asymmetry in the electron structure of zinc atoms it will be due to the valence electrons. At $(\sin\frac{1}{2}\phi)/\lambda=0.6$ the contributions of these electrons to the f values may be neglected and so f and also ΣE_r^2 may be considered as independent of ψ. Now (2) may be written in the form

$$M=\{b+(a-b)\cos^2\psi\}(\sin^2\tfrac{1}{2}\phi)/\lambda^2 \quad (9)$$

and so, from (1), (2), (4) and (5), we have at

[12] G. E. M. Jauncey and G. G. Harvey, Phys. Rev. **38**, 1071 (1931).

[13] G. E. M. Jauncey and W. D. Claus, Phys. Rev. **46**, 941 (1934).

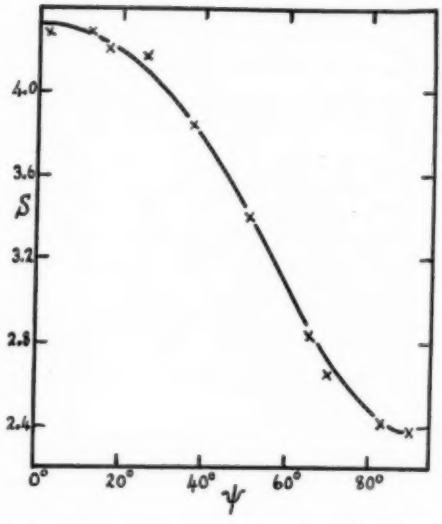

FIG. 2. Diffuse scattering of $\lambda=0.435$A from single crystals of zinc at $\phi=30°$ but for the orientation angle ψ varying from 0° to 90°.

$(\sin\frac{1}{2}\phi)/\lambda=0.6$

$$S_\psi=\text{const}-(F_{90°}^2/Z)\exp\left[-2(a-b)(\cos^2\psi\sin^2\tfrac{1}{2}\phi)/\lambda^2\right]. \quad (10)$$

For convenience we here introduce two notations: $F(10\bar{1}0)$ and $f(10\bar{1}0)$ are the F and f values for the $(10\bar{1}0)$ reflection, respectively, while $F(0.218, 90°)$ and $f(0.218, 90°)$ are the F and f values for $(\sin\frac{1}{2}\phi)/\lambda=0.218$ and $\psi=90°$. From Fig. 1, Brindley's most recent experimental value of $F(0.585, 80°)$ is 7.6. Now, from the form of (2), $M(80°)$ must nearly be equal to $M(90°)$ and so from the trend of the curve in Fig. 1 we estimate $F(0.6, 90°)=7.5$. But this last F is for Cu $K\alpha$ rays and contains the effect of dispersion. From data given on p. 806 of Brindley's paper,[5] this value must be multiplied by $11.7/(11.7-2.14)$ in order to obtain the F value for $\lambda=0.435$A, which is fairly far on the short wave-length side of the K absorption edge for zinc. This new value is 9.2 and is the value used for $F_{90°}$ in (10). From (10)

$$S_{0°}-S_{90°}=(F_{90°}^2/Z)\cdot(1-\exp\left[-2(a-b)\cdot(\sin^2\tfrac{1}{2}\phi)/\lambda^2\right]). \quad (11)$$

Our experimental value of $S_{0°}-S_{90°}$ is 1.94, so that upon solving (11) for $(a-b)$ we obtain 1.61. This amount of anisotropy is greater than that given by Brindley and much greater than the later value given by Zener. Putting this value of $(a-b)$ in (10) and using an arbitrary constant, we have plotted the curve shown in Fig. 2. The very good agreement between the experimental points and the curve shows the excellence of Zener's formula (2) and also of the method of diffuse scattering. Moreover, the agreement gives us some confidence in the value, $a-b=1.61$. Diffuse scattering experiments which do not involve the use of Brindley's experimental results and in which the method of integration over all wave-lengths in the spectrum of the primary rays is used give $a-b=1.66$ in reasonably good agreement with $a-b=1.61$. We shall take the higher value to be the more reliable. Further, these diffuse scattering experiments, which will be reported later, also give $b=0.68$ and therefore $a=2.34$. These values are shown in the fourth row of Table I.

Since[3] $$M=8\pi^2\overline{u_\psi^2}(\sin^2\tfrac{1}{2}\phi)/\lambda^2, \quad (12)$$

where $\overline{u_\psi^2}$ is the mean square displacement of an atom due to its thermal vibrations, we find from (2) that

$$(\overline{u_\psi^2})^{\frac{1}{2}}=\{(a\cos^2\psi+b\sin^2\psi)/8\pi^2\}^{\frac{1}{2}}. \quad (13)$$

Hence our results give

ψ	$(\overline{u_\psi^2})^{\frac{1}{2}}$
0°	0.172A
90°	0.093A

at room temperature. It is probably a coincidence that the ratio of these root-mean-square displacements very nearly equals the axial ratio.

Using the values of a and b shown in the fourth row of Table I we have calculated f values from Brindley's experimental F values. These f values are shown as white circles in Fig. 1. The curve in the figure is the quantum-mechanical f curve for zinc atoms estimated by Brindley[5] and corrected for dispersion. It is remarkable that the points for $f(20\bar{2}3)$, $f(21\bar{3}1)$, and $f(0006)+f(21\bar{3}2)$ fall so closely to the theoretical f curve. The point for $f(10\bar{1}5)+f(11\bar{2}4)$, however, departs considerably from the curve. But, if we use Brindley and Spiers' F value as represented by the black circle, we obtain an f point, represented by a white square, which does fall upon the theoretical curve. We feel therefore that there is good evidence for all these four f points

falling upon the theoretical f curve. This is very satisfactory because at reasonably high values of $(\sin\frac{1}{2}\phi)/\lambda$, such as 0.532 to 0.610, the outer electrons contribute a negligible amount to f and the calculated theoretical f values are therefore more reliable. We note that at lower values of $(\sin\frac{1}{2}\phi)/\lambda$ the f points calculated from Brindley's F values fall above the curve. However, the f points calculated from Brindley and Spiers' values and represented by white squares tend to fall upon the theoretical curve. On the whole we believe that there is good evidence that all the f points fall close to the theoretical curve but with some tendency for the f points to be above the curve at small values of $(\sin\frac{1}{2}\phi)/\lambda$. It is in this region of $(\sin\frac{1}{2}\phi)/\lambda$ that the calculated theoretical f values become somewhat unreliable due to the contributions of the outer electrons. Considering errors of experiment and of theoretical calculation, the agreement is satisfactory with the notable exception of the point for $f(10\bar{1}0)$.

4. Asymmetry in the Electron Structure?

From (1) and (2)

$$f(0002)/f(10\bar{1}0) = (F(0002)/F(10\bar{1}0))e^{0.0413(a-1.15b)}, \quad (14)$$

since $(\sin\frac{1}{2}\phi)/\lambda$ has the values 0.203 and 0.218 for the (0002) and (10$\bar{1}$0) reflections, respectively. Using our values of a and b and Brindley's $F(0002)$ and $F(10\bar{1}0)$ values for Cu $K\alpha$ rays, we thus obtain

$$f(0002)/f(10\bar{1}0)=0.958. \quad (15)$$

From the trend of the curve in Fig. 1, we estimate that

$$f(0.203, 90°)=1.015f(0.218, 90°).$$

Hence

$$f(0.203, 0°)/f(0.203, 90°) = 0.958/1.015=0.944. \quad (16)$$

For simplicity we shall assume that this ratio also holds for $(\sin\frac{1}{2}\phi)/\lambda=0.2$. According to p. 806 of Brindley's paper $f(0.2)$ for symmetrical zinc atoms is $23.7-2.14=21.6$ (say). We shall suppose that this is an average of $f(0.2, 0°)$ and $f(0.2, 90°)$, so that (16) gives $f(0.2, 0°)=21.0$ and $f(0.2, 90°)=22.2$. Although we place no great confidence in these f values, they indicate that $f(0.2, 0°)$ is somewhat less than $f(0.2, 90°)$ and so suggest the existence of some asymmetry in the electron structure of the zinc atoms. It is interesting to note that the asymmetry is such that the electron atmosphere is more diffuse in the direction of the c axis than in a direction normal to this axis.[14] It is the (0002) and (10$\bar{1}$0) reflections which, because $(\sin\frac{1}{2}\phi)/\lambda$ is small and the values of ψ differ by the maximum amount, give the best chance of showing asymmetry in the electron structure. These reflections should be investigated further. The (0004) and (20$\bar{2}$0) reflections should also prove of interest if they can be obtained unmixed with other reflections. The intensity of the (0004) reflection should prove to be low.

If there is asymmetry in the electron structure, it will be found that the f values obtained by correcting the F values for thermal vibrations will depart slightly from a smooth curve. The points will fall between two curves,[15] one for $\psi=0°$ and the other for $\psi=90°$. These curves will separate from each other at small values of $(\sin\frac{1}{2}\phi)/\lambda$.

5. Conclusion

We conclude that the experiments on diffuse scattering together with those on powdered crystals of zinc prove that the anisotropy of the thermal vibrations is much more than previously suspected. The anisotropy is almost sufficient to explain the anomalous F values obtained for the (0002) and (10$\bar{1}$0) reflections. However, we hold the tentative opinion that these reflections indicate some asymmetry in the electron structure of the atoms of a zinc crystal.

We wish to thank Professor E. P. T. Tyndall and Mr. D. O. Holland of the State University of Iowa for valuable information in regard to the growing of zinc crystals.

[14] The difference between $f(0.2, 90°)$ and $f(0.2, 0°)$ is 1.2. If this is due to the two valence electrons, then for each such electron $E(0.2, 90°)-E(0.2, 0°)=0.6$. The electron structure factor for each valence electron is probably somewhat like that for the electron in the hydrogen atom. For this latter electron $E(0.2)=0.5$ approximately. Taking this as the average of $E(0.2, 90°)$ and $E(0.2, 0°)$ we obtain $E(0.2, 90°)=0.8$ and $E(0.2, 0°)=0.2$. These are possible values.

[15] *Note added in proof:* In paper III of this series, Miller and Foster find evidence for $F(10\bar{1}1)=20.1$ for Cu $K\alpha$ rays. Using our values of a and b, we calculate $f(10\bar{1}1)=21.3$ for Cu $K\alpha$ rays. Referring to Fig. 1, we see that this f point falls between the curves which may be imagined as respectively passing through the f points for the (0002) and (10$\bar{1}$0) reflections. Miller and Foster also confirm the value of $F(0002)/F(10\bar{1}0)$ found by Brindley.

Anisotropy in the Atomic Vibrations of Zinc Crystals

II. Diffuse Scattering of X-Rays from Single Crystals

G. E. M. JAUNCEY* AND W. A. BRUCE, *Wayman Crow Hall of Physics, Washington University, St. Louis*

(Received June 29, 1936)

The general radiation from a tungsten tube was used together with Jauncey and Claus' method of integration over all wave-lengths. Because of the high absorption coefficient of zinc it was necessary to scatter the x-rays from the front surface of the zinc crystals. Correction for the presence of fluorescent rays was made. A number of zinc crystals were grown. The control of the direction of the major and minor axes with respect to the surface of the crystal is described. Two types of experiment were made: (1) the variation of S with ψ, the orientation angle, for a fixed value of ϕ, the scattering angle; and (2) the variation of S with ϕ for two fixed values of ψ, one near 90° and the other near 0°. (1) gave remarkable confirmation of the correctness of the form of Zener's formula for the Debye-Waller M for hexagonal crystals, while (2) confirmed in a general way our values as obtained in (1) for a and b in Zener's formula. We find a much higher anisotropy, $a-b=1.66$, than that suggested by Brindley, $a-b=0.785$.

1. INTRODUCTION

AS described in the previous article,[1] papers by Zener and by Brindley and Spiers suggested that a study of the diffuse scattering of x-rays from single crystals of zinc should prove of interest. According to the theory of diffuse scattering

$$S=S_{\text{coh}}+S_{\text{inc}}/(1+\alpha \text{ vers } \varphi)^3, \quad (1)$$

where

$$S_{\text{coh}}=(f^2/Z)(1-e^{-2M}) \quad (2)$$

and

$$S_{\text{inc}}=1-(1/Z)\sum E_r^2. \quad (3)$$

Since according to Zener's theory for hexagonal crystals M is related to the angle of orientation ψ by

$$M=(a\cos^2\psi+b\sin^2\psi)\cdot(\sin^2\tfrac{1}{2}\varphi)/\lambda^2, \quad (4)$$

the diffuse scattering S depends upon the orientation of the crystal. The root-mean-square displacement of an atom in a direction making an angle ψ with the c axis of the crystal is given by[1]

$$(\overline{u_\psi^2})^{\frac{1}{2}}=\{(a\cos^2\psi+b\sin^2\psi)/8\pi^2\}^{\frac{1}{2}}. \quad (5)$$

2. EXPERIMENTAL METHOD

Because of the high absorption coefficient of x-rays in zinc we could not use monochromatic x-rays and used instead the general radiation from a tungsten tube. The spectrum of this radiation is shown in Fig. 1. Also because of the high absorption in zinc we were unable to use the method of transmission through a thin crystal and used instead the method of scattering from the front face as used by the senior author[2] in his original experiments on diffuse scattering.

In Fig. 2, θ is the glancing angle of incidence on the surface of the crystal and ϕ is the angle of scattering. Our angle θ is not to be confused with the θ of the Bragg law. The line BD lies in the plane of scattering and bisects the angle ABC. It is the vibrations of the atom of a crystal in the direction of BD which give rise to the coherent part of the diffuse scattering[3] in the direction BC. The angle ψ is the angle between BD and the c axis of the crystal.

If the Compton effect is neglected the intensity of the scattered rays of wave-length λ is given by[2]

$$I_{\phi,\theta}=(s_\phi A I_0/2R^2\mu_1)\cdot u(\phi,\theta), \quad (6)$$

where I_0 is the intensity of the primary rays of wave-length λ, s_ϕ is the scattering coefficient per unit solid angle in the direction ϕ, μ_1 is the absorption coefficient of the x-rays in the crystal, and

$$u(\phi,\theta)=\frac{2\sin(\phi-\theta)}{\sin(\phi-\theta)+\sin\theta}, \quad (7)$$

In a hexagonal crystal, if the c axis is normal to the plane of scattering in Fig. 2, s_ϕ is not a func-

* The senior author was aided in part by a grant from the Rockefeller Foundation to Washington University for research in science.

[1] G. E. M. Jauncey and W. A. Bruce, Phys. Rev. **50**, 408 (1936). See this article for further references.

[2] G. E. M. Jauncey, Phys. Rev. **20**, 405 (1922). Figs. 2 and 6 in this reference should be interchanged.

[3] G. E. M. Jauncey, Phys. Rev. **37**, 1193 (1931); G. E. M. Jauncey, Phys. Rev. **42**, 453 (1932).

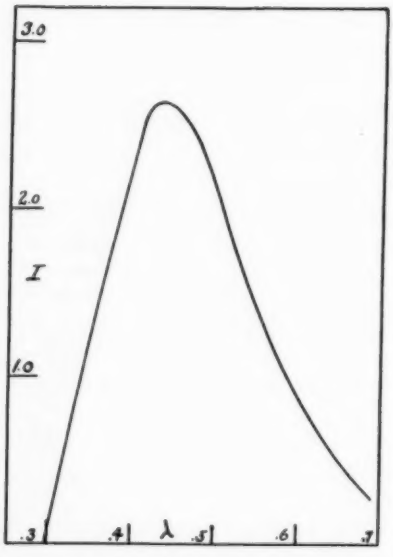

FIG. 1. Spectral distribution curve for the x-rays falling upon the crystal.

tion of θ, so that, if $I_{\phi,\theta}/u(\phi, \theta)$ is plotted against θ for a given value of ϕ, a horizontal line is obtained except for those values of θ at which Laue spots occur. If the c axis is in some other direction, the graph of $I_{\phi,\theta}/u(\phi, \theta)$ *vs.* θ will be a monotonic curve except for the Laue spots. We are thus enabled to eliminate the Laue spots as shown in Fig. 3.

From previous papers,[4] we obtain for front face scattering when a band of wave-length is used

$$(S\rho/\mu_1)_{\text{exp}}=\frac{4R^2Wm^2c^4}{ANZe^4(1+\cos^2\phi)}\cdot\frac{D_{\phi,\theta}}{D_0u(\phi,\theta)}, \quad (8)$$

where μ_1/ρ is the mass absorption coefficient of the primary rays of wave-length λ in the crystal, and $D_{\phi,\theta}$ and D_0 are, respectively, the ionization currents produced by the scattered and the primary rays. Now, if the distribution-in-wave-length of the intensity in the primary spectrum is $I(\lambda)d\lambda$, we can define another quantity

$$(S\rho/\mu_1)_{\text{th}}=\int(S\rho'/\mu_1)Id\lambda/\int Id\lambda, \quad (9)$$

where, because the Compton effect is taken into account,

$$S'=S_{\text{coh}}+\frac{2K_\phi\mu_1S_{\text{inc}}}{K_0(\mu_1+\mu_2)(1+\alpha\ \text{vers}\ \phi)^3} \quad (10)$$

and μ_2 is the absorption coefficient in the crystal of primary rays of wave-length λ after the Compton change of wave-length. K_ϕ is the fraction of modified rays of original wave-length λ and K_0 the fraction of unmodified rays of this wave-length absorbed in the ionization chamber.

3. METHOD OF GROWING THE CRYSTALS

We used a slight modification of the method described by Cinnamon.[5] Crystals were grown in a Lavite mould of 18 cm length with thermocouples at 6 cm intervals. Instead of a ceramic cover for the mould, a thick strip of mica with a hole for pouring was placed on the mould and was held down by a $\frac{3}{8}$-inch iron bar. The hole was above one end of the mould. A cup of alundum cement was made around the mica hole to facilitate pouring the casting and also to provide an easily accessible cleavage surface. We shall refer to this as the well of the mould. The nucleus used was a wire pulled out by the Czochralski-Gomperz method. The nucleus was placed at the opposite end of the mould from the well. The top surface of the casting in the mould was the surface which was later used for the scattering of x-rays. The available part of this surface measured 12 cm by 1 cm. The thickness of the crystal was 0.6 cm. In most cases the crystals were grown with the c axis perpendicular to the length

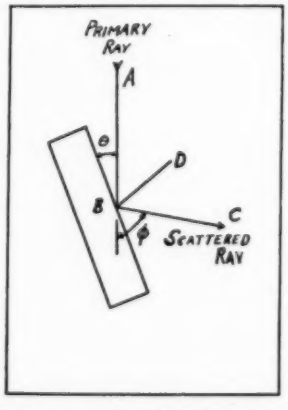

FIG. 2. Scattering from front face.

[4] G. E. M. Jauncey and W. D. Claus, Phys. Rev. **46**, 941 (1934). See this article for further references.

[5] C. A. Cinnamon, Rev. Sci. Inst. **5**, 187 (1934).

of the crystal but making various angles with the surface of the crystal. By using various crystals a number of values of ψ could thus be obtained in the experiments on the diffuse scattering of x-rays. Also, with one and the same crystal, variation in ψ could be obtained by tilting the crystal about an axis parallel to its length, the length being parallel to the plane of scattering in Fig. 2. In this way it is possible to obtain diffuse scattering measurements for the same value of ψ and ϕ but for crystals with different angles between the c axis and the surface.

The control of the major axis is very simple and in the 90° crystal (i.e., the c axis is perpendicular to the length of the crystal) the minor axis may be placed within one or two degrees. This latter is possible because zinc has a tendency to slip among planes of highest atomic density and to cleave along these planes when cooled to the temperature of liquid air.[6] The portion grown in the well of the mould was useful for finding the direction of the c axis with respect to the surface of the crystal. The growth of the crystal is best under control when the temperature gradient along the casting is about 5°C per cm and the rate of growth about 0.16 cm/min. The crystal casting when finished is covered with oxide. This is removed with 20 percent hydrochloric acid, which leaves a slightly etched surface. Examination of the etching tells whether or not the crystal is single.

If no cleavage can be found along a minor axis the orientation of this axis may be found by carefully examining the bright surface of an exposed basal plane. Faint twinning marks are usually found and indicate the minor axes. These twinning marks do not mean that the crystal is a twin but that when it was cleaved twins started and almost immediately recrystallized leaving only the marks at the very surface of cleavage. A freshly cleaved basal plane surface is highly reflecting and it is a simple matter to determine by optical means the direction cosines of the c axis with respect to the coordinate axes of the spectrometer. The angle θ is also determined by optical means by pasting a mirror on the surface of the crystal. It is interesting to note that diffuse scattering measurements cannot be obtained for $\psi=0°$ since a Laue spot necessarily occurs at this setting of the crystal. Knowing the directions of the major and minor axes with respect to the spectrometer, the values of θ in Fig. 2 at which Laue spots occur can be predicted and so avoided.

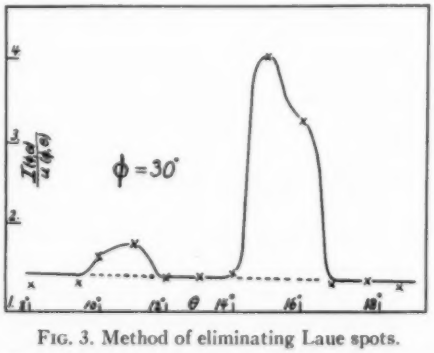

FIG. 3. Method of eliminating Laue spots.

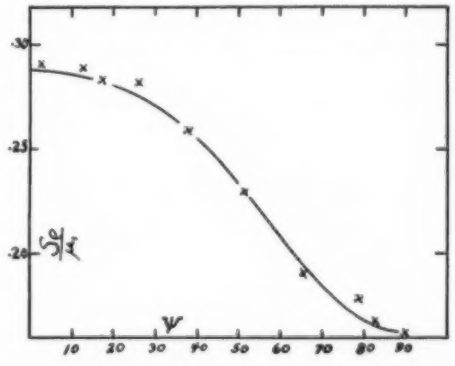

FIG. 4. Variation of diffuse scattering with the angle of orientation for a scattering angle of 30°.

4. Correction for Fluorescence Rays

The x-rays which were used were of shorter wave-length than that of the K absorption edge of zinc and so the K fluorescence radiation of zinc was excited. The fluorescence radiation entering the ionization chamber was considerably reduced by placing 0.0336 cm of aluminum in front of the chamber window. However, a small amount of fluorescence radiation still penetrated into the chamber. By a modification of the method described by Jauncey and DeFoe[7] we were able to correct for this small amount. We found that the part of $(D_{\phi,\theta})/D_0$ due to fluorescence radiation

[6] R. F. Miller, Metals Technology, Tech. Pub. 703 (1936).

[7] G. E. M. Jauncey and O. K. DeFoe, Phil. Mag. **1**, 711 (1926) and Proc. Nat. Acad. Sci. **11**, 520 (1925).

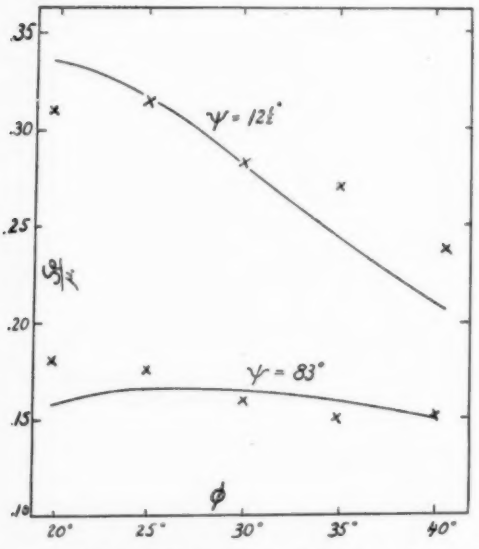

FIG. 5. Variation of diffuse scattering with angle of scattering for fixed values of ψ.

when $\theta=\phi/2$ was $(2.0\pm0.4)\times10^{-7}$. For $\phi=30°$, $\psi=90°$, and $\theta=\phi/2$, the value of $(D_{\phi,\theta})/D_0$ due to both fluorescence and scattered rays was 94×10^{-7}. The values for $D_{\phi,\theta}/D_0$ corrected for fluorescence radiation are used in (8) for calculating $(S\rho/\mu_1)_{\text{exp}}$. The area A of the ionization chamber window was 0.897 cm² and the distance R of the window from the axis of the spectrometer was 12.24 cm.

5. Results for the Variation of ψ for a Given Value of ϕ

By using several crystals we were able to obtain values of $(S\rho/\mu_1)_{\text{exp}}$ for various values of ψ between 2.5° to 90° for a fixed scattering angle of 30°. These values of $(S\rho/\mu_1)_{\text{exp}}$ are shown as crosses in Fig. 4. In order to calculate values for plotting $(S\rho/\mu_1)_{\text{th}}$ it was necessary to use quantum-mechanical values of f and ΣE_r^2. We have used Brindley's estimated values[8] of f. Unfortunately Brindley does not give values of ΣE_r^2. We have therefore used ΣE_r^2 values which have been extrapolated from the ΣE_r^2 values for copper given by Compton and Allison.[9] The incoherent part of the diffuse scattering in the case of zinc is only a small fraction of the total diffuse scattering so that the error introduced by using Compton and Allison's ΣE_r^2 values is insignificant. Next, it was necessary to assume values of a and b in (4). We tried various values and found that the values

$$a=2.34\ A^2, \qquad b=0.68\ A^2$$

give the best fit. The curve of $(S\rho/\mu_1)_{\text{th}}$ *vs.* ψ is that shown in Fig. 4. Because of the excellence of the fit between the experimental points and the curve we feel confidence in the above values of a and b. The excellent fit gives remarkable confirmation of the form of Zener's formula (2) for hexagonal crystals containing atoms of one kind. Putting these values of a and b in (5), we obtain the root-mean-square displacements reported in the previous paper.[1]

6. Results for the Variation of ϕ for Two Values of ψ

We used two crystals, one with $\psi=12.5°$ and the other with $\psi=83°$, and obtained values of $(S\rho/\mu_1)_{\text{exp}}$ for scattering angles ranging from 20° to 40°. The experimental values are shown as crosses in Fig. 5. The curves are graphs of $(S\rho/\mu_1)_{\text{th}}$ *vs.* ϕ for $\psi=12.5°$ and $\psi=83°$, respectively. The values of a and b shown in the preceding section have been used in calculating values of $(S\rho/\mu_1)_{\text{th}}$. The points do not fall upon the curves as well as we would like. However, there was some trouble with Laue spots at $\phi=40°$ so that the value of $(S\rho/\mu_1)_{\text{exp}}$ at this angle is somewhat unreliable. Also at $\phi=20°$ the theoretical f and ΣE_r^2 values which are used in calculating $(S\rho/\mu_1)_{\text{th}}$ are somewhat uncertain. At any rate our points do show a big difference between the diffuse scattering for $\psi=12.5°$ and that for $\psi=83°$ over the range of scattering angles investigated. The points roughly follow the trend of the curves. All of the points demand values of a and b that are distinctly greater than Brindley's values of a and b shown in Table I of our first paper[1] and still greater than Zener's values for the modified Debye model. Perhaps it is still more important that our value for the anistropy is $a-b=1.66$ as compared with Brindley's value 0.785 and Zener's value 0.465.

[8] G. W. Brindley, Phil. Mag. **21**, 760 (1936).
[9] A. H. Compton and S. K. Allison, *X-Rays in Theory and Experiment*, p. 782.

Anisotropy in the Atomic Vibrations of Zinc Crystals.
III. The (0002) and (10$\bar{1}$0) Reflections of Mo $K\alpha$ X-Rays from Powdered Zinc

R. D. MILLER AND E. S. FOSTER, JR., *Wayman Crow Hall of Physics, Washington University, St. Louis*

(Received June 30, 1936)

The ratio of the F value for the (0002) reflection to the F value for the (10$\bar{1}$0) reflection of Mo $K\alpha$ x-rays from powdered zinc was found to be 0.891. This compares very well with Brindley's value of 0.894. Our results suggest that the value of F for the (10$\bar{1}$1) reflection of Cu $K\alpha$ rays is 20.1, which is somewhat higher than Brindley's value.

BRINDLEY[1] first noticed that the F value for the (10$\bar{1}$0) reflection is much greater than that for the (0002) reflection when Cu $K\alpha$ x-rays are used. Hence Brindley has applied the term anomalous to the (10$\bar{1}$0) reflection. He has suggested that this high value may be due to an impurity, but he finds a similar result for the same reflection from cadmium.[2] However, it is possible that the difference between these two reflections is partially due to anisotropy in the vibrations of the atoms and perhaps partially due to the asymmetry of the electron structure of the atoms in the zinc crystals, as pointed out by Jauncey and Bruce.[3] Since Brindley's results were obtained by a photographic method for Cu $K\alpha$ x-rays, it is important to determine whether the same difference between $F(0002)$ and $F(10\bar{1}0)$ is obtained when Mo $K\alpha$ rays are used and when the observations are made by means of an ionization chamber instead of by a photographic film.[4]

The method used was that described by Wollan.[5] Very fine zinc powder was prepared by the sublimation of pure zinc filings heated in a vacuum to prevent oxidation, as described by Brindley and Spiers.[6] X-rays from a molybdenum target tube operated at 32 kv peak and 29 ma fell upon the briquet of zinc powder at a glancing angle, α, of 8° 35′. A zirconium filter was placed in front of the ionization chamber and thus absorbed not only the Mo $K\beta$ line but also the fluorescent zinc K radiation. The slit before the ionization chamber was curved to a radius corresponding to that of the average curvature of the (0002) and (10$\bar{1}$0) lines. Its width was 1 mm at a distance of 14.8 cm from the axis of the spectrometer. Our results are shown in Fig. 1 and are the average of several runs over the range of scattering angles shown. In this figure the hump for the (10$\bar{1}$1) reflection is also shown. The ratio of the area under the (0002) hump to that under the (10$\bar{1}$0) hump is 1.156, while the ratio of the heights of the two maxima is 1.150. Now,

$$\text{Area} = \text{const.}\; p s_c^2 \left(\frac{1+\cos^2 2\theta}{\sin\theta \sin 2\theta}\right) \frac{\sin(2\theta-\alpha) F^2}{\sin(2\theta-\alpha)+\sin\alpha}, \quad (1)$$

where p is the number of planes cooperating in producing the reflection, s_c is the crystal structure

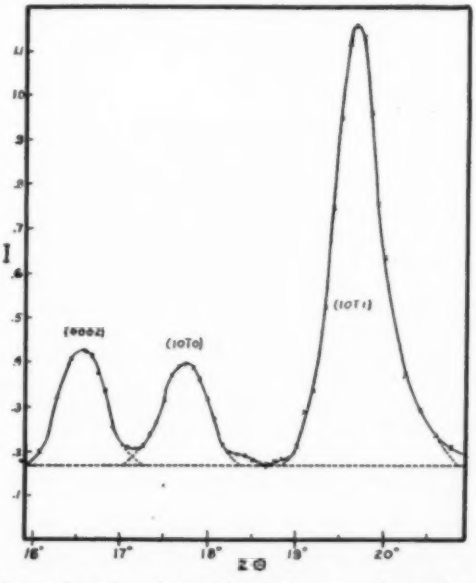

FIG. 1. Intensity of scattering against scattering angle.

[1] G. W. Brindley, Phil. Mag. **21**, 790 (1936).
[2] G. W. Brindley, Proc. Leeds Phil. Soc. **3**, 200 (1936).
[3] G. E. M. Jauncey and W. A. Bruce, Phys. Rev. This issue.
[4] For notation used in the above paragraph, see reference 3.
[5] E. O. Wollan, Phys. Rev. **35**, 1019 (1930).
[6] G. W. Brindley and F. W. Spiers, Phil. Mag. **20**, 865 (1935).

TABLE I. *F values.*

Reflection	θ	Area	Relative F Mo $K\alpha$	Cu $K\alpha$
0002	8° 17′	1.156	0.891	0.897
$10\bar{1}0$	8° 54′	1.000	1.000	1.000
$10\bar{1}1$	9° 49′	4.72	.898	.866

The $(10\bar{1}1)$ reflection of the β-line falls very nearly on the $(10\bar{1}0)$ reflection of the α-line. The areas in the figure are uncorrected. Measurement of the spectrum of the rays penetrating the zirconium filter give $\beta/\alpha = 0.5/100$. The F values are for pure $K\alpha$ rays.

factor (2 for (0002), 1 for $(10\bar{1}0)$, $\sqrt{3}$ for $(10\bar{1}1)$), θ is the Bragg angle of reflection, and F is the atomic structure factor including the effect of thermal vibrations. From the ratio of the areas the ratio of the F's may be obtained. Our final results are shown in Table I. The ratios $F(0002)/F(10\bar{1}0)$ and $F(10\bar{1}1)/F(10\bar{1}0)$ as found by us are shown in the fourth column while Brindley's ratios are shown in the fifth column of the table.

Because of dispersion,[1] the f values (i.e., F values corrected for thermal vibration) should be greater by 2.14 when Mo $K\alpha$ rays are used than when Cu $K\alpha$ rays are used. Hence our value of $F(0002)/F(10\bar{1}0)$ should be slightly less than Brindley's value. Our estimate of Brindley's value for Mo $K\alpha$ rays is 0.894, which is in very good agreement with our value of 0.891. Our estimate of Brindley's value of $F(10\bar{1}1)/F(10\bar{1}0)$ for Mo $K\alpha$ rays is 0.863. We feel that this is really lower than our value of 0.898.

Since Brindley made repeated experiments on $F(10\bar{1}0)$, we take his value of 22.4 for Cu $K\alpha$ rays to be correct. From our ratio, given above, is obtained $F(10\bar{1}1) = 20.1$. If this value is used in Fig. 1 of Jauncey and Bruce's paper,[3] and $f(10\bar{1}1)$ found by using their values of a and b, the f point falls between the curve for $\psi = 0°$ which passes through the f point for (0002) and the curve for $\psi = 90°$ which passes through the f point for $(10\bar{1}0)$. This fact gives some support to the idea of asymmetry in the electron structure of the atoms.[3]

The authors wish to thank Professor G. E. M. Jauncey for suggesting this problem and Mr. W. A. Bruce for aid in making the powdered crystals and in the experimental details.

SEPTEMBER 1, 1936 PHYSICAL REVIEW VOLUME 50

Fundamental Absorption Bands of the Deuteroammonias

M. V. MIGEOTTE* AND E. F. BARKER, *University of Michigan*

(Received May 13, 1936)

The four fundamental vibration bands of ND_3 have been obesrved in infrared absorption, ν_3 being a double band as in NH_3. The frequencies of the parallel vibrations, expressed in cm^{-1}, are $\nu_1 = 2420$, $\nu_3 = 749.2$ and 745.8, and of the perpendicular vibrations, $\nu_2 = 2556$ and $\nu_4 = 1191.3$. The rotational structure for ν_3 is completely resolved. The perpendicular bands consist of many components with zero branches spaced at intervals of 1.7 cm^{-1} in ν_2 and 5.2 cm^{-1} in ν_4. The former cannot be resolved: they coalesce into a broad central absorption region, but the spacing of the most intense rotation lines in the composite band indicates the interval between centers. These frequency intervals agree well with the predictions of Johnston and Dennison. The moments of inertia for ND_3 are determined from the structure of the band ν_3, by comparison with observations upon NH_3. They are $C = 8.985 \times 10^{-40}$ g cm² with respect to the symmetry axis, and $A = 5.397 \times 10^{-40}$ g cm² for any perpendicular axis. From these the molecular dimensions are obtained. The height of the pyramid is 0.360×10^{-8} cm and the distance between hydrogen atoms is 1.645×10^{-8} cm. New information regarding the potential curve is obtained (1) from observations upon the doubling of the first excited levels in the four varieties of ammonia, and (2) from the positions of higher excited levels in ND_3. Four vibration levels are located which lie above the central potential hump, and correspond to oscillations of the nitrogen atom from side to side through the plane formed by the hydrogen atoms.

THE ammonia molecule is known to have the form of a low equilateral triangular pyramid. Its spectrum is rich, including many harmonic and combination bands in addition to the four fundamental frequencies, but the analysis and interpretation of the available observations is by no means complete. The moment of inertia A with respect to an axis normal to the symmetry line may be obtained immediately

* C. R. B. Fellow 1934–5, now at the University of Liége.

from the line spacing in the parallel bands, and also from the pure rotation frequencies. The spectrum, however, does not yield a direct determination of the moment C with respect to the symmetry axis itself, from which the molecular dimensions could be computed. In the perpendicular bands[1] the dependence of line spacing upon A and C is complicated by an interaction arising from the twofold degeneracy of the vibration. This effect has been completely formulated[2] but is difficult to evaluate precisely. The height of the pyramid may be estimated indirectly[3] in terms of the observed doubling in parallel bands, which serves to define the potential curve representing the bond between N and the H_3 group. The following observations upon the spectrum of ND_3 determine the moment of inertia A for that molecule, from which the molecular dimensions may be computed on the assumption that they are the same for ND_3 as for NH_3.

The gas used at the beginning of this investigation was a mixture of the deuteroammonias, with ND_3 in rather low concentration.[4] Through the courtesy of Professor Taylor we were later privileged to examine a very pure sample of ND_3 prepared at Princeton University by Dr. J. C. Jungers. In transferring this gas to absorption cells with windows of rocksalt, which could not be baked out, some contamination with H was unavoidable: this did not lead to any serious ambiguity in the results, however. The bands were examined under fairly high resolution with the usual prism-grating spectrometer.

In the mixed sample the double frequency parallel bands ν_3 for the various ammonias were observed, and these are shown in Fig. 1. The four pairs of zero branches stand out distinctly, but the rest of the structure is extremely complicated due to superposition. Since a considerable amount of NH_3 was present it seemed advisable to remap a part of the pure NH_3 spectrum for comparison. This is represented by the broken lines. The arrows upon the horizontal axis indicate band centers. The lower pair of levels

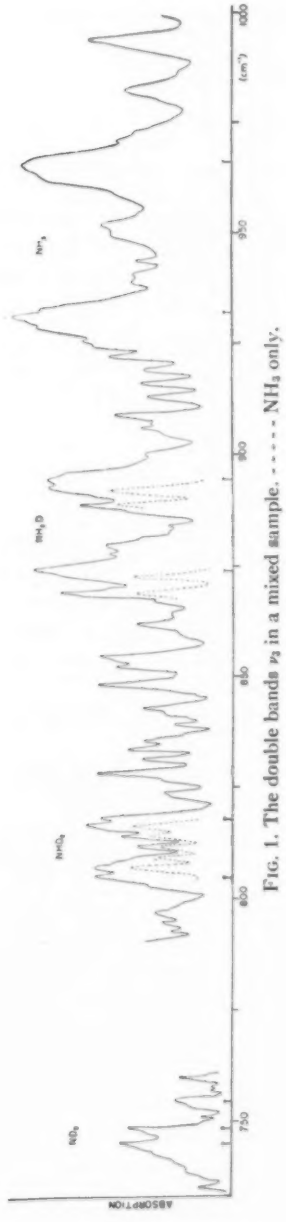

FIG. 1. The double bands ν_3 in a mixed sample. - - - - - NH_3 only.

may be designated 0_s, 0_a and the upper pair 1_s, 1_a. The permitted transitions are $0_s \rightarrow 1_a$ and $0_a \rightarrow 1_s$, the former giving the higher frequency. Table I shows the observed positions of the band centers. The computed doublet separations are first approximations obtained by the method

[1] An analysis of the perpendicular band ν_4 for NH_3 at 6μ has been completed and is soon to be published.
[2] Johnston and Dennison, Phys. Rev. **48**, 868 (1935).
[3] Dennison and Uhlenbeck, Phys. Rev. **41**, 313 (1932).
[4] This sample was prepared by Mr. W. A. Webb of Berkeley, Cal., and was purchased through a grant from the Faculty Research Fund.

TABLE I. *Positions of band centers in cm⁻¹.*

	$0_s \rightarrow 1_a$	$0_a \rightarrow 1_s$	$\Delta\nu$ obs.	$\Delta\nu$ comp.
NH_3	966	933	33	(33)
NH_2D	894	874	20	10.7
NHD_2	818	808	10	4.5
ND_3	749.2	745.8	3.4	2.2

of Dennison and Uhlenbeck, assuming identical potential curves in each case. It is not surprising that they agree with the observed intervals only moderately well, for the potential energy is actually a function of two variables, depending not only upon the displacement of the nitrogen atom from its equilibrium position, but also upon the distance between the hydrogen atoms. The relative importance of these two coordinates is not the same for vibrating molecules with different mass distributions. Our results indicate, as might be expected, that a section of the two-dimensional potential surface appropriate to one of the heavier molecules has a slightly lower central maximum than does that of NH_3. In the unsymmetrical molecules there is, of course, the added complication that the motion of the nitrogen atom is not precisely along the axis of the pyramid.

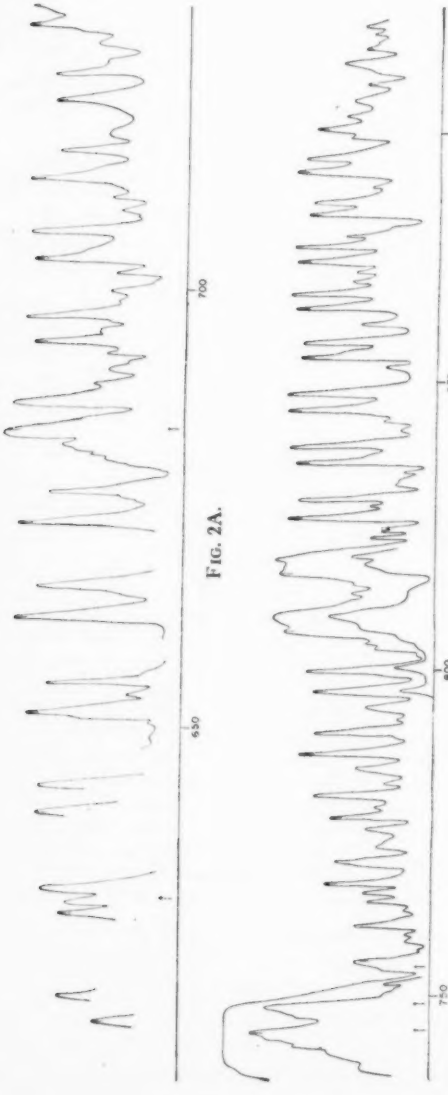

FIG. 2A.

FIG. 2B.

FIG. 2. ν_3 in ammonia with high ND_3 concentration.

The rotational structure of the pair of bands representing ν_3 for ND_3 is shown in Fig. 2, the lines belonging to the component with lower frequency ($0_a \rightarrow 1_s$) being indicated by marks. For these observations ND_3 was used at a pressure of 11 cm in a cell 10 cm long. The windows were KBr plates 6 mm thick. A slight contamination with ordinary hydrogen is indicated by the presence of broad absorption maxima due to NHD_2 at about 808 cm^{-1} and 818 cm^{-1}. Another rather broad line at 683.4 cm^{-1} includes the sixth negative member of the low frequency component band and also a weak zero branch corresponding to absorption by excited ND_3 molecules executing the transition $1_s \rightarrow 2_a$. Similarly, the band center for $2_s \rightarrow 3_a$ appears at 754.5, almost at the $+1$ position for the low frequency fundamental band. This $+1$ line is absent, however, while the corresponding member of the $0_s \rightarrow 1_a$ band is clearly present at 759.6, the change is statistics when deuterons replace protons reversing the situation observed in NH_3.[5] The change in spin from $\frac{1}{2}$ for protons to 1 for deuterons also results in a smaller variation in the intensities of the successive lines across the band. At about 632 cm^{-1} there is a weak absorption maximum marked with a broken arrow which is perhaps the $1_a \rightarrow 2_s$ frequency for NHD_2. On the low frequency side these bands extend into the region of intense absorption due to atmospheric CO_2, where satisfactory observations may be made only at intervals between the CO_2 lines.

[5] Dennison and Hardy, Phys. Rev. **39**, 938 (1932).

TABLE II. *Structure of the bands ν_3 for* ND_3.

High frequency component, $\nu_0 = 749.2$				Low frequency component, $\nu_0 = 745.8$							
ν obs.	ν comp.	Difference	m	ν obs.	ν comp.	Difference	m	ν obs.	ν comp.	Difference	m
759.57	759.42	−0.15	1	739.00	738.92	−0.08	1	755.96	756.02	+0.06	1
769.63	769.58	−0.05	2	728.60	728.59	−0.01	2	766.25	766.20	−0.05	2
779.63	779.67	+0.04	3	718.16	718.20	+0.04	3	776.32	776.32	0.00	3
789.71	789.70	−0.01	4	707.77	707.77	0.00	4	786.32	786.38	+0.06	4
799.70	799.66	−0.04	5	697.12	697.28	+0.16	5	796.40	796.38	−0.02	5
809.02	809.54	+0.52	6	686.81	686.76	−0.05	6	806.40	806.32	−0.08	6
818.95	819.35	+0.40	7	676.28	676.20	−0.08	7	816.26	816.19	−0.07	7
829.16	829.09	−0.07	8	665.55	665.60	+0.05	8	826.00	825.99	−0.01	8
838.80	838.73	−0.07	9	654.85	654.96	+0.11	9	835.56	835.72	+0.16	9
848.28	848.30	+0.02	10	644.21	644.30	+0.09	10	845.37	845.37	0.00	10
857.80	857.77	−0.03	11	633.61	633.60	−0.01	11	855.01	854.94	−0.07	11
867.26	867.16	−0.10	12	623.13	622.89	−0.24	12	864.43	864.43	0.00	12
876.50	876.45	−0.05	13					873.63	873.83	+0.20	13
885.56	885.64	+0.08	14					883.06	883.14	+0.08	14
894.77	894.73	−0.04	15					892.22	892.36	+0.14	15
903.46	903.72	+0.26	16					901.10	901.48	+0.38	16
								910.16	910.51	+0.35	17

The positions of the rotation lines in the two bands are very well represented by the two equations

$$\nu = 749.2 \pm 10.25m - 0.029m^2 \mp 0.00050m^3,$$
$$\nu = 745.8 \pm 10.25m - 0.024m^2 \mp 0.00053m^3,$$

where m is the ordinal number of any line counted from the band center. Table II shows the positions of observed lines, and the frequencies indicated by these formulae, expressed in cm^{-1}. The differences are generally small, though in a few cases they clearly exceed the errors in observation. This is the result of blends, either with lines of the upper stage bands or with absorption due to other molecules, such as NHD_2, NH_2D and CO_2.

The curves in Fig. 3 are traced from records of an automatic prism spectrograph, showing (a) the absorption in the region of 16μ due to ND_3 in a 10 cm cell at 40 cm pressure, and (b) the same region with the cell empty. A parallel type band corresponding to the transition $1_a \rightarrow 2_s$ shows very clearly, with its center at 610 ± 2 cm^{-1}. It is not completely separated from the negative branches of the intense fundamental bands whose unresolved zero branches (746 and 749) appear at the left.

In Fig. 4 a small section of the 10μ region is represented, the lower curve indicating absorption due to NH_3, while the upper one shows the changes resulting from the addition of ND_3. A very strong peak at 1081.5 cm^{-1} indicates the $1_a \rightarrow 3_s$ transition, while the weaker absorption at 1066 cm^{-1} is interpreted as the band center for $2_a \rightarrow 4_s$. A much weaker line at 1038.5 may represent the next step from 3_s to 4_a. These observations serve to define the potential curve much more precisely than do any previously available.

Manning[6] has recently discussed the problem of the double minimum in ammonia, utilizing a modified Morse function which may be solved exactly. He has computed the approximate positions for the first eight levels of ν_3 in ND_3, and compared them with numerical values obtained by Benedict from ultraviolet absorption measurements. Our values are in very good agreement with these predictions, and with Benedict's observations. Fig. 5 shows the curve employed by Manning with the observed levels indicated. The separation of the lowest pair, which is predicted to be about 0.2 cm^{-1}, has not yet been determined experimentally. Levels above the central maximum tend to assume an equal spacing, and correspond to vibrations in which the nitrogen atom passes completely through from one side to the other of the plane formed by the hydrogen atoms. Higher levels would, of course, converge as they approach the dissociation level, which lies somewhat above 40,000 cm^{-1}.

[6] Manning, J. Chem. Phys. **3**, 136 (1935).

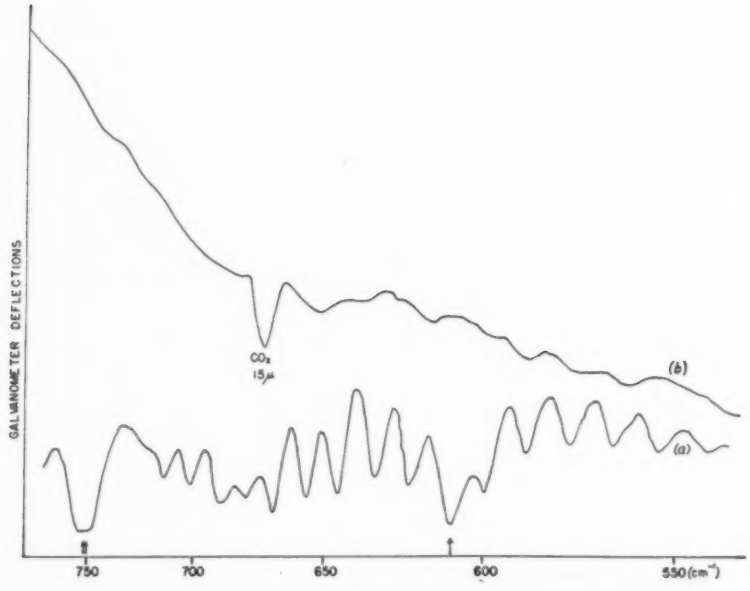

FIG. 3. a. ND_3 band near 16μ, from a recording spectrograph with KBr prism.
b. Empty cell record.

The other parallel vibration, ν_1, corresponds to a symmetrical motion of the three hydrogen atoms approximately in their own plane. For ND_3 it lies at 2420 cm^{-1}, and the zero branch is shown in Fig. 6a. The rotation structure cannot be satisfactorily resolved. It is obscured on the low frequency side by the intense absorption due to atmospheric CO_2, and on the high frequency side by the perpendicular band ν_2 of ND_3. This latter band also is only partially resolved. It consists of a sequence of zero branches spaced approximately 5.2 cm^{-1} apart, the most intense one lying 2.6 cm^{-1} to the high frequency side of the band center at 2556 cm^{-1}. There is some indication of further absorption, perhaps due to NHD_2, at 2570 cm^{-1} and at 2620 cm^{-1}.

The fourth fundamental band, also of the perpendicular variety, has been located at 1191.3 cm^{-1}. This too is an aggregate of many component bands, but their relative displace-

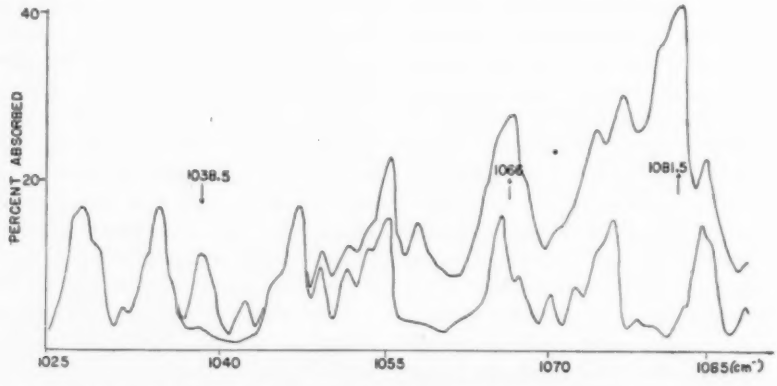

FIG. 4. Absorption of NH_3 (lower curve) and of ND_3+NH_3 (upper curve) near 10μ.

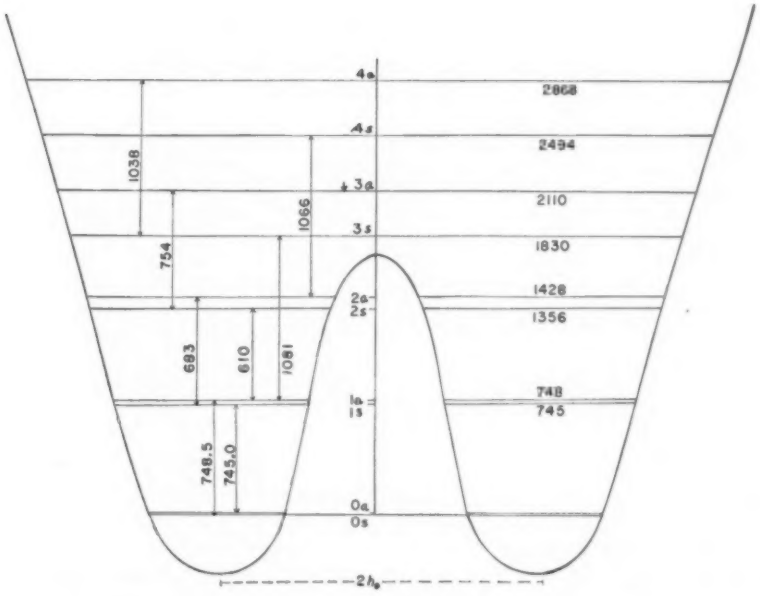

FIG. 5. Potential curve and observed transitions for the low frequency symmetrical vibration in ND_3.

ments are so small that the zero branches are not separated. The observed pattern is indicated in Fig. 6b. On the low frequency side the rotational structure is fairly well resolved, the interval between lines being 8.5 cm^{-1} but on the high frequency side it is not so clear because one of the bands of NHD_2 is superposed upon it. The spacing of successive zero branches is estimated at 1.7 cm^{-1}. Table III shows the measured positions of the lines, and, in the third column, the mean positions by pairs, indicating the convergence.

TABLE III. *Rotational structure of the band* $\nu_4 = 1191.3$ cm^{-1}.

m	Negative	Positive	Mean	Interval
1	—	1200.0		
2	1174.0	1209.0	1191.5	8.8
3	1165.4	1217.0	1191.2	8.6
4	1156.8	1225.0	1190.9	8.5
5	1148.5	1234.1	1191.3	8.6
6	1140.3	1241.8	1191.0	8.5
7	1132.0	1249.5	1190.8	8.4
8	1123.8	1258.1	1191.0	8.4
9	1115.4	1265.8	1190.6	8.4
10	1106.2	1273.5	1189.8	8.4
11	1097.9	1281.3	1189.6	8.3
12	1089.6	—		
13	1081.2	1297.3	1189.2	8.3
14	1073.4			
15	1065.5			
16	1058.2			

The structure and line spacing in these two perpendicular bands is actually in accord with the predictions of band theory. Degenerate vibrations of this type have been discussed in detail by Johnston and Dennison,[2] who show that the resulting internal axial angular momentum $\zeta h/2\pi$ consists of two terms having opposite signs, one due to the mutual rotation of the N atom and the D_3 group, and the other due to the oscillations of the three D atoms, with respect to their own center of mass. Each fundamental or combination band of the perpendicular type has a characteristic ζ, either positive or negative, the value of which may be computed approximately. The line spacing is $[(1-\zeta)/C-1/A]h/4\pi^2$. Dennison's computed values for $\Delta\nu_2$ and $\Delta\nu_4$ in cm^{-1} are 4.8 and 2.7, as compared with our observed spacings 5.2 and 1.7.

The equations representing the bands ν_3 indicated a line interval of 10.25 cm^{-1}. This yields immediately the moment of inertia $A = 5.397 \times 10^{-40}$ g cm^2 for ND_3. The corre-

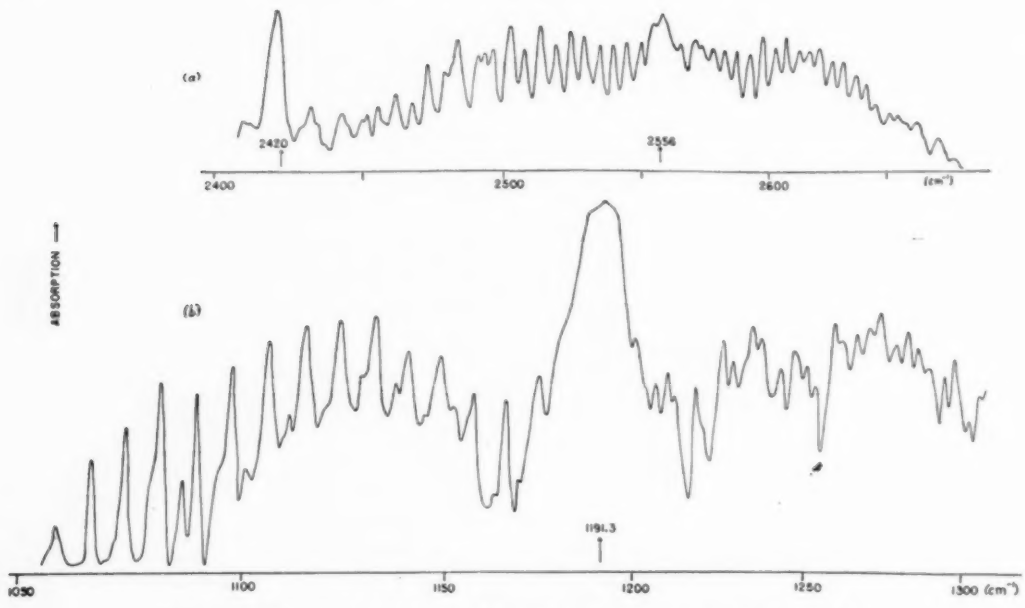

FIG. 6. Fundamental vibration bands of ND_3. a. ν_1 and ν_2 near 4μ. b. ν_4 near 8μ.

sponding value for NH_3 is 2.782×10^{-40}, as indicated by the data of Wright and Randall.[7] From a comparison of these two numbers the molecular dimensions may be computed immediately. Our values agree well with those obtained with somewhat less precision from the pure rotation spectrum of ND_3, by Barnes.[8] They are:

$H-H$ distance	1.645×10^{-8} cm
$N-H$ distance	1.016×10^{-8}
height of pyramid	0.360×10^{-8}

moment of inertia,

$C=4.497\times10^{-40}$ g cm² for NH_3
and $C=8.985\times10^{-40}$ g cm² for ND_3.

The mechanical problem of the vibrations of symmetrical tetratomic molecules has been treated by Rosenthal,[9] though without taking into account the effect of the double minimum. The normal frequencies are represented by her equations (4) consisting of two quadratic expressions containing six arbitrary constants. The four observed frequencies for ND_3, together with any two of those for NH_3, provide information for selecting a consistent set of values for the six constants. Since the effects of anharmonicity and of the double minimum can only be estimated, these coefficients are not precisely determined. The approximate values are useful, however, in the interpretation of the atomic binding, and in the classification of the bands due to NH_2D and NHD_2. We have chosen the following group:

$A=10.2\times10^{-5}$, $B=5.46\times10^{-5}$,
$C=1.68\times10^{-5}$, $D=1.18\times10^{-5}$,
$E=2.12\times10^{-5}$, $F=2.44\times10^{-5}$.

[7] Wright and Randall, Phys. Rev. **44**, 391 (1933).
[8] Barnes, Phys. Rev. **47**, 658 (1935).
[9] Rosenthal, Phys. Rev. **47**, 235 (1935).

Deuteron-Induced Radioactivities

J. J. LIVINGOOD, *Radiation Laboratory, University of California*

(Received June 29, 1936)

Bombardment of several elements with 5-MEV deuterons produces the following radioactivities. Commercial *copper* decays with a half-life of 130±10 days, emitting gamma-rays and very slow electrons. Attempts at chemical identification of probable radioactive products have been inconclusive, and the activity may be due to some unknown impurity in the copper. *Zinc* emits electrons with half-lives of 97±10 hours, 25±2 hours, 12±1 hours and 1±0.3 hours; the third of these is possibly due to radio Cu^{64} which has the same period. *Antimony* exhibits electron activities with half-lives of 50±4 days, 68±2 hours (confirming the 2.5 day period found by Fermi with neutrons) and 24±2 hours. *Ruthenium* shows half-lives of 46±3 days, 11±2 days, 39±1 hours and 4±1 hours, all due to electrons. *Bismuth* yields electrons of 5 days half-life and alpha-particles which increase in number for three weeks and then remain practically constant. This is interpreted as the synthesis of radium E through the reaction $_{83}Bi^{209}+{}_1H^2\rightarrow{}_{83}Bi^{210}$ (i.e., Ra E)$+{}_1H^1$, followed by its natural decay to polonium and thence to lead. The range of the alpha-particles agrees with that of the alphas from natural polonium to within 0.5 mm, and the time required to reach maximum alpha-activity is consistent with the 140 day half-life of polonium.

BOMBARDMENT of the elements herein reported has been made with the cyclotron of Lawrence and Livingston.[1] The targets were mounted in the bombardment chamber which was roughly evacuated with a Hyvac pump, the deuterons entering this region through a window of thin platinum foil supported on a brass grid. The magnitude of current was read by rotating a tungsten or platinum target into the beam near the inner side of the window; during the bombardment this target was turned aside and a small fraction of the current, employed as an indicator of correct synchronization, was picked up on an internal probe wire. The transmission factor of the window was approximately 50 percent, and the bombarding currents given below are therefore one-half of the current actually produced. The energy of the deuterons was observed by visual observation of the range in air across the bombardment chamber after passage through aluminum foils of known stopping power. Most of the targets were wrapped in aluminum foil as a protection against contamination from recoil atoms distilled onto the window during previous use. Correction for the stopping power of these wrappers has been made in the data given.

The observations of radioactivity were made on a quartz-fiber electroscope of the Lauritsen type. The yields of active atoms per impinging deuteron have all been computed for an infinite duration of bombardment, when equilibrium would be reached between the production of the nuclei and their spontaneous decay. Due to a number of uncertainties, such as the calibration of the electroscope, the transparency of the window through which the deuterons pass, etc., the absolute values of the yields are not to be taken too seriously, but the relative values are probably quite good, particularly among the activities of a single element, in which fluctuations in bombarding current would effect all isotopes equally. The errors given in the periods of decay have been obtained from inspection of the curves and are limits of error of generous size.

COPPER

Extended observations[2] have been made on filings scraped from the copper deflecting plate in the interior of the cyclotron. This is subjected to bombardment by stray deuterons of probably the full 5 MEV energy. The first sample was examined after about one month's intermittent use, and for the first 200 hours of observation showed a radioactivity with half-life of 14 hours. This is doubtless a combination of the 12.8-hour activity of radio Cu^{64} (originally given as 10 hours by Fermi but more recent observations by Van Voorhis[3] quote the former figure) and the 15.5-hour activity of radio Na^{24}. After this interval the sample exhibited a half-life of 25 days,

[1] Lawrence and Livingston, Phys. Rev. **45**, 608 (1935).

[2] Presented before the Physical Society at Seattle, June 18, 1936.

[3] Van Voorhis, Phys. Rev. **49**, 876 (1936).

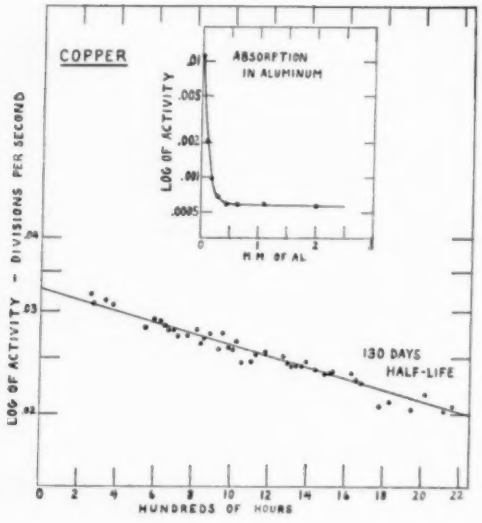

FIG. 1.

the observations extending over an additional 42 days time.

Assuming that it is really copper and not some impurity that has been transmuted, the radio isotope responsible must be one that can be attained by some known or hypothetical deuteron reaction. The known types may be classified as follows:

(I) $${}_{Z}X^{A}+{}_{1}H^{2}\rightarrow{}_{Z}X^{A+1}+{}_{1}H^{1},$$

(II) $$\rightarrow{}_{Z+1}X^{A+1}+{}_{0}n^{1},$$

(III) $$\rightarrow{}_{Z-1}X^{A-2}+{}_{2}He^{4}.$$

The first of these, the net effect of which simply is to add a neutron to the target nucleus (Oppenheimer-Phillips[4] transmutation), would here be ruled out, since only two stable copper isotopes are known, Cu^{63} and Cu^{65}, and the resulting radio isotopes Cu^{64} and Cu^{66} have half-lives of 12.8 hours and 6 minutes, respectively. The second type must also be discarded, since it leads to Zn^{64} or Zn^{66}, both of which are stable; while if Cu^{62} existed, the result would be radio Zn^{63}, which should be positron active, whereas (see below) the observed activity is of negative electrons. The third case would seem to fit the present situation:

$${}_{29}Cu^{65}+{}_{1}H^{2}\rightarrow{}_{28}Ni^{63}+{}_{2}He^{4}$$

$${}_{28}Ni^{63}\rightarrow{}_{29}Cu^{63}+e^{-}.$$

In spite of the unlikelihood of all of these possibilities except that of nickel, a chemical analysis for nickel, copper and zinc was attempted on a second set of copper filings. A little zinc and nickel was added to an acid solution of the irradiated copper; CuS was precipitated out with H_2S, then Ni $(OH)_2$ was precipitated from alkalinity, and finally ZnS was brought down with more H_2S.

The results of this showed that the previously found 25 day half-life, was entirely spurious; the Ni (OH_2) has been followed for three months and shows an apparent half-life of 130 ± 10 days; the CuS decayed with the 14.5 days activity characteristic of the omnipresent radio phosphorous (probably occluded or brought down as some phosphate); while the ZnS had an initial activity only one-seventh that of the nickel hydroxide and was consequently discarded. The sum of the Ni $(OH)_2$ and CuS (P^{32}) activities showed the original false 25 day half-life, which emphasizes very clearly the necessity for caution when contaminants may be present and when only a relatively short time of observation is employed to compute a half-life.

The character of the radiation from the Ni $(OH)_2$ has been observed to be negative electrons accompanied by gamma-rays, through visual observation with a Wilson chamber equipped with Helmholtz coils. For the use of this instrument I am grateful to Dr. F. N. D. Kurie and Mr. H. Paxton. The absorption curve is shown in Fig. 1. The beta and gamma-rays are both evident, the latter about one-twentieth as strong as the former, with no absorber. According to Feather's rule,[5] the energy of the electrons, as determined from the maximum range of 0.05 cm of aluminum, is about 0.4 MEV.

Although these results favored the hypothesis of the creation of Ni^{63}, it was felt desirable to use a test that would be more specific for nickel than merely precipitating its hydroxide. In collaboration with Mr. Philip Abelson further chemical analysis has been carried on with a third sample of filings. The result has been to

[4] Oppenheimer and Phillips, Phys. Rev. **48**, 500 (1935).

[5] Feather, Phys. Rev. **35**, 1559 (1930).

shake our faith in the Ni^{63} supposition and to suggest that possibly the reaction is

$$_{29}Cu^{65}+{}_{1}H^{2}\rightarrow{}_{26}Fe^{59}+{}_{2}He^{4}+{}_{2}He^{4}$$

$$_{26}Fe^{59}\rightarrow{}_{27}Co^{59}+e^{-}.$$

However, the analysis is still very inconclusive with regard to both hypotheses and more work must be carried on. It is quite possible that the activity is due to some unknown impurity in the commercial copper. The Ni^{63} interpretation is also improbable on other grounds: the production[6] of an activity of half-life 3 hours$\pm$10 minutes when nickel is bombarded with slow neutrons. If this latter radiation is of electrons, it is very probably due to the production of radio Ni^{63} through neutron capture by Ni^{62} (present to 3.8 percent abundance), although a similar capture by Ni^{64} (0.9 percent) to form electron emitting radio Ni^{65} must not be overlooked. On the other hand, if the 3 hours period is due to positrons, it is probably due to the formation of radio Ni^{59} out of Ni^{58}, of 68.1 percent abundance.

The longer range of the 130 days' activity and the presence of a gamma-ray are sufficient to distinguish it from the 3 months activity observed by McMillan[7] in deuteron activated brass and molybdenum.

Zinc

The bombardment of zinc for 2 hours with 3.5 microamperes of 3.2 MEV deuterons yields[8] a

[6] Rotblat, Nature **136**, 515 (1935); Naidu, Nature **137**, 578 (1936).

[7] McMillan, Phys. Rev. **49**, 876 (1936).

[8] Presented before the Physical Society at Berkeley, Dec. 20, 1935.

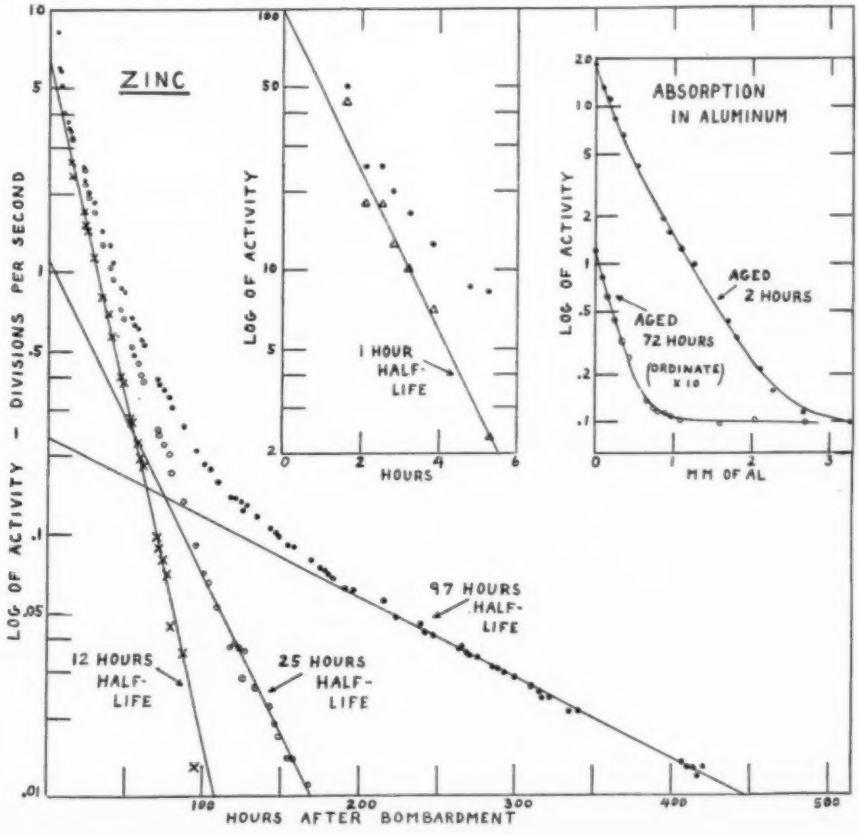

FIG. 2.

radioactivity of which the decay curve is shown in Fig. 2. The longest period, followed for about two half-lives, shows a half-life of 97 ± 10 hours. Subtraction of this activity from the experimental readings gives the open circles of the figure, in which a definite curvature precludes the possibility of but a single period. It is feasible to fit a 25 ± 2 hour line to the later points and on subtraction of this, the earlier readings are seen to fall on a fairly well established activity of 12 ± 1 hours half-life. The insert reveals an additional radiation of 1 ± 0.3 hours half-life. The thick target yields, computed for equilibrium by correcting for the finite length of the exposure, are as follows:

Half-life	Yield (H^2 per active atom)
97 ± 10 hours (negative electrons)	1.2×10^8
25 ± 2 hours (negative electrons)	1.5×10^8
12 ± 1 hours (negative electrons)	0.5×10^8
1 ± 0.3 hours (? ?)	0.2×10^8

The sign of the charges were determined from visual examination with a cloud chamber in a magnetic field. Absorption curves taken 2 hours and 72 hours after activation, are shown in Fig. 2, and indicate at least one gamma-ray as well as a complex of electron groups.

The stable isotopes of copper, zinc, gallium and germanium are:[9]

$_{29}$Cu		63		65				
$_{30}$Zn	64		66	67	68		70	
$_{31}$Ga				69		71		
$_{32}$Ge			70		72	73	74	76

Under neutron bombardment zinc exhibits[10] the 6-minute and 12-hour activities characteristic of radio Cu^{66} and Cu^{64}, while an additional activity with 100 minutes half-life has been observed by McLennan, Grimmet and Read;[11] gallium shows[10] a 20-minute radiation that has been chemically identified as due to a gallium isotope and also a 23-hour activity that is slightly water sensitive. These two periods may probably be assigned to radio Ga^{70} and Ga^{72}.

No usual reaction with deuterons could transmute zinc to an electron-emitting form of gallium; if the observed 25 ± 2-hours period were identified with the 23-hours activity of radio gallium, recourse would have to be made to the type of reaction as yet unestablished for deuterons:

$$_{30}Zn^{68,\,70}+{}_1H^2\rightarrow{}_{31}Ga^{70,\,72}+\text{gamma-ray}$$

$$_{31}Ga^{70,\,72}\rightarrow{}_{32}Ge^{70,\,72}+e^-.$$

(A reaction of this type, but with the proton as projectile, is known[12] in the case of $_6C^{12}+{}_1H^1\rightarrow$radio $_7N^{13}+$gamma.) The only possible electron-emitting isotopes of zinc, Zn^{69} and Zn^{71}, may be called on to explain two of the observed activities. If the one-hour radiation is of positrons, its origin could be in

$$_{30}Zn^{64}+{}_1H^2\rightarrow{}_{30}Zn^{65}+{}_1H^1$$

$$_{30}Zn^{65}\rightarrow{}_{29}Cu^{65}+e^+.$$

or

$$_{30}Zn^{66,\,67}+{}_1H^2\rightarrow{}_{31}Ga^{67,\,68}+{}_0n^1$$

$$_{31}Ga^{67,\,68}\rightarrow{}_{30}Zn^{67,\,68}+e^+.$$

One would be tempted to identify the 12 hour activity with the 12.8-hour period of radio Cu^{64}, through

$$_{30}Zn^{66}+{}_1H^2\rightarrow{}_{29}Cu^{64}+{}_2He^4$$

$$_{29}Cu^{64}\rightarrow{}_{30}Zn^{64}+e^-$$

were it not for the fact that this isotope has recently been shown by Van Voorhis[3] to decay both to stable Zn^{64} by the emission of an electron and also to stable Ni^{64} by emitting a positron. More careful examination must be made to establish whether or not the 12-hour period of zinc does exhibit positrons as well as electrons.

Antimony

A piece of metallic antimony, wrapped in thin aluminum foil, was exposed for 1 hour to 1 microampere of 5 MEV (net) deuterons.[13] The subsequent radioactive decay curve can be analyzed into three well-defined components, as shown in Fig. 3. The half-lives and the thick target saturation yields (corrected for the finite time of exposure) are as follows.

[9] Aston, *Mass Spectra and Isotopes* (1933).
[10] Amaldi, d'Agostino, Fermi, Pontecorvo, Rasetti and Segrè, Proc. Roy. Soc. **A149**, 522 (1935).
[11] McLennan, Grimmet and Read, Nature **135**, 505 (1935).
[12] Cockcroft, Gilbert and Walton, Proc. Roy. Soc. **A148**, 225 (1935).
[13] Presented at the Seattle meeting of the Physical Society, June 18, 1936.

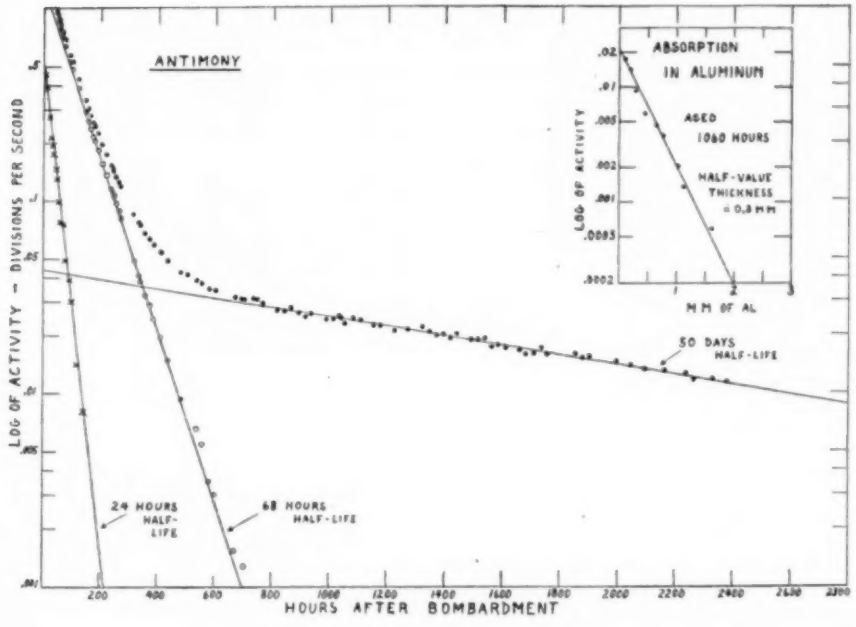

FIG. 3.

Half-life	Yield (H^2 per active atom)
50±4 days (negative electrons)	1.4×10^7
68±2 hours (negative electrons)	0.7×10^7
24±2 hours (negative electrons)	1.2×10^8

A residual activity of about 2.5 minutes, not very well established, is probably due to adsorbed oxygen and nitrogen, which yield radio F^{17} and O^{15} with half-lives of 1 minute 10 seconds and 2 minutes 6 seconds, respectively. Observation with a Wilson chamber in a magnetic field has shown that these three longer period activities are due to negative electrons. An absorption curve in aluminum, taken 44 days after the bombardment when only the longest period remained, is shown in Fig. 3. This apparently indicates a single distribution of electrons, with a half-value thickness of 0.03 cm Al. If there is a gamma-ray present, it is too weak to be detected.

The antimony, tellurium and relevant tin isotopes are[14]

$_{50}$Sn···118	119	120		122	124		
$_{51}$Sb	121		123				
$_{52}$Te 122	123	124	125	126	128	130	

[14] Aston, *Mass Spectra and Isotopes* (1933), and Nature **137**, 613 (1936); Bainbridge and Jordan, Phys. Rev. **49**, 416 (1936).

It is evident that no radio tellurium can be formed by deuteron bombardment of antimony, for deuteron capture, whether followed by neutron emission or not, would yield stable tellurium in every case. The two possibilities involving radioactive antimony are

$$_{51}Sb^{121,\,123}+{}_1H^2\rightarrow{}_{51}Sb^{122,\,124}+{}_1H^1$$

$$_{51}Sb^{122,\,124}\rightarrow{}_{52}Te^{122,\,124}+e^-.$$

Only one possibility exists for the production of radio tin:

$$_{51}Sb^{123}+{}_1H^2\rightarrow{}_{50}Sn^{121}+{}_2He^4$$

$$_{50}Sn^{121}\rightarrow{}_{51}Sb^{121}+e^-.$$

Fermi[10] has observed a 2.5 days half-life activity when antimony is bombarded with neutrons, and has shown the isotope to be one of antimony, necessarily either Sb^{122} or Sb^{124}. It seems reasonable to identify this with the 68-hour activity reported in the present paper. The 50-day and 24-hour periods are then to be assigned to the other radio-antimony isotope and to Sn^{121}, or *vice versa*. No chemical test has yet been made. It is tempting to assign the 24±2-

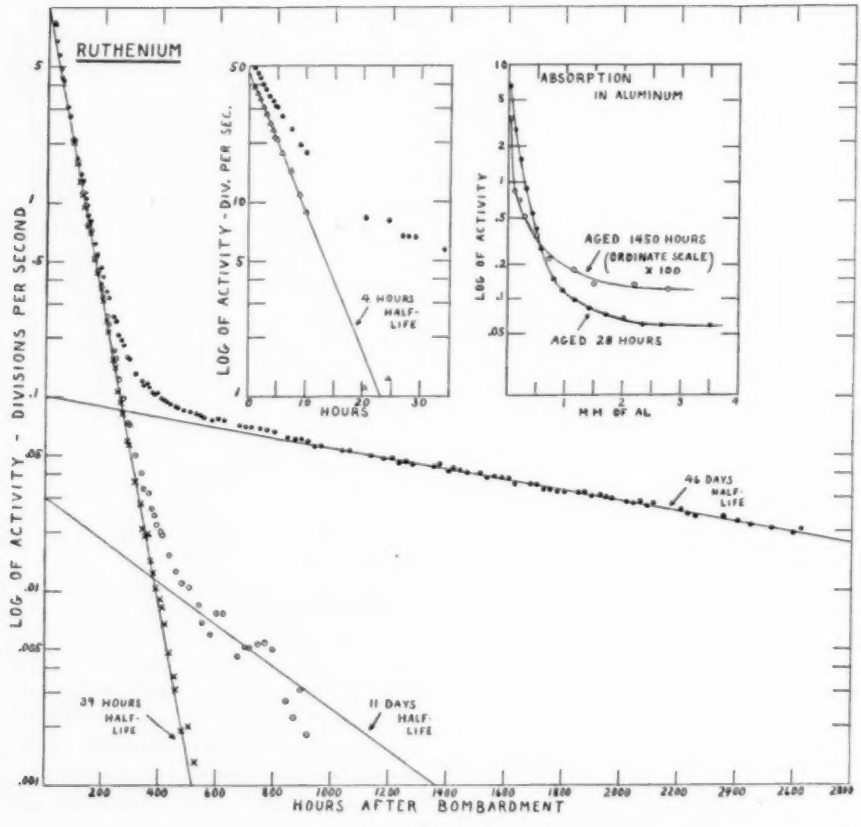

FIG. 4.

hour period to Sn^{121} and to identify it with the 28 ± 2-hour activity found when tin is transmuted to radio tin by deuteron bombardment.[15]

RUTHENIUM

Ruthenium was bombarded[16] for 2 hours with 2.5 microamperes of deuterons at a net energy of 5.3 MEV, the sample being wrapped in very thin aluminum foil to prevent deposition on it, by recoil, of the sodium and phosphorus generally present in the bombardment chamber of the cyclotron. The metal had previously been heated red hot with a blow torch and thoroughly washed, being handled only with tweezers. The radioactive decay curve is shown in Fig. 4.

The longest period, of half-life 46 ± 3 days, appears to be well established, having shown no deviation for almost two half-lives. A shorter period, with half-life 39 ± 1 hours, is apparent from the early data. An intermediate activity, of half-life around 9 to 13 days, may be detected only by the fact that when the 46-day data are subtracted from the original experimental points, the 39-hour activity shows a persistent flattening out as time goes on. These points (open circles in Fig. 4, in the region along the time axis from 400 to 900 hours) are too badly scattered to determine the slope and intensity of this middle activity, but by working backward one can adjust the slope and intensity to such values that when the resulting 11-day period is subtracted, the earlier points fall well along the 39-hour line without any consistent deviation. It is then seen that the 11-day line fits reasonably well along the points from which it could, in theory, be located.

[15] Livingood and Seaborg. See following paper.
[16] Presented before the Physical Society at Seattle, June 18, 1936.

This activity is so weak that whether or not it is included makes no noticeable difference in the half-life of the 39 hours radiation. The insert of Fig. 4, on a more open time scale, reveals a further short period activity with half-life 4 ± 1 hours.

Visual cloud chamber observations, made 20 hours after bombardment, showed only negative electrons and gamma-rays. If the 11-day activity were of positrons, they probably would not have been noticed since the intensity of this component is so weak.

The thick target yields, calculated for infinite exposure, are given below.

Half-life	Yield (H^2 per disintegration)
46 ± 3 days (negative electrons)	2.5×10^{7}
11 ± 2 days ? ?	1×10^{10}
39 ± 1 hours (negative electrons)	0.8×10^{7}
4 ± 1 hours (negative electrons)	1.5×10^{7}

Fig. 4 also exhibits the absorption curves in aluminum, one taken when the sample was 28 hours old, the other at the age of 60 days. The former is complex, as would be expected, since three and possibly four electron activities are contributing, with at least one associated gamma-ray. The rather similar curve obtained when only the 46-day activity is appreciable is somewhat surprising. There would be little physical significance in an analysis of these complex curves into components, since the determination of energy distributions from absorption curves is notoriously erroneous.

The isotopic constitution of ruthenium and of neighboring elements, as given by Aston[9] and Dempster[17] are

${}_{42}$Mo	92	94	95	96	97	98	100	
${}_{43}$Ma								
${}_{44}$Ru	96	98	99	100	101	102	104	
${}_{45}$Rh					103			
${}_{46}$Pd		102		104	105	106	108	110

Masurium has been identified only by its x-ray spectrum, but one of its stable isotopes is surely Ma^{99}, since molybdenum has been activated[10, 18] with slow neutrons to give two periods, of 25 to 30 minutes and 36 hours half-lives. As slow neutron capture usually leads to the formation of a heavier isotope of the element hit, and since Mo^{99} is unknown while Mo^{98} is the most prevalent, it seems likely that one of these periods is due to the production of radio Mo^{99} which emits an electron and becomes stable Ma^{99}.

The possible radioactivities of ruthenium bombarded with deuterons are therefore

$$
\begin{aligned}
{}_{44}Ru^{104}+{}_{1}H^{2}&\rightarrow{}_{44}Ru^{105}+{}_{1}H^{1}\\
{}_{44}Ru^{105}&\rightarrow{}_{45}Rh^{105}+e^{-}\\
{}_{45}Rh^{105}&\rightarrow{}_{46}Pd^{105}+e^{-}\\
{}_{44}Ru^{102}+{}_{1}H^{2}&\rightarrow{}_{44}Ru^{103}+{}_{1}H^{1}\\
{}_{44}Ru^{103}&\rightarrow{}_{45}Rh^{103}+e^{-}\\
{}_{44}Ru^{101,\,104}+{}_{1}H^{2}&\rightarrow{}_{45}Rh^{102,\,105}+{}_{0}n^{1}\\
{}_{45}Rh^{102,\,105}&\rightarrow{}_{46}Pd^{102,\,105}+e^{-}.
\end{aligned}
$$

Reaction similar to the last couplet, but starting from $Ru^{98,\,99,\,100}$, would give rise to positron active rhodium isotopes decaying into stable ruthenium, since there are no stable palladium isotopes to which the rhodium could go by electron emission. If the only stable masurium isotope is Ma^{99}, there are several paths by which radio masurium could be formed:

$$
\begin{aligned}
{}_{44}Ru^{n}+{}_{1}H^{2}&\rightarrow{}_{43}Ma^{n-2}+{}_{2}He^{4}\\
{}_{43}Ma^{n-2}&\rightarrow{}_{44}Ru^{n-2}+e^{-},
\end{aligned}
$$

where $n=98, 100, 102, 104$.

Summing up, there are possible four radio isotopes of masurium, two of rhodium and two of ruthenium which could be formed directly by deuteron bombardment of ruthenium and which would be electron emitters; there are at least three possible positron emitters. As yet, no chemical analysis has been attempted in an endeavor to assign the four observed activities to various of these possibilities.

Kurtschatow, Nemenow and Selenow[19] have reported four activities when ruthenium is bombarded with slow neutrons, with periods of 40 seconds, 100 seconds, 11 hours and 75 hours, the intensity ratios being 100, 100, 10, 40, respectively. (Whether these are the observed

[17] Dempster, Nature **135**, 65 (1935).
[18] McLennan, Grimmet and Read, Nature **135**, 147 (1935).
[19] Kurtschatow, Nemenow and Selenow, Comptes rendus **200**, 2162 (1935).

initial ratios or whether they have been corrected for the finite exposure time is not stated.) Because of the equal intensity of the first two, they suggest as the relevant reaction the double disintegration listed above. These two shortest periods could not have been observed in the present work with deuterons, for observation did not begin until 20 minutes after the exposure was finished. The failure to observe 11-hour and 75-hour activities suggests that these may be due to masurium or molybdenum isotopes accessible with neutron bombardment but not with deuterons. On the other hand, the 75-hour period might have been deduced erroneously if observations had ceased during the transition interval just before the 46-day activity would have made itself known.

The interpretation of the deuteron induced activities is complicated further by the fact that rhodium, under neutron bombardment yields[10, 20] two periods of half-lives 35 to 44 seconds and 3.8 minutes. One of these must be due to radio Rh^{104} and the other to either radio Ru^{103} or radio Ma^{100}, these three isotopes being formed respectively, by neutron capture, capture plus proton emission, and capture plus alpha-emission.

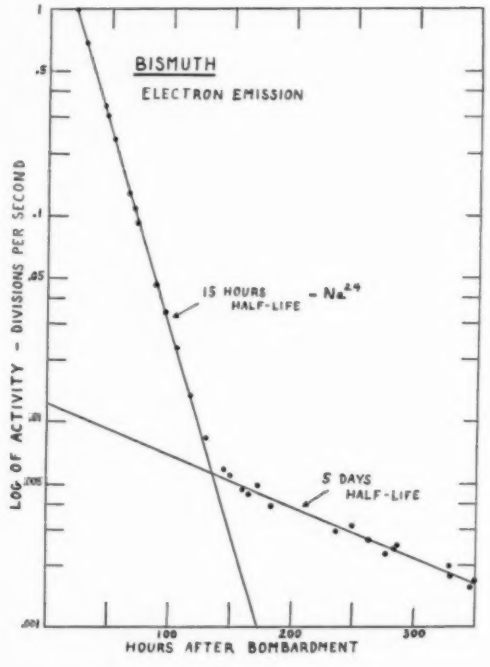

FIG. 5.

BISMUTH[21]

Since it is well known that radium *E*, which emits electrons with a half-life of five days, is isotopic with bismuth, several attempts have been made to convert bismuth into this radioactive form by neutron bombardment, the expected reaction being

$$_{83}Bi^{209} + {}_0n^1 \rightarrow {}_{83}Bi^{210}(\text{Ra E})$$

$$_{83}Bi^{210} \rightarrow {}_{84}Po^{210} + e^-.$$

Fermi and his collaborators,[10] and McLennan, Grimmet and Read[11] have found no detectable activity after such an attempt. Sosnowski[22] has reported an electron activity with a half-life of about 1 hour, and since a chemical analysis showed no radioactive thallium or lead, concluded that a bismuth isotope must be responsible and hence that the synthetic Ra E must have a different internal arrangement of its constituent parts than the natural variety, because of the lack of agreement in the decay periods. Subsequently, Preiswerk and von Halban[23] using a much stronger source of neutrons (1200 mc of Rn+Be and 300 mc of Rn+B) have not confirmed Sosnowski's findings. More recently Andersen[24] has reported no activity in bismuth after neutron bombardment.

Following the successful attempt of Cork and Lawrence[25] to produce disintegrations in platinum by deuteron bombardment in the neighborhood of 5 MEV, it was felt that the available deuteron energy was perhaps sufficient to effect a transmutation in bismuth, through the Oppenheimer-Phillips[4] type of reaction

$$_{83}Bi^{209} + {}_1H^2 \rightarrow {}_{83}Bi^{210}(\text{Ra E}) + {}_1H^1.$$

It was hoped that the almost universal negative result with neutrons was due to a relative insuf-

[20] Dopel, Physik. Zeits. **37**, 96 (1936).
[21] Presented before the Washington meeting of the Physical Society, May 2, 1936.
[22] Sosnowski, Comptes rendus **200**, 1027 (1935).
[23] Preiswerk and von Halban, Comptes rendus **201**, 722 (1935).
[24] Andersen, Nature **137**, 457 (1936).
[25] Cork and Lawrence, Phys. Rev. **49**, 788 (1936).

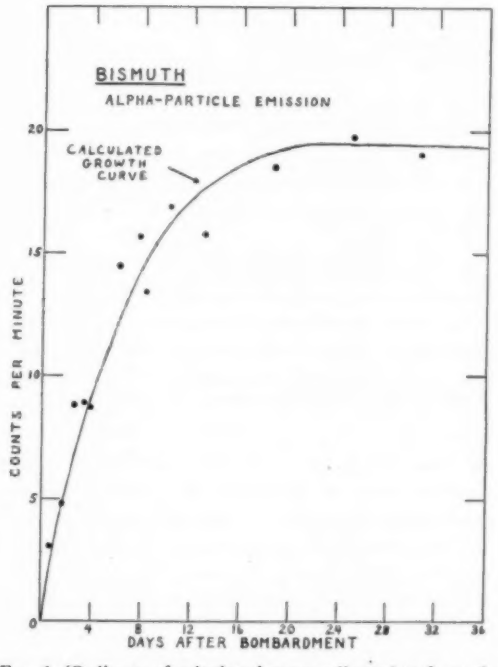

FIG. 6. (Ordinate of calculated curve adjusted to fit at the maximum.)

ficiency of their numbers and that the much greater bombarding currents of deuterons might give a detectable effect.

To prevent its melting during the exposure, a thick layer of bismuth was soldered to a heavy copper plate; this was wrapped in aluminum foil in an effort to prevent contamination with radio sodium present in the bombarding chamber of the cylotron due to a recent preparation of this material. An exposure of 4 hours to 1.2 microamperes of deuterons with a net energy of 4.4 MEV was made, and the subsequent radioactivity observed with an electroscope. The decay curve is shown in Fig. 5. In spite of the precautions to avoid it, a very strong activity with the 15-hour half-life of radio sodium was present, and only after 150 hours (when the net activity was about equal to the background) did a departure from this period occur. The following feeble activity decayed at a rate which was quite consistent with the 5 days half-life of Ra E. By correcting for the time of exposure, the equilibrium thick target yield was found to be 2×10^9 deuterons per active nucleus.

If the manner of formation of this isotope is immaterial to its subsequent behavior, then a confirmatory test of its production would be the detection of alpha-particles with the range of 3.9 cm of air characteristic of polonium, through the natural decay of this into lead:

$$_{84}Po^{210}\rightarrow{}_{82}Pb^{206}+{}_{2}He^{4}.$$

Furthermore, as the Ra E is gradually converted into Po, the alpha-particle activity of the latter should first increase with time up to a maximum value and then die away with the 140 days half-life of natural polonium. The well-known theory of radioactive growth and decay shows that this time of maximum activity, after the preparation of the parent substance, is given by

$$t_{\max}=\frac{1}{\lambda_2-\lambda_1}\log_e\frac{\lambda_2}{\lambda_1},$$

where λ_1 and λ_2 are the decay constants ($\lambda=0.693/$ half-life) of the parent and product. For the case of Po growing in fresh Ra E, this time works out as 23 days.

Consequently, a search for alpha-particles was made with a linear amplifier, commencing on the day after bombardment. During the following two weeks counts greater than background were obtained on nine days, but the greatest net activity was only 1.5 alpha-particles per minute and no consistent rise in activity was noticeable. (The background was taken by replacing the irradiated bismuth with another sample from the same supply and mounted on copper in an identical manner, in order to eliminate any possible natural radioactive contamination.)

In an endeavor to strengthen this activity, if it were genuine, a second bombardment was made, for a total of 13 microampere hours at 5.4 MEV, and to further increase the yield, the aluminum foil wrapper was omitted. The resulting 5-day period of Ra E was completely masked by the 15 hours radio sodium and 14.5 days radio phosphorus contamination activities, but the alpha-particle emission was established as genuine from the outset. The growth curve is indicated in Fig. 6, and is seen to follow the theoretical curve not too badly, a maximum being reached in approximately 3 weeks. Since the calculation of this interval involves the 140-

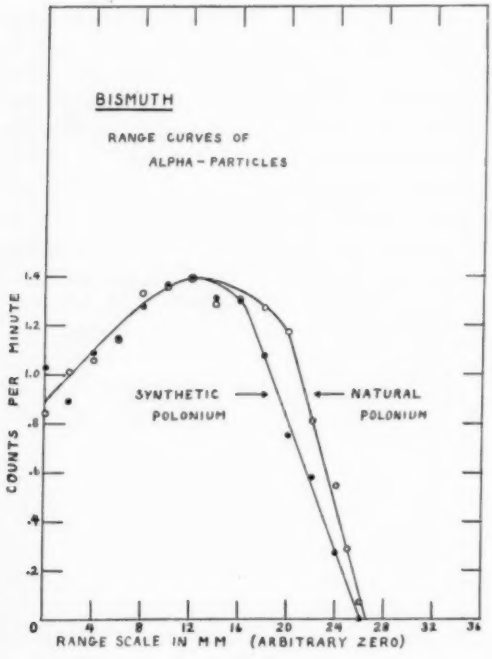

FIG. 7.

day half-life of polonium, it was not felt necessary to establish this period by direct continued observation.

After the attainment of this very nearly constant yield of the maximum activity, a measurement of the range of the alpha-particles was made, not on an absolute basis, but by comparison with that of the alphas from natural polonium deposited onto a silver plate, the two samples being alternately attached to a frame mounted on a micrometer screw and counts being taken at varying distance from the amplifier. The resulting curves are shown in Fig. 7, after a geometrical correction has been made for change in solid angle with distance. The scale of ordinates for the much stronger natural sample has been reduced to a fit at the maximum activity, to facilitate comparison. The extrapolated ranges are seen to agree to within 0.5 mm. which is as good as could be expected with the simple procedure used.

If the chance of transmutation were markedly increased for particular deuteron energies, the range curve would show a series of steps, corresponding to the emission of alpha-particles from layers more densely populated with active atoms at particular distances below the surface. Such a resonance phenomenon with deuterons has been found by Cork and Lawrence[25] in the transmutation of platinum into radio iridium, wherein the deuteron is captured and an alpha-particle emitted. On the other hand, the observed smooth range curve, of somewhat lesser slope than that of the natural particles, indicates the emission of alphas in gradually decreasing numbers at greater depths below the surface; this is consistent with the postulated Oppenheimer-Phillips type of disintegration, the chance of the deuteron being split, into a repelled proton and a captured neutron, diminishing with reduced deuteron energy.

ACKNOWLEDGMENTS

It is a pleasure to acknowledge the cooperation and friendship of the other members of the Laboratory staff, and to express our gratitude to the Chemical Foundation, the Research Corporation and the Josiah Macy, Jr. Foundation for their continued support.

Deuteron-Induced Radioactivity in Tin

J. J. LIVINGOOD, *Radiation Laboratory, University of California*
AND
GLENN SEABORG, *Chemistry Department, University of California*

(Received June 29, 1936)

Tin has been bombarded with 5 MEV deuterons and chemically analyzed for transmutation into radioactive indium, tin and antimony isotopes. The indium fraction exhibits a strong electron emission of 26±2 hours' half-life and an extremely weak activity of undetermined sign and with half-life probably several months. The tin precipitate emits an intense electron group with half-life 28±2 hours and a weak activity also of several months period. Two antimony isotopes are formed with half-lives of 13.3±1 hours and 112±30 days. The former gives evidence of being a branching decay, both electrons and positrons being observed; the sign of the longer period has not been determined. Short period activities from bombarded tin are of 12±2 minutes' and 45±5 minutes' half-life. Absorption curves in aluminum are given and the possible transmutations that are responsible are discussed.

TIN was bombarded for 3 hours with 3.5 microamperes of 5.2 MEV deuterons produced in the cyclotron of Lawrence and Livingston.[1] A chemical separation into fractions of indium ($Z=49$), tin ($Z=50$) and antimony ($Z=51$) was performed in the following manner.

The irradiated tin, plus a little indium and antimony, was dissolved in HCl with a few crystals of potassium chlorate, and the acidity adjusted to about 2 normal. H_2S was bubbled through the hot solution and a precipitate of Sb_2S_5 filtered off. This precipitate was redissolved in HCl plus $KClO_3$, and into the solution a piece of tin foil was placed. The tin replaced the antimony ions from solution and black metallic antimony was plated out on the foil. Through the original filtrate, containing chlorides of tin and indium, H_2S was again passed while the solution was hot, to insure the complete removal of antimony. The H_2S was then boiled off and NaOH added until the $Sn(OH)_4$ which was precipitated was just redissolved; the white $In(OH)_3$ precipitate was filtered off, washed, redissolved in HCl and reprecipitated with NaOH. The previous filtrate was adjusted to 1 normal HCl concentration and yellow SnS_2 precipitated with H_2S. The remaining solution was made alkaline and through it H_2S was bubbled; the absence of a precipitate indicated that indium had been completely removed previously. The observed radioactivities of these three fractions, as determined with a quartz fiber electroscope, are shown in Figs. 1, 2, and 3.

[1] Lawrence and Livingston, Phys. Rev. **45**, 608 (1934).

INDIUM FRACTION

The indium precipitate exhibits three activities; a very intense 26±2 hours' half-life, the 14.5-day radiation of radio phosphorus contamination, and an extremely feeble activity as yet insufficiently well established to permit an estimate of its period, but the half-life must be at least several months. (In computing the life of the 26-hour activity this extremely weak component has been neglected. The errors here given are generous limits of error, obtained by inspection of the curves.) Visual observations with a Wilson chamber in a magnetic field made 10 and 26 hours after activation, respectively, in two entirely separate bombardments and analyses, showed only negative electrons and gamma-rays, which are to be ascribed to the 26 hours' component, for the several months' activity was far too weak to contribute to the observed tracks. (We are indebted to Dr. F. N. D. Kurie and Mr. H. Paxton for the use of this instrument.) The thick target saturation yields, corrected for the finite length of exposure, are as follows:

Half-life	Yield (H^3 per active atom)
26±2 hours (negative electrons)	4.0×10^7
Several months (? ?)	—

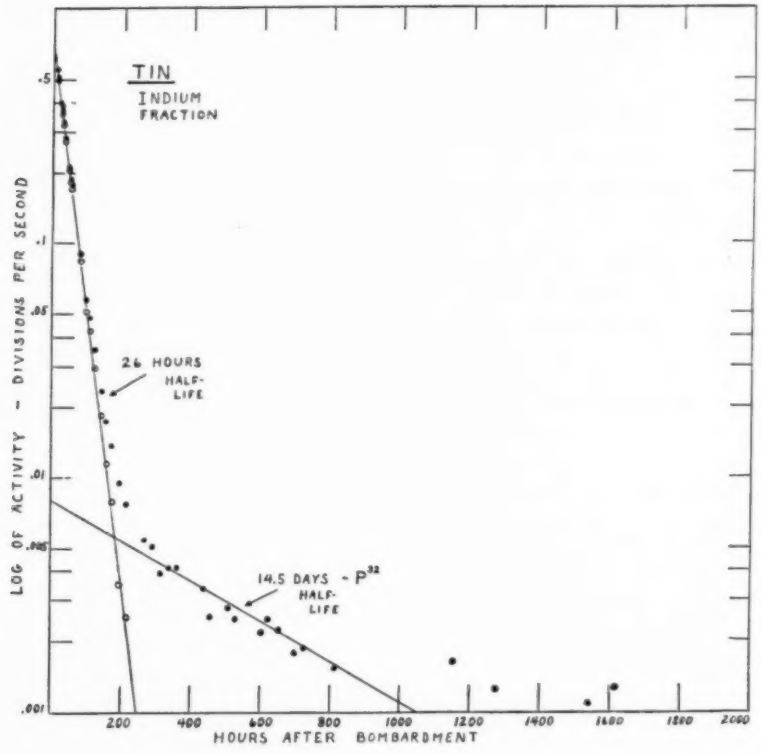

FIG. 1.

The isotopes of tin and neighboring elements are[2]

$_{49}$In			113		115						
$_{50}$Sn	112	114	115	116	117	118	119	120		122	124
$_{51}$Sb							121		123		

It is therefore apparent that a number of possibilities exist for the formation of electron-emitting isotopes of indium from the bombardment of tin with deuterons:

$$_{50}\mathrm{Sn}^{n}+{}_{1}\mathrm{H}^{2}\rightarrow{}_{49}\mathrm{In}^{n-2}+{}_{2}\mathrm{He}^{4}$$

$$_{49}\mathrm{In}^{n-2}\rightarrow{}_{50}\mathrm{Sn}^{n-2}+e^{-},$$

where $n=114, 116, 118, 119, 120, 122, 124$. The first or fourth of these possibilities, leading to radio In^{112} or In^{117}, seem the most likely origin of the 26 hours' activity, since the higher isotopes would be unreasonably far removed from any stable neighbors, while radio In^{114} and In^{116} have already been assigned to the 13 seconds and 54 minutes activities found when indium is bombarded with slow neutrons;[3] a 3.5 hours' half-life initiated with fast neutrons[4] can be ascribed to radio Cd^{115}, which Bainbridge and Jordan[2] have shown does not exist as a stable isotope. If the several months' activity should turn out to be a positron emitter, a possible source could be radio In^{112}, formed as above but decaying to stable $_{48}\mathrm{Cd}^{112}$.

TIN FRACTION

The tin precipitate shows a strong activity of 28 ± 2 hours' half-life, the 14.5-days contamination of radio phosphorous and a further weak activity the half-life of which is as yet undetermined but must be several months. The thick

[2] Aston, *Mass Spectra and Isotopes* (1933); Nature **137**, 613 (1936); Blewett and Sampson, Phys. Rev. **49**, 778 (1936); Bainbridge and Jordan, Phys. Rev. **49**, 416 (1936).

[3] Amaldi, d'Agostino, Fermi, Pontecorvo, Rasetti, Segrè, Proc. Roy. Soc. **A149**, 522 (1935).

[4] Szilard and Chalmers, Nature **135**, 98 (1935).

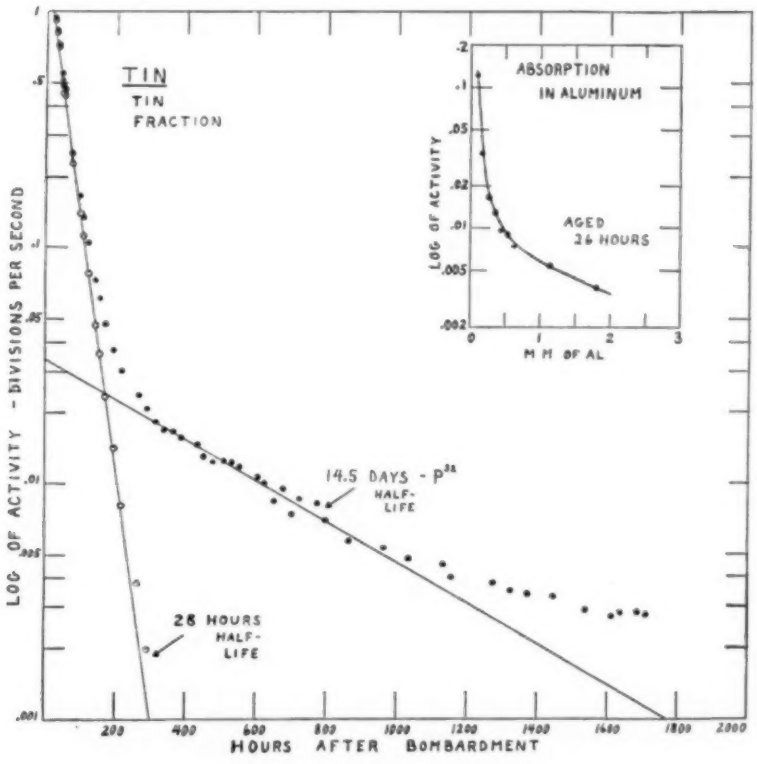

FIG. 2.

target yields, again corrected to infinite exposure, are:

Half-life		Yield (H^3 per active atom)
28±2 hours	(negative electrons)	1.5×10^7
Several months	(? ?)	—

The electron nature of the shorter period has been observed with a cloud chamber.

The separation of tin from indium is reputedly difficult, and the similarity of the activities found in the two fractions suggests that the separation has been incomplete. If so, it is more likely that the tin precipitate should contain a contamination of indium than *vice versa*. On the other hand, the ratio of the initial intensities of the tin to indium precipitates was 2.3 to 1 in one determination, and 2.5 to 1 in a second entirely separate bombardment and chemical analysis; this variation of only 10 percent argues against the supposition of incomplete separation. If one assumes that the activities are genuinely due to tin isotopes, an explanation can be found in the disintegrations[5]

$$_{50}Sn^{120,\ 122}+{}_1H^2\rightarrow{}_{50}Sn^{121,\ 123}+{}_1H^1$$

$$_{50}Sn^{121,\ 123}\rightarrow{}_{51}Sb^{121,\ 123}+e^-.$$

Whether positrons or electrons are emitted during the many months' decay is not known; if the former, the only possibility is

$$_{50}Sn^{112}+{}_1H^2\rightarrow{}_{50}Sn^{113}+{}_1H^1$$

$$_{50}Sn^{113}\rightarrow{}_{49}In^{113}+e^+.$$

The scarcity of Sn^{112} (1 percent) can be used as an argument either for or against this explanation of the very weak observed activity.

[5] It is tempting to choose the first alternative for the 28 hours' activity and to identify it with a 24±2 hours' activity found by Livingood (see previous paper in this issue) when antimony is bombarded with deuterons, this latter disintegration yielding radio Sn^{121} through

$$_{51}Sb^{123}+{}_1H^2\rightarrow{}_{50}Sn^{121}+{}_2He^4$$
$$_{50}Sn^{121}\rightarrow{}_{51}Sb^{121}+e^-.$$

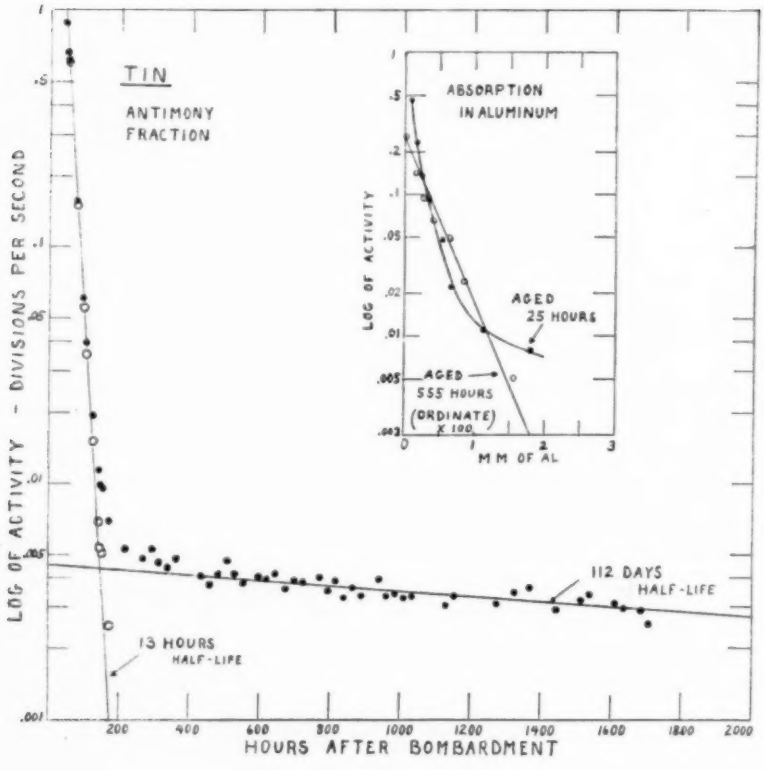

FIG. 3.

These speculations on the origins of the activities found in the tin precipitate are complicated by the recent announcement of Naidu[6] that tin under slow neutron bombardment yields radiations with half-lives of 8 ± 2 minutes and 18 ± 2 minutes. The necessity for slow neutrons implies their simple capture and the formation of radio tin; if the interpretations given above are correct, there are no radio isotopes of tin available to explain Naidu's work. The production of radio Sn^{125} might be invoked, since it would result in two successive electron emissions to radio Sb^{125} and thence to stable Te^{125}, except that an initial increase in activity in the longer period should be observed if it involved the second of the two transformations, which has not been reported, whereas only the longer period would be observed if it were the first disintegration since the atoms of short period would decay as rapidly as they were formed. Furthermore, the existence of Sn^{125} as a stable isotope is suggested below, to explain other phenomena. Possible explanations may be that Naidu's activities do not really require slow neutrons and hence may be due to radio cadmium or indium, or else that the radiations reported in the present paper are really due to indium contamination.

ANTIMONY FRACTION

The antimony fraction shows an initially strong activity with 13.3 ± 1.0 hours' half-life, followed by a weak radiation with half-life 112 ± 30 days. (This latter activity has been reported in a preliminary announcement[7] to be of 52 days life, but continued measurements have doubled this early estimate. The particular value chosen makes no appreciable difference in the

[6] Naidu, Nature **137**, 578 (1936).

[7] Livingood, Seattle Meeting of the Physical Society, June 18, 1936.

value of the 13-hour period.) Because of the plating-out in the chemical procedure, no radio phosphorous contamination was brought down with the antimony. The thick target equilibrium yields are

Half-life	Yield (H^2 per active atom)
13.3±1 hour (electrons and positrons)	5.6×10^6
112±30 days (? ?)	3.0×10^6

Both electrons and positrons were observed by means of a Wilson chamber in a magnetic field at 10 and 26 hours after activation, respectively, in two entirely separate bombardments and subsequent analyses, the electrons predominating by a factor of from 5 to 10. Since the 112-day activity was so very weak, it could not possibly have contributed to any of the observed tracks, and one might invoke the possibility that the 13-hour activity embraces a branching disintegration of both positrons and electrons. Such a case among the artificially radioactive elements has recently been reported by Van Voorhis,[8] with radio Cu^{64} disintegrating to Ni^{64} by the emission of positrons and to Zn^{64} by the emission of electrons, both with the same half-life of 12.8 hours. It seems impossible that the 13-hour activity reported here can be due to a contamination of copper because of the very strong intensity and because of the lack of a carrier for the copper through the chemical separation; furthermore, other elements mounted and bombarded in an identical manner have not exhibited this period.

Fermi[3] has established that either radio Sb^{122} or Sb^{124} disintegrates with a 2.5-day half-life, while Livingood[9] has presented evidence for either a 50±4 days or a 24±2 hours' electron activity to be associated with the other of these isotopes. The origin of the branching decay of the 13-hour activity can then only be found in

$$_{50}Sn^{119,\,124}+{}_1H^2\rightarrow{}_{51}Sb^{120,\,125}+{}_0n^1$$

$$_{51}Sb^{120,\,125}\rightarrow{}_{50}Sn^{120,\,125}+e^+$$

$$_{51}Sb^{120,\,125}\rightarrow{}_{52}Te^{120,\,125}+e^-.$$

These two possibilities require the postulated existence of either stable Sn^{125} or stable Te^{120}, neither of which are so far known.*

The sign of charge in the 112-day activity has not been determined, but whatever its nature, an explanation can be found in the remaining alternative of the above pair of reactions.

Tin Not Chemically Analyzed

Tin given a short bombardment with deuterons and examined without chemical analysis shows two short periods with half-lives of 12±2 minutes and 45±5 minutes. The signs of the charges have not been determined. The first of these might be taken as associated with Naidu's 8±2-minute activity or else ascribed to the 10.3-minute positron activity of radio N^{13} formed from carbon contamination. It is possible that the 45 minutes' radiation should be identified with the known 54 minutes' activity of either In^{114} or In^{116}, by the disintegration

$$_{50}Sn^{116,\,118}+{}_1H^2\rightarrow{}_{49}In^{114,\,116}+{}_2He^4$$

$$_{49}In^{114,\,116}\rightarrow{}_{50}Sn^{114,\,116}+e^-.$$

Acknowledgments

These experiments have been made possible by the continued support of the Research Corporation, the Chemical Foundation and the Josiah Macy, Jr. Foundation.

[8] Van Voorhis, Phys. Rev. **49**, 876 (1936).
[9] Livingood. See preceding paper.

*_Note added in proof:_ The existence of stable Te^{120} has been recently established by Dempster (Phys. Rev. **51**, 186 (1936)).

Lifetimes of Potassium Doublets λ4047–4 and λ3447–6

DAVID SINCLAIR AND HAROLD W. WEBB, *Columbia University*

(Received July 2, 1936)

The lifetimes of the potassium doublets λ4047–4 and λ3447–6 were measured by the a.c. excitation method previously described. A sodium-hydride vacuum photo-cell of special design was used to measure the radiation from a potassium cell containing a hot cathode and two anodes. Measurements were made throughout a range of vapor pressures from 4×10^{-6} mm to 10^{-3} mm. The lifetime of λ4047–4 was found to be 3.79×10^{-7} sec., the lifetime of λ3447–6 to be 8.50×10^{-7} sec., with an estimated precision of one percent. It was shown that the radiation emitted after electron excitation followed a simple exponential law. No change in the measured value of the lifetime was found for either of the doublets throughout the whole pressure range studied. This could be accounted for by the assumption that only 10 percent of the absorbed λ4047–4 is re-emitted at the same wave-length, and similarly for λ3447–6. Measurements made of the variation of the emission with pressure, and of the absorption, were consistent with this assumption.

INTRODUCTION

THE first doublet of the principal series of the alkali metals has been extensively studied and the lifetimes and f values of Li, Na, K and Cs have been measured by absorption and magneto-rotation methods. No direct measurements of the lifetimes of the second or higher doublets have hitherto been made. The ratios of the f values for the first and second doublets have been determined,[1] but since there is more than one transition from the upper level of the second doublet, its lifetime cannot be derived from its f value.

In the present investigation a direct determination was made of the lifetime of the second and third doublets of potassium, each doublet being treated as a single line. The method of measurement was that developed in this laboratory.[2] Potassium vapor at low pressure was excited by electron impact, with a pure sinusoidal exciting voltage applied in such a way that radiation was emitted during the positive half-cycle only. The radiation was measured by a photo-cell to which the same voltage was applied in phase. At low frequency the radiation was all emitted during the positive half-cycle and the photo-current was a maximum. As the frequency was increased, the total excitation being held constant, the photo-current decreased due to the persistence of the radiation, some of which reached the photo-cell during the negative half-cycle. From the relation between the photo-current and the frequency, the lifetime, τ, was calculated as previously described.[3]

APPARATUS

The apparatus is shown schematically in Fig. 1. The potassium excitation cell was a Pyrex tube, containing electrodes C, G, and G'. C was an equipotential hot cathode, consisting of a nickel cylinder 3 cm long and 6.5 mm in diameter, with an internal tungsten heater. The accelerating grid G was a coaxial half cylinder of 9 mm radius. It was made of 1.6 mm mesh nickel gauze and placed in front of the cathode. The electrode G' was a nickel gauze cylinder 2.6 cm in diameter fitted against the wall of the tube, with a curved nickel sheet partition 5 mm in back of C.

The vapor pressure of the potassium in the excitation cell was controlled by the temperature of a small side tube containing the excess potassium. This was immersed in melted Woods metal in a brass cup, the lower end of which was in an oil bath thermostatically controlled to $\frac{1}{4}$°C. The rest of the cell was superheated 50°C above the temperature of the oil bath. The values of the vapor pressure given in this paper are those computed from the temperature of the oil bath, without any correction.

The vacuum photo-cell was a Pyrex tube 4 cm in diameter containing electrodes P, H, and W. The sodium-covered electrode P, a nickel

[1] A. C. G. Mitchell and M. W. Zemansky, *Resonance Radiation and Excited Atoms*, pp. 146–151; S. A. Korff and G. Breit, Rev. Mod. Phys. **3**, 499–501 (1932).

[2] H. W. Webb, Phys. Rev. **24**, 113 (1924); F. G. Slack, Phys. Rev. **28**, 1 (1926); H. W. Webb and H. A. Messenger, Phys. Rev. **33**, 319 (1929); R. H. Randall, Phys. Rev. **35**, 1161 (1930); P. H. Garrett, Phys. Rev. **40**, 779 (1932).

[3] Slack, reference 2, p. 2.

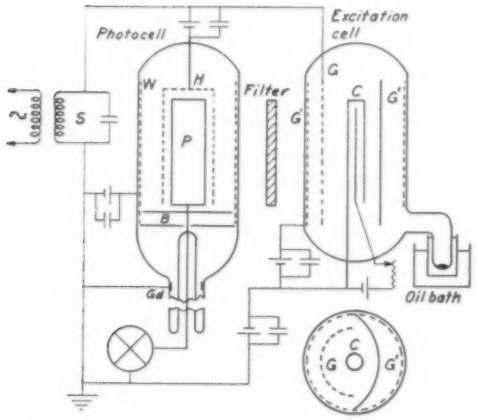

FIG. 1. Schematic diagram of apparatus and electrical circuits.

cylinder 13 mm in diameter and 5 cm long, was supported centrally on a re-entrant glass tube, made 17 cm long to increase the electrical leakage path. As a further precaution, an internal guard ring, *Gd*, which was held at ground potential, was fitted to the walls of the cell. In addition, nickel disk baffles, *B*, prevented evaporation of sodium into the re-entrant tube. With this design, the resistance between *P* and the rest of the tube was about 10^{16} ohms. The sodium-covered electrode H was a coaxial nickel gauze cylinder 19 mm in diameter. Fitted against the wall was a cylindrical electrode *W* of sheet nickel, with a gauze window to allow the passage of radiation. A photo-sensitive sodium-hydride surface was formed on *P* and *H* according to the method given by Nottingham.[4]

In the construction of each cell all metal parts were pre-outgassed and the cells were baked out at 500°C for several hours before distilling in the alkali metals. A liquid-air trap prevented the entrance of mercury into the cells, which were pumped out to a pressure of about 10^{-5} mm and sealed off when cold.

The photo-cell was placed 5 cm from the excitation cell. Between them was a heat insulating partition consisting of alternate layers of wood and metal, except for a window 6 cm long by 3 cm wide. A large part of the heat radiated through this window was absorbed by the filters described below. The temperature of the photo-cell did not exceed 25°C, at which temperature the sodium had little tendency to evaporate and destroy the insulation.

In all observations Corning glass filters were used between the excitation cell and the photo-cell to isolate the doublet under observation; filter No. 511, 1½ mm thick, and No. 428, 3½ mm thick for λ4047–4; and No. 584, 5 mm thick for λ3447–6. Photographs of an iron spark taken through the filters showed that the λ4047–4 filter was opaque to all subordinate series lines and the radiation from the hot cathode, and allowed the passage of one percent of λ3447–4; and that the λ3447–6 filter was opaque to λ4047–4 and allowed the passage of one percent of λ3218–7, the fourth doublet of the principal series. Furthermore, the photo-cell was very insensitive to λ5461 and longer wave-lengths.

D.c. bias voltages were supplied by small dry cells. The a.c. voltage, supplied by vacuum-tube oscillators, was applied to the grids *G* and *H* of the experimental cells by connecting these electrodes to a parallel resonant circuit, *S*, which was loosely coupled to the oscillator. The peak value of this voltage was measured with a vacuum tube voltmeter and could be held constant over the whole range of frequencies used, to within 0.5 percent. For all frequencies the a.c. voltage was shown to be practically free from harmonics by tuning the resonant circuit to the first and second harmonics, for which the voltage was less than 0.5 percent of the voltage when tuned to the fundamental frequency.

The photo-currents were measured with a Compton quadrant electrometer of about 5000 mm per volt sensitivity. The steady leakage current, about 10^{-16} amperes, amounted to 1 to 10 percent of the true photo-current, which was corrected accordingly.

PROCEDURE AND RESULTS

In the calculation of the lifetime, τ, from the measurements made with a.c. voltage applied simultaneously to the excitation cell and photo-cell, the d.c. voltage- or static-characteristics of the two cells should be known. The typical excitation curves, Fig. 2, show the relation between the photo-current and the exciting voltage on *G*, the voltage difference between *H*

[4] W. B. Nottingham, J. Frank. Inst. **205**, 637 (1928).

and P, $H-P$, being held constant. The excitation potential $G-C$, was varied between 0 and 7.5 volts. The wall grid potentials $G'-C$ and $W-P$ were held constant at 1.5 and 6.0 volts, respectively. The photo-currents in the two curves are drawn to different scales.

These curves show that λ4047–4 and λ3447–6 appeared at approximately the theoretical voltages for these radiations, 3.1 and 3.6, respectively. The curve for λ4047–4 is practically linear, whereas that for λ3447–6 departs somewhat from a straight line.

The typical photo-cell curves, Fig. 3, show the relation between the photo-current and the voltage $H-P$, the radiation from the excitation cell being held constant. $H-P$ was varied between -5 and 3. The wall grid voltages were the same as given above. The photo-currents in the two curves are drawn to different scales. It will be observed that for negative voltages on the grid, the current never reaches saturation. The voltage for zero current differs in the two curves by about 0.5 volt, due to the difference in the positive and negative photo-currents and the difference in wave-lengths.

Fig. 4 shows typical curves obtained with a.c. voltage applied simultaneously to the excitation cell and the photo-cell. The vapor pressure and other conditions were the same as for the static characteristic curves. The abscissas are the frequencies. The ordinates are the ratios, R, of the photo-current at high frequency to that at 12,000 ~. Such a curve will be referred to below as the $R-f$ curve. The a.c. voltage, which had a peak value of 4.0 volts, was applied in phase to the excitation grid G and the photo-cell grid H. These grids were biased so that the excitation started and the photo-current reversed at the beginning of the positive half-cycle, see Figs. 2 and 3. Since the wall grid G' of the excitation cell was kept 1.5 volts positive with respect to C, all electrons which passed out through G were removed rapidly, thus preventing them from exciting radiation in the negative half-cycle. Similarly the positive potential of 6 volts on the wall grid W of the photo-cell prevented photo-electrons which passed out through H from going back to P in the following half-cycle.

From the experimental observations the life-time, τ, was deduced in a manner similar to that described in the earlier papers[3] on the assumption of a simple exponential decay of the excitation. The excitation, which was confined to the positive half-cycle, was closely given by $A \sin 2\pi ft$ for λ4047–4, and $B \sin 2\pi ft - 0.06C \sin 2\pi 3ft$ for λ3447–6. The radiation emitted as a function of the time was calculated as before. It was conveniently expressed using $t' = t/\tau$ as the time variable and $\psi = 2\pi f\tau$ instead of f, giving a curve depending only on the parameter ψ. For different values of ψ the intensity-time curves were constructed. By multiplying each point on these curves by the ordinate of the photo-cell characteristic corresponding to the simultaneous value of the voltage applied to the grid of the photo-cell, new curves were obtained showing the variation of the photo-current with the time, during one complete cycle. By graphical integration, the average photo-currents were then

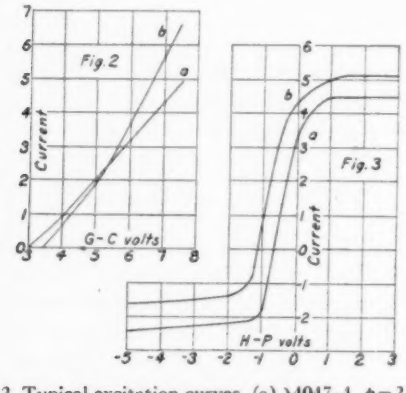

FIG. 2. Typical excitation curves, (a) λ4047–4, $p = 2\times10^{-4}$ mm, (b) λ3447–6, $p = 10^{-3}$ mm.
FIG. 3. Typical photo-cell curves, (a) λ4047–4, $p = 2\times10^{-4}$ mm, (b) λ3447–6, $p = 10^{-3}$ mm.

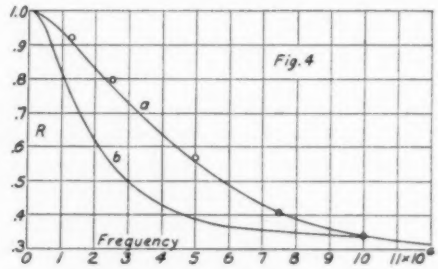

FIG. 4. Typical R–f curves, (a) λ4047–4, $p = 2\times10^{-4}$ mm, (b) λ3447–6, $p = 10^{-3}$ mm.

found for each value of ψ, and an $R-\psi$ curve was constructed. τ was then obtained from the relation $\psi=2\pi f\tau$ by substituting for any given value of R the corresponding values of ψ and f on the $R-\psi$ and $R-f$ curves, respectively. The most precise results were obtained from the curve in the neighborhood of $\psi=1$, and this part of the experimental curve was determined with very great care by taking a large number of observations.

The mean life of λ4047–4 was found to be 3.79×10^{-7} sec., and the mean life of λ3447–6 to be 8.50×10^{-7} sec. with an estimated precision of one percent.

These values were determined from measurements made at $p=2\times10^{-4}$ mm for λ4047–4 and $p=10^{-3}$ mm for λ3447–6. As the effect of absorption and re-emission within the excitation cell is to decrease the rate of decay of the emitted radiation,[5] τ can be determined only from measurements at such low pressures that the effect of this "imprisonment of radiation" is negligible. Experimentally it is sufficient to decrease the pressure until the observed rate of decay no longer increases, this limiting value determining the correct value of τ. In the present measurements no change in the value of the rate of decay was observed over a range of pressures extending from 4×10^{-5} mm to 10^{-2} mm for λ4047–4, and from 5×10^{-4} mm to 10^{-2} mm for λ3447–6. The pressures at which the precise determinations of τ were made were within these limits and were selected to give the best experimental conditions.

A suspected source of error in these measurements was the effect on the rate of decay of the radiation resulting from the population of the 5^2P levels by transitions from higher levels excited by electron impact. In the case of λ4047–4, the next higher level has an energy difference of 0.3 volt. Since the relative contributions of directly excited radiation and that due to the "cascading" depend on the peak voltage, measurements of the decay rate were also made with three other values of the peak voltage: 2, 1, and 0.5. No difference in the values of decay rate was found, indicating that practically only direct excitation was present. Similar tests with λ3447–6 were made with two other values of the peak voltage 2, and 1.5, with similar results. Additional tests were made with other values of the d.c. bias on G and H. These gave the same value of τ.

To check the behavior of the two cells with high frequency impressed, two tests were made. First, a steady potential was impressed on the photo-cell and the same a.c. and d.c. potentials were applied to the excitation cell as were used for the $R-f$ curves. The photo-current was found to be the same for all frequencies used, 10^3 to 2×10^6 cycles, showing that with constant peak voltage the total energy emitted was independent of the frequency. This served also as a test of variation in wave form. In the second test a constant d.c. potential was applied to the excitation cell while the photo-cell was subject to the same potentials as for the $R-f$ curves, and it was found that the photo-current was the same for all frequencies, showing that the form of the photo-cell characteristic was independent of frequency.

As a further check on the method and especially on the assumption that the radiation excited at any instant falls off exponentially, τ was determined by a second method which did not involve knowledge of the photo-cell characteristics. Using a low frequency for which the effect of the persistence of the excited radiation was negligibly small, the conditions under which the $R-f$ curves were taken were reproduced in the following manner. A half-wave rectified sine voltage of 1000~ was applied across two noninductive resistances, r_1 and r in series; and a variable capacity, C, and the excitation cell were connected in parallel across r. Considering the result for one cycle only, we find that for r_1 large with respect to r, and the current through the excitation cell small with respect to the current through r, the voltage across r at any time is given by:

$$E_r=\text{const. } e^{-t/rC}\int_0^t e^{\beta/rC}\sin 2\pi f\beta d\beta$$

for $0<t<\frac{1}{2}f$. When $t>\frac{1}{2}f$ the voltage, E_r, decreases as $e^{-\beta/rC}$. With a linear excitation characteristic the radiation produced is proportional to E_r, and except for the change in the time scale, the relation between radiation and time at the low frequency is the same as that

[5] Webb and Messenger, reference 2, p. 325.

resulting from the persistence of the radiation at high frequency.[6]

Consequently, if we vary C and plot as ordinates, R, the ratios of the photo-current obtained to that for $C=0$, and as abscissas $\tau C\omega/2\pi$, we have a curve identical with the $R-f$ curve except that the abscissas are reduced by a factor equal to τ. The points marked by circles in Fig. 4 for λ4047–4 were obtained by this method using the value of τ already found, 3.79×10^{-7} sec. The agreement is satisfactory, affording a valuable check on the method and the assumption that the radiation decays exponentially.

Owing to the fact that the excitation characteristic for λ3447–6 was not a straight line, the above method could not be used to determine τ for this wave-length.

Discussion

As stated above the measured rate of decay of the radiation for each of the wave-lengths studied was found to be the same for pressures at which the absorption was negligible (10^{-4} mm) as for pressures at which the absorption was 90 percent (10^{-2} mm). If at the higher pressures more than a small fraction of the radiation absorbed were re-emitted at the same wave-length, a marked decrease in the rate of decay of the radiation excited in the mass of vapor should have been observed. Webb and Messenger[5] found that because of this "diffusion of radiation" the rate of decay of the λ2537 radiation from a mass of mercury vapor excited by electron impact varied very nearly inversely as the pressure over a 100-fold pressure range. λ2537 when absorbed is practically all re-emitted at the same wave-length. We conclude therefore that in potassium only a small fraction of λ4047–4 when absorbed is re-emitted at the same wave-length, and similarly for λ3447–6.

An atom excited to the 5^2P level can return to the normal state by three processes: first, by radiation of λ4047–4 (4^2S-5^2P); second, by successive radiation of the lines λ27,215–27,066 (5^2S-5^2P), λ12,523–12,434 (4^2P-5^2S), and λ7699–65 (4^2S-4^2P); third, by successive radiation of the lines λ31,597–31,395 (3^2D-5^2P), λ11,772–11,690 (4^2P-3^2D) and λ7699–65 (4^2S-4^2P). Let α be the ratio of the probability of the direct transition to the sum of the probabilities of the two indirect transitions. From the present measurement a maximum value for α of 1/10 is estimated since a measurable change in the rate of decay would have been observed if more than 10 percent of the radiation incident on the photo-cell were re-emitted radiation of the same wave-length.

This estimate is in agreement with that made from a study of the variation in the intensity of the radiation emitted from the excitation cell as a function of the vapor pressure. The cell was placed close to the photo-cell so that the latter received, in addition to the λ4047–4 radiation excited by electron impact, the major part of that which was absorbed and re-emitted at the same wave-length. As the vapor pressure in the excitation cell was increased the radiation increased, first in direct proportion to the vapor pressure, then at a less rapid rate due to the absorption by the outer layers of vapor; and finally the emitted radiation decreased with increase of vapor pressure. This was as expected since the re-emission at other wave-lengths of energy absorbed as λ4047–4 is equivalent to dissipative absorption. From the relation obtained between the emitted radiation and the vapor pressure and from the absorption coefficient previously determined, a value of α was computed equal to $\frac{1}{4}$. However, owing to the difficulty of estimating the effective thickness of vapor layer and other factors, this determination is subject to large error and can be regarded only as roughly confirming the estimate of α made from the lifetime measurements. For λ3447–6 the lifetime measurements also indicate that α does not exceed the above value.

From a study of the anomalous dispersion, Prokofiew and Gamow[7] found for the ratio of the transition probability of the first doublet to that of the second, for the principal series of potassium, a value of 30.3. From magneto-rotation measurements Weiler[8] obtained for the first doublet $\tau_1=2.7\times10^{-8}$ sec. This is equal to the reciprocal of the transition probability, since for this doublet α is equal to unity. The

[6] Slack, reference 2, p. 8.

[7] W. Prokofiew and G. Gamow, Zeits. f. Physik **44**, 887 (1927).

[8] J. Weiler, Ann. d. Physik **1**, 361 (1929).

experimental value of the lifetime of the second doublet λ4047–4 as found above is $\tau_2 = 3.79 \times 10^{-7}$ sec. This is equal to the product of α and the reciprocal of the transition probability for this doublet, since τ equals the reciprocal of the sum of the probabilities of emission from the upper level. This gives $\alpha = \tau_2/30.3\tau_1 = 0.46$, which is considerably larger than our estimate.

It is interesting to compare this with the value $\alpha = \frac{1}{2}$, obtained for the sodium doublet λ3202–3, by Christensen and Rollefson.[9] They illuminated a bulb containing sodium vapor at a pressure of 10^{-4} mm and measured the relative intensities of λ5890–6 and λ3202–3 emitted at right angles to the illumination, from which they computed α. On the other hand Weiss[10] found α to be about 1/25 by comparing the relative intensities of these same doublets emitted by an arc.

The preceding discussion is based on the assumption that all radiation not directly transmitted is absorbed and re-emitted, the mean time for the process being equal to τ. Coherent scattering has been assumed negligible and the pressures were too low for dissipative absorption by collision. The effect of coherent scattering superposed on absorption would be to give too small a value for α as estimated from the lifetime measurements. On the other hand the effect on the results of Christensen's and Rollefson's[9] experiment would be to give too large a value for α.

[9] C. J. Christensen and G. K. Rollefson, Phys. Rev. **34**, 1157 (1929).

[10] C. Weiss, Ann. d. Physik **1**, 565 (1929).

SEPTEMBER 1, 1936 PHYSICAL REVIEW VOLUME 50

The $^1\Sigma^* - {}^1\Sigma$ Band System of Copper Deuteride

MYRON A. JEPPESEN,* *Department of Physics, Pennsylvania State College*

(Received May 8, 1936)

The copper deuteride bands have been photographed with high dispersion and an analysis is given of the $^1\Sigma^* - {}^1\Sigma$ system. The $Cu^{63}D$ and $Cu^{65}D$ isotopic bands are separated and an independent analysis is given for each. From data obtained for the normal $^1\Sigma$ state, ρ for $Cu^{65}D$ to $Cu^{63}D$ is 0.999503 which agrees with the best mass spectrographic data. A comparison with Heimer and Heimer's CuH analysis gives a value of ρ equal to 0.7131 for $Cu^{63}D$ to $Cu^{63}H$. The electronic isotope displacement of CuD relative to CuH is 19 cm^{-1}.

INTRODUCTION

THE spectrum of CuH has been photographed by several investigators.[1–4] None of these has given a complete analysis of the copper isotopic bands. The purpose of the present investigation was to obtain data for a comparison of the hydride and deuteride spectra, and also to make a rigorous copper isotope analysis. After the experimental work and much of the analysis was finished it was learned that the copper deuteride spectrum had been photographed in another laboratory.[5] Since no mention was made of a copper isotope analysis it appeared worth while to complete the present study.

EXPERIMENTAL

The spectrum was excited in a water-cooled metal arc chamber. Deuterium, produced by the vacuum distillation of heavy water onto powdered zinc, was admitted to the chamber and kept at a pressure of 40 cm of mercury. Following the suggestion of Heimer and Heimer[2] we used an anode of bismuth copper alloy and a cathode of pure copper. The arc chamber was evacuated and refilled with deuterium five or six times during a 24-hour exposure. The arc was run from a 220 volt line and carried a current of approximately 3 amperes.

* From a dissertation submitted in partial fulfillment of the requirements for the Ph.D. degree at the Pennsylvania State College.

[1] Jevons, *Band Spectra of Diatomic Molecules* (1932), p. 300.

[2] A. Heimer and T. Heimer, Zeits. f. Physik **84**, 222 (1933).

[3] T. Heimer, Zeits. f. Physik **95**, 321 (1935).

[4] B. Grundstrom, Zeits. f. Physik **98**, 128 (1935).

[5] T. Heimer, Naturwiss. **23**, 372 (1935).

The plates were taken on a Johns Hopkins University spectrograph, consisting of a 21-foot, 30,000 lines per inch grating in Paschen mounting. The photographs were taken in the first order, which gave a dispersion of about 1.3A/mm. Nearly all the wave numbers given are mean values of measurements of two spectrograms. The wave-lengths should be accurate to within 0.005A.

Analysis

The bands analyzed involve the first four vibrational levels in each of the $^1\Sigma$ and $^1\Sigma^*$ states, the former being the normal state of the CuD molecule. They were located when possible by making use of the published data on CuH and theoretical isotope relations. Other bands were found by application of the combination principle. The rotational analysis was done by the usual methods. There is considerable overlapping of bands causing rather numerous blends. Atomic lines of copper, bismuth, and hydrogen obscure many of the CuD lines.

The resolving power is sufficient to permit a complete analysis of the system under consideration for each of the two molecules, $Cu^{63}D$ and $Cu^{65}D$, the isotopic lines being completely resolved for the bands involving a change in the vibrational quantum number v greater than zero. In other bands resolution is not attained at the lower values of the rotational quantum number J. In Table I are listed the lines identified in twelve different bands with their quantum number assignments. The first entry for a given value of J is for $Cu^{63}D$, the second for $Cu^{65}D$. Where the lines are unresolved there is a single entry.

Derivation of Constants

The well-known analytic least-squares method given by Birge[6] was used in performing the calculations. In order to use lines belonging to transitions between levels having large J values the rotational energy function was carried out to the term involving $(J+\frac{1}{2})^8$, and expressed as

$$F(v, J)=B_v(J+\tfrac{1}{2})^2+D_v(J+\tfrac{1}{2})^4 +F_v(J+\tfrac{1}{2})^6+H_v(J+\tfrac{1}{2})^8. \quad (1)$$

For each level F_v was taken equal to F_e and H_v to H_e. This equation forms the basis for the evaluation of the rotational constants. Taking into account the difference between the finite difference and the derivative in the terms in which this difference is appreciable one obtains for the rotational energy intervals

$$\Delta_2F=4B_v(J+\tfrac{1}{2})+(8D_v+12F_e)(J+\tfrac{1}{2}) +(8D_v+40F_e)(J+\tfrac{1}{2})^3 +12F_e(J+\tfrac{1}{2})^5+16H_e(J+\tfrac{1}{2})^7. \quad (2)$$

Δ_2F^* is now defined as follows:

$$\Delta_2F^*=\Delta_2F-(8D_v+12F_e)(J+\tfrac{1}{2}) -(8D_v+40F_e)(J+\tfrac{1}{2})^3-12F_e(J+\tfrac{1}{2})^5 -16H_e(J+\tfrac{1}{2})^7=4B_v(J+\tfrac{1}{2}). \quad (3)$$

D_v, F_e, and H_e are calculated from the theoretical relations given by Jevons,[1] hence Δ_2F^* may be determined directly from the observed rotational intervals. B_v then occurs as the slope of a linear least squares equation with $4(J+\frac{1}{2})$ as the independent and Δ_2F^* as the dependent variable.

The work of Almy and Irwin[7] on the $^1\Sigma-{}^1\Sigma$ system of Li_2 indicates that the accuracy of constants evaluated from lines of large rotational quantum number may be open to question. The close agreement between the values of Δ_2F^* determined directly from the data and those calculated by substituting the least-squares values of B_v in Eq. (3) indicates that in the normal $^1\Sigma$ state the use of lines having values of J as great as 45 is justified.

In the $^1\Sigma^*$ state it was found that lines of large rotational quantum number could not be used. Beginning at approximately $J=20$ the calculated B_v's for a given level show a gradual decrease. Apparently D_v in the rotational energy function should have a larger absolute value than that given by the theoretical relations, and should increase rather than decrease (in absolute value) with v. Instead of using empirical values of D_v it was thought best to use the theoretical ones having their usual significance and limit the calculations to low values of J. For small values of J the derived constants would have the same value in either case. Anomalous behavior of the rotational energy function for the $^1\Sigma^*$ state was also observed in the copper hydride spectrum,[2] where it was found necessary to use a *positive D*

[6] R. T. Birge, National Research Council Bulletin No. 57, *Molecular Spectra in Gases*, pp. 172–175 (1926).

[7] G. M. Almy and G. R. Irwin, Phys. Rev. **49**, 72 (1936).

TABLE I. *Wave numbers of the copper deuteride bands.*

J	R	P
	0−0 BAND	
0	23332.88	
1	38.86	23318.06
2	43.74	09.04
3	47.55	23298.93
4	50.32	87.91
5	52.03	75.83
6	52.76	62.72
7	52.40	48.63
8	51.07	33.51
9	48.58	17.41
10	45.12	00.35
11	40.57	23182.24
12	35.00	63.20
13	28.40	43.15
14	20.71	22.12
15	12.02	00.15
16	02.28	23077.31
17	23291.51	53.47
18	79.69	28.58, 8.83
19	66.89	02.88, 3.15
20	51.97	22976.26, 6.59
21	38.18	48.73, 9.08
22	22.30	19.68, 0.74
23	05.22	22891.05, 1.48
24	23187.53	60.88, 1.34
25	68.59	29.87, 0.30
26	48.75	22797.98, 8.45
27	27.87	65.23, 5.71
28	05.97	31.63, 2.21
29	23083.13	22697.22, 7.85
30	59.29	61.98, 2.56
31	23034.40, 4.64	26.07, 6.70
32	08.60, 8.92	22589.21, 9.95
33	22981.88, 2.24	51.65, 2.38
34	54.20, 4.57	13.23, 4.01
35	25.57, 6.00	22474.12, 4.92
36	22895.98, 6.43	34.21, 5.03
37	65.44, 5.90	22393.54, 4.39
38	33.98, 4.51	52.16, 3.07
39	01.58, 2.11	10.00, 0.94
40	22768.22, 8.66	22267.14, 8.13
41	33.91, 4.55	23.58, 4.61
42	22698.70, 9.28	22179.29, 0.36
43	62.70, 3.32	34.29, 5.40
44	25.49	22088.59, 9.74
45	22587.55, 8.35	42.34, 3.48
46	48.60, 9.42	21995.12, 6.37
47	08.73, 9.56	47.36, 8.63
48	22467.93, 8.78	21898.90, 0.26
49	26.12, 7.00	49.70, 1.04
50	22383.39, 4.37	21799.88, 1.30
51	39.72, 0.74	49.32
52	22295.00	21698.08
53	49.32	46.06
54	02.63	21593.43
55	22154.96	40.16
56	06.07	21486.12
57	22056.16	
58	05.18	
59	21953.09	
60	00.26	
61	21846.46	
	0−1 BAND	
0	21986.73	
1	92.81	21971.93, 2.65
2	98.08	63.27, 3.92
3	22002.40	53.82, 4.52
4	05.91	43.46, 4.12
5	08.60	32.33, 2.98
6	10.50	20.32, 1.02
7	11.36, 1.99	07.50, 8.20
8	11.36, 1.99	21893.85, 4.58
9	10.50, 1.35	79.39, 0.12
10	09.00, 9.57	64.12, 4.83
11	06.46, 7.12	48.04, 8.84
12	03.03, 3.70	31.24, 1.98
13	21998.80, 9.41	13.50, 4.28
14	93.66, 4.34	21795.08, 5.87
15	87.73, 8.36	75.84, 6.67
16	80.92, 1.56	55.89, 6.73
17	73.25, 3.88	35.17, 6.21
18	64.72, 5.37	13.66, 4.59
19	55.35, 6.00	21691.39, 2.29
20	45.12, 5.81	68.30, 9.31
21	34.08, 4.76	44.67, 5.67
22	22.19, 2.87	20.44, 1.21
23	10.44, 0.07	21595.15, 6.31
24	21895.88, 6.56	69.32, 0.28
25	81.48, 2.23	42.90, 3.83
26	66.26, 7.04	15.64, 6.79
27	50.28, 1.06	21487.73, 8.80
28	33.38, 4.17	59.21, 9.91
29	15.74, 6.57	30.02, 1.02
30	21797 29, 8.13	00.16, 1.25
31	78.12	21369.68, 0.79
32	58.03, 8.78	38.56
33	37.11, 7.99	06.83
34	15.48, 6.37	21274.53
35	21693.05, 3.92	41.57
36	69.87	08.05
37	45.70	

J	R	P
	0−2 BAND	
10	20710.72	
11	10.24	20551.74, 3.00
12	09.01, 9.76	37.12, 8.50
13	07.04, 8.28	21.88, 3.19
14	04.56, 5.90	05.96, 7.23
15	01.36, 2.49	20489.24, 0.41
16	20697.45, 8.60	
17	92.83	
18	87.23	
	1−0 BAND	
0	24503.28	
1	08.90	24488.48
2	13.15	79.27
3	16.32, 5.64	68.81
4	18.07, 7.44	57.13
5	18.68, 8.06	44.37
6	18.07, 7.44	30.41
7	16.32, 5.64	15.24
8	13.15, 2.53	24398.73
9	08.90, 8.20	81.13
10	03.28, 2.69	62.33
11	24496.55, 5.90	42.39
12	88.48, 7.89	21.23
13	79.30, 8.72	24298.95
14	68.82, 8.24	75.52
15	57.11, 6.53	50.97
16	44.04, 3.61	25.23, 4.45
17	29.88, 9.37	24198.36, 7.18
18	14.46, 4.05	70.39, 9.40
19	24397.77, 7.44	41.33, 0.44
20	79.94, 9.62	11.11, 0.25
21	60.93	24079.86, 8.94
22	40.68	47.43, 6.37
23	19.22	14.02, 3.09
24	24296.51	23979.38
25	72.21	43.86
26	47.61	07.18
27	21.28	23869.44
28	24193.83	30.69
29	65.16	23791.16
30	35.25	50.10
31	04.18	08.16
32	24071.93	23665.35
33	38.58	21.54
34	03.86	23576.73
35	23967.94	30.84
36	31.14	23483.80
37	23892.76	35.89
38	53.08	23387.09
39	12.25	37.13
40	23770.25	23286.28
41		34.36
42		23181.34
	1−1 BAND	
0	23156.66	
1	62.51	
2	67.21	23133.78
3	71.03	23.89
4	73.69	13.03
5	75.28	01.15
6	75.82	23088.16
7	75.28	74.23
8	73.69	59.29
9	71.03	43.36
10	67.21	26.40
11	62.51	08.60
12	56.66	22989.51
13	49.78	69.61
14	41.90	48.73
15	32.89	26.82
16	22.89	04.03
17	11.77	22880.27
18		55.55
19	23086.60	29.86
20	72.33	03.38
21	57.09	22775.85
22	40.84	22747.41, 7.87
23	23.51	18.08, 8.64
24	05.17	22687.85, 8.45
25	22985.79	56.76, 7.32
26	65.50	24.79, 5.47
27	43.91	22591.94, 2.58
28	21.52	58.15, 8.92
29	22898.22	23.63, 4.32
30	73.54	22488.20, 8.86
31	47.96	51.85, 2.61
32	22821.30, 1.71	14.69, 5.52
33	22793.73, 4.17	22376.72, 7.50
34	65.13, 5.81	37.87, 8.70
35	35.46, 5.90	22298.23, 9.08
36	04.76, 5.24	57.68, 8.61
37	22672.93, 3.59	16.33, 7.31
38	40.05, 0.91	22174.12, 5.18
39	06.33, 6.97	31.15, 2.15
40	22571.28	22087.26
41	35.19	
	1−2 BAND	
0	21848.84	
1	54.79, 5.51	21834.17, 5.07

J	R	P
	1−2 BAND	
2	59.82, 0.53	25.99
3	64.12, 4.83	16.57, 7.40
4	67.34, 8.05	06.58, 7.26
5	69.75, 0.89	21795.87
6	71.43, 2.02	83.72, 4.46
7	72.02, 2.70	71.06, 1.82
8	72.02, 2.70	57.55, 8.24
9	70.88, 1.43	43.23, 4.00
10	69.00, 9.75	28.12, 8.89
11	66.27, 7.02	12.17, 2.93
12	62.60, 3.31	21695.41, 6.23
13	58.08, 8.79	77.86, 8.69
14	52.70, 3.39	59.61, 0.38
15	46.45, 7.16	40.36, 1.22
16	39.31, 0.01	20.35
17	31.24, 1.98	21599.83, 0.72
18	22.45, 3.18	78.39, 9.30
19	12.72, 3.50	56.18, 7.11
20	02.14, 2.88	33.22
21	21790.69, 1.44	09.53, 0.49
22	78.31, 9.02	21485.12, 6.08
23	65.20, 5.97	59.96, 0.92
24	51.17, 1.95	33.46, 5.00
25	36.21	07.36, 8.45
26	20.48, 1.19	21379.93, 1.08
27	03.96, 4.72	51.98, 3.10
28	21686.46, 7.26	23.24, 4.35
29	68.30, 9.31	93.83, 4.99
30	48.98, 9.89	21263.71, 4.91
31	28.91, 9.78	32.94
32	08.04, 8.93	01.45
33	21586.32, 7.28	
34	63.69, 4.74	
35	40.15, 1.22	
36	15.89, 6.79	
37	21490.70, 1.75	
38	64.50, 5.59	
39	37.50, 8.59	
	2−0 BAND	
0	25628.83, 7.58	
1	33.71, 2.74	25612.77
2	37.25, 6.36	03.28
3	39.82, 8.87	25592.79
4	40.59, 9.98	80.89
5	39.98, 9.74	67.98, 7.46
6	38.08, 7.25	52.93, 2.12
7	34.74, 3.71	36.74, 5.71
8	30.05, 8.83	18.93, 7.96
9	23.67, 2.65	25499.76, 8.91
10	16.01, 4.93	79.33, 8.30
11	06.86, 5.91	57.25, 6.40
12	25596.32, 5.22	34.00, 3.15
13	84.35, 3.44	09.43, 8.58
14	71.04, 0.04	25383.47, 2.68
15	56.18, 5.23	56.17, 5.48
16	39.92, 8.96	27.50, 6.73
17	22.17, 1.22	25297.71, 6.82
18	03.07, 2.21	66.28, 5.47
19	25482.51, 1.73	33.49, 2.66
20	60.51, 9.66	25199.61, 8.47
21	37.07, 6.12	64.41, 3.73
22	12.28, 1.53	27.83
23	25386.02, 5.18	25090.03
24	58.46, 7.80	50.86
25	29.25, 8.51	10.36
26		24968.63
27		25.85
28		24881.61
29		36.18
30		24789.41
31		41.44
32		24692.24
33		41.70
34		24589.94
35		36.93
36		24482.68
	2−1 BAND	
0	24282.42	
1	87.60	24268.32
2	91.71	
3	94.61	48.80
4	96.51	37.22
5	96.51	
6	95.79	10.59
7	93.61	24195.49
8	90.26	79.18
9	85.36	61.69
10	79.79	42.96
11	72.63	23.09
12	64.33	02.08
13		24079.86
14	43.93	56.45
15	31.79	31.90
16	18.47	06.15
17	03.52	23979.38
18	24188.02	51.30
19	71.06	22.12
20	52.65	23891.77
21	33.02	60.40

J	R	P
	2−1 BAND	
22	12.20	28.02
23	24090.11	23794.16
24	66.79	59.43
25	42.16	
	2−2 BAND	
5	22991.44	
6	91.44	
7	90.56	
8	88.64	
9	85.85	
10	82.06	22844.99
11		26.98
12		07.83
13	63.08	
14	54.76	
15	45.19	22745.56
16		
17	23.63	22698.71
18	10.61	74.16
19		48.37
20	22882.64	21.71
21	66.98	22594.00
22	50.00	65.42
23		35.94
	2−3 BAND	
4		21661.80, 2.85
5		51.28, 2.06
6		39.56, 0.40
7		27.02, 7.77
8	21724.69, 5.26	13.61, 4.43
9	23.39, 4.11	21599.35
10	21.19, 1.87	84.33, 5.16
11	18.05, 8.85	68.39, 9.39
12	14.05, 4.59	51.52, 2.60
13	09.14, 9.88	34.21, 5.08
14	03.35, 4.15	15.61, 6.79
15	21696.69, 7.45	21496.69, 7.63
16	89.12, 9.85	76.78, 7.69
17	80.64, 1.38	56.05, 6.98
18	71.31, 2.15	34.49, 5.46
19	61.06, 1.80	12.17, 3.17
20	49.89, 0.71	21389.05, 0.11
21	37.90, 8.59	65.17, 6.20
22	24.93, 5.74	40.51, 1.57
23	11.10, 1.92	15.10, 6.20
24	21596.32, 7.19	21288.95, 0.04
25	80.72, 1.55	62.04, 3.11
26	64.17, 4.93	34.24, 5.46
27	46.70, 7.56	05.87, 7.03
28	28.39, 9.20	
	3−1 BAND	
2	25368.38	25336.82
3	70.57	26.11
4	71.42	14.09
5	70.57	00.67, 9.76
6	68.38	25285.70, 4.94
7	64.48, 3.77	69.42, 8.63
8	59.37, 8.46	51.69, 0.96
9	52.71, 1.98	32.66, 1.86
10	44.71, 3.80	12.08, 1.32
11	35.13, 4.26	25190.19, 9.44
12	24.14, 3.30	66.78, 6.13
13	11.62, 0.86	42.19, 1.47
14	25297.71, 6.82	16.13, 5.44
15	82.36, 1.57	25088.68, 8.14
16	65.48, 4.79	59.92, 9.28
17	47.19, 6.45	29.66
18	27.39, 6.63	24998.17
19	06.08, 5.44	65.25
20	25183.40, 2.78	31.07
21	59.21, 8.52	24895.40
22	33.50, 9.19	58.41
23	06.32	20.26
24	25077.67, 4.56	24780.63
25	47.49	39.61
26	15.87	24697.34
27	24982.58	53.69
28	48.01	
29	11.79	24562.87
30		15.64
	3−2 BAND	
1	24057.60	
2	61.10	
3	63.61	24019.03
4	64.94	07.58
5	64.94	23995.05
6	63.61	81.37
7	61.10	66.46
8	57.60	50.11
9	24052.67	23932.50
10	46.39	13.41
11	38.52	• 23893.91
12	30.05	72.90
13	19.98	50.09
14	08.55	26.97
15	23995.89	02.25
16	81.90	23776.43
17		49.26

TABLE II. *Values of B_v for the normal $^1\Sigma$ state.*

	$Cu^{63}D$		$Cu^{65}D$	
	Obs.	Obs.–Calc.	Obs.	Obs.–Calc.
B_0	3.99197	+0.00013	3.98804	+0.00002
B_1	3.90034	−0.00011	3.89698	0.00000
B_2	3.80900	−0.00004	3.80589	−0.00006
B_3	3.71795	+0.00031	3.71498	+0.00006

TABLE III. *Values of B_v for the $^1\Sigma^*$ state.*

	$Cu^{63}D$		$Cu^{65}D$	
	Obs.	Obs.–Calc.	Obs.	Obs.–Calc.
B_0	3.4740	−0.0005	3.4711	−0.0010
B_1	3.3809	+0.0001	3.3777	+0.0003
B_2	3.2829	−0.0002	3.2788	−0.0003
B_3	3.1819	+0.0004	3.1785	+0.0010

TABLE IV. *Summary of constants.*

	$Cu^{63}D$		$Cu^{65}D$	
	$^1\Sigma$	$^1\Sigma^*$	$^1\Sigma$	$^1\Sigma^*$
ω_e	1381.38	1213.16	1383.65	1212.60
$x_e\omega_e$	19.14	20.65	19.12	20.45
$y_e\omega_e$	0.037	−0.41	0.027	−0.45
T_e	0	23412	0	23412
B_e	4.03754	3.5199	4.03353	3.5182
α_e	0.09140	0.0898	0.09103	0.0919
γ_e	——	−0.0020	——	−0.0017
D_e	-1.3737×10^{-4}	-1.185×10^{-4}	-1.3710×10^{-4}	-1.183×10^{-4}
β_e	1.442×10^{-6}	5.51×10^{-7}	1.241×10^{-6}	4.28×10^{-7}
F_e	3.285×10^{-9}	1.901×10^{-9}	3.317×10^{-9}	2.058×10^{-9}
H_e	-1.20×10^{-13}	-8.34×10^{-14}	-1.28×10^{-13}	-9.33×10^{-14}

for the $v=3$ level. The perturbation giving rise to this abnormal value is evidently removed in the copper deuteride molecule. Here D_3 is negative as theory demands.

The values of B_v for the normal $^1\Sigma$ state are given by the following least-squares equations:

$$\text{For } Cu^{63}D: B_v = 4.03754 - 0.09140(v+\tfrac{1}{2}). \quad (4)$$

$$\text{For } Cu^{65}D: B_v = 4.03353 - 0.09103(v+\tfrac{1}{2}). \quad (5)$$

In the determination of the constants of these equations each value of B_v was given a weight proportional to the number of values of Δ_2F^* used in its calculation.

In the $^1\Sigma^*$ state the B_v's are given by the following quadratic equations:

$$\text{For } Cu^{63}D: B_v = 3.5199 - 0.0898(v+\tfrac{1}{2}) - 0.00197(v+\tfrac{1}{2})^2. \quad (6)$$

$$\text{For } Cu^{65}D: B_v = 3.5182 - 0.0913(v+\tfrac{1}{2}) - 0.00173(v+\tfrac{1}{2})^2. \quad (7)$$

Table II gives the experimental values of B_v for the normal $^1\Sigma$ state as determined from Eq. (3), and the differences between these values and those calculated from Eqs. (4) and (5). Table III gives similar information for the $^1\Sigma^*$ state.

The vibrational intervals $\Delta G_{v+\frac{1}{2}}$ are obtained from the observed band lines by the use of relations such as these:

$$\Delta G_{1\frac{1}{2}} = R_{(0-1)}(J) - R_{(0-2)}(J) + \alpha J(J+1) - \beta J^2(J+1)^2 = P_{(0-1)}(J) - P_{(0-2)}(J) + \alpha J(J+1) - \beta J^2(J+1)^2. \quad (8)$$

In each case α and β are obtained from the rotational data already given.

The values of the vibrational constants ω_e, $x_e\omega_e$, and $y_e\omega_e$ were obtained from the equation

$$\Delta G_{v+\frac{1}{2}} = \omega_e - 2x_e\omega_e(v+\tfrac{1}{2}) + 3y_e\omega_e(v+\tfrac{1}{2})^2, \quad (9)$$

into which the observed $\Delta G_{v+\frac{1}{2}}$ were substituted. A summary of the usual band spectra constants is given in Table IV.

ISOTOPE RELATIONS

Corrections that may be applied to the band spectra values of ρ have been conveniently listed by Watson.[8] In view of the irregularities observed in the $^1\Sigma^*$ state in CuH and to a lesser degree in CuD there is probably quantum-mechanical interaction with the neighboring $^1\Pi$ states[3] which would make the B_v determined from the data an *effective B* not having the simple relation to the true moment of inertia. Analysis of the CuH spectrum is not sufficiently complete to permit a calculation of this correction in the present paper. Accordingly, the values of ρ which are considered to be most accurate are determined from the normal state.

TABLE V. *Isotope ratios.* (Heimer and Heimer's values of the constants for $Cu^{63}H$ are used for the $Cu^{63}D$ to $Cu^{63}H$ ratios.)

	$Cu^{65}D : Cu^{63}D$		$Cu^{63}D : Cu^{63}H$	
	$^1\Sigma$	$^1\Sigma^*$	$^1\Sigma$	$^1\Sigma^*$
$(B_e^i/B_e)^{\frac{1}{2}}$	0.999503	0.99976	0.7131	0.7153
ω_e^i/ω_e	0.99947	0.99954	0.7135	0.7129
$(\mu/\mu_i)^{\frac{1}{2}}$	0.99952		0.7129	

[8] W. W. Watson, Phys. Rev. **49**, 70 (1936).

A consideration of the other corrections indicates that the only ones which might be appreciable in the normal state are those given by Dunham[9] for the anharmonicity terms. They involve a power series in B_e^2/ω_e^2, which is of the order of 10^{-6} for the CuD molecule, making even these corrections negligible.

The values of ρ calculated from the vibrational and rotational constants are given in Table V and compared with the value of $(u/u_i)^{\frac{1}{2}}$ from mass-spectrograph data. The agreement is excellent with the exception of $(B_e^i/B_e)^{\frac{1}{2}}$ in the $^1\Sigma^*$ state. Here the value is 0.99976 for $Cu^{65}D$ to $Cu^{63}D$, which differs by 0.00024 from the calculated value. This difference may be due in part to difficulty in reduction of the data as is indicated above since only the low values of J can be used in this state. The fact that $(B_e^i/B_e)^{\frac{1}{2}}$ for CuD to CuH in the $^1\Sigma^*$ state is also much larger than the calculated value indicates that the discrepancy is real, however, and that B_e should in this case be corrected as mentioned above.

Rather limited data are available for the determination of the $\Delta G_{v+\frac{1}{2}}$ values for $Cu^{65}D$, especially in the normal state. This makes the uncertainty in the value of ω_e^i/ω_e much greater than the uncertainty in $(B_e^i/B_e)^{\frac{1}{2}}$ for this state. An estimate of the probable error in ω_e^i/ω_e based on the individual probable errors in the values of $\Delta G_{v+\frac{1}{2}}$ is 0.00015. In the $^1\Sigma$ state ω_e^i/ω_e for $Cu^{65}D$ to $Cu^{63}D$ has the value 0.99947, and in the $^1\Sigma^*$ state 0.99954. The corresponding values for $Cu^{63}D$ to $Cu^{63}H$ are 0.7135 and 0.7129, respectively.

The large number of individual values used in the determination of the B_v constants makes $(B_e^i/B_e)^{\frac{1}{2}}$ for the normal state the most reliable value of ρ determined from the present work. This value for the molecules $Cu^{65}D$ and $Cu^{63}D$ is 0.999503. The calculated values of the probable errors of the values of B_e as given by Eqs. (4) and (5) are 0.000071 and 0.000018, respectively. A consideration of the probable error of the individual values of B_v would indicate that these values are too small. It is believed, however, that $(B_e^i/B_e)^{\frac{1}{2}}$ for $Cu^{65}D$ to $Cu^{63}D$ can have a probable error no greater than 0.00006. The value of this ratio for $Cu^{63}D$ to $Cu^{63}H$ for the $^1\Sigma$ state is 0.7131.

In conclusion the author wishes to express his sincere thanks to the Physics Department of The Johns Hopkins University for the use of the spectrograph on which the plates were taken.

[9] J. L. Dunham, Phys. Rev. **41**, 721 (1932).

SEPTEMBER 1, 1936 PHYSICAL REVIEW VOLUME 50

The Temperature Variation of the Elastic Moduli of NaCl, KCl and MgO

MILO A. DURAND, *Columbia University*

(Received June 29, 1936)

The principal adiabatic and isothermal elastic moduli and elastic constants of NaCl, KCl and MgO have been measured over the temperature ranges 80°K to 270°K (Balamuth and Rose) and 270°K to 480°K for NaCl; 80°K to 280°K for KCl; and 80°K to 560°K for MgO. The Debye characteristic temperatures of these substances at 80°K, calculated from the adiabatic elastic constants, are 320°K, 246°K and 946°K, respectively. The variation of the isothermal c_{11} and c_{44} with temperature is described very accurately by the formula: $(c_{ii})_u = (c_{ii})_0 \exp(-A_{ii}F_{ii}(u))$, where $u = (T/\theta)$, T is the absolute temperature and θ the characteristic temperature, $(c_{ii})_0$ denotes the value at absolute zero, A_{ii} is a constant of the material, and $F_{ii}(u)$ is a function of u which assumes the value unity when $u = 1$, *and which is the same for all three substances.* Experimental values of $F_{11}(u)$ and $F_{44}(u)$ are given for values of u between 0.1 and 1.5. The isothermal c_{12} does not vary with temperature, over the specified ranges, by more than the error of measurement.

THE temperature variations of the three principal elastic constants of sodium chloride between 80°K and 270°K have been reported in this journal by Balamuth[1] and Rose.[2] These investigators perfected their experimental method for use only at temperatures below that of melting ice. The object of the present research is, in the first instance, to extend the scope of the method and the observations on sodium chloride to higher temperatures. In addition, observations

[1] Balamuth, Phys. Rev. **45**, 715 (1934).
[2] Rose, Phys. Rev. **49**, 50 (1936).

have been made on single crystals of potassium chloride and, over the extended temperature range, of magnesium oxide, both of which have the same lattice structure as sodium chloride. A scrutiny of the data reveals a remarkable correlation between the thermo-elastic properties of the three substances, of such a sort, in fact, as to suggest that it is characteristic at least of the lattice type. Apart from its theoretical interest, this correlation permits the calculation of any one of the elastic constants at a given temperature when its value at two other temperatures is known, and so yields plausible values for the constants at absolute zero.

Experimental Method

The experimental method, which is described in detail in the papers of Balamuth and Rose heretofore cited, utilizes the properties of a separately excited composite piezoelectric oscillator constructed by cementing a suitably cut, right circular cylinder of crystalline quartz to one end of a cylinder of specimen material whose cross section is the same as that of the quartz. The diameter of the cylinders is about 4 mm and their lengths vary between 1 cm and 5 cm. The fundamental frequency of free longitudinal or torsional vibration of this system, hereafter called the "resonance frequency," is measured by observing the variation of the electrical impedance of the piezoelectric oscillator with the frequency of the applied voltage, and the Young's or the rigidity modulus of the specimen material for the direction of the cylinder axis is calculated from this and other readily measurable quantities.

The present research is concerned with only two directions in a cubic lattice, namely, (0,0,1) and (0,1,1). Accordingly, the Young's modulus, G, and the rigidity modulus, μ, are related to the principal moduli of the crystal by the formulae,[3]

$$\begin{aligned} 1/G &= s_{11}, \\ 1/G' &= s_{11}' = \tfrac{1}{2}(s_{11}+s_{12}+\tfrac{1}{2}s_{44}), \\ 1/\mu &= s_{44}, \\ 1/\mu' &= s_{11}-s_{12}+\tfrac{1}{2}s_{44}, \end{aligned} \qquad (1)$$

in which the unprimed and the primed quantities refer, respectively, to the (0,0,1) and the (0,1,1) directions. It follows from these equations that

$$s_{12} = 1/G' - 1/2\mu', \qquad (2)$$

or

$$= 1/G + 1/2\mu - 1/\mu'. \qquad (3)$$

The elastic moduli and elastic constants are related by the formulae,

$$\begin{aligned} c_{11} &= (s_{11}+s_{12})/(s_{11}-s_{12})(s_{11}+2s_{12}), \\ c_{12} &= -s_{12}/(s_{11}-s_{12})(s_{11}+2s_{12}), \\ c_{44} &= 1/s_{44}\,. \end{aligned} \qquad (4)$$

Lastly, the compressibility, κ, is given by the formulae,

$$\begin{aligned} \kappa &= 3(s_{11}+2s_{12}), \\ &= 3/(c_{11}+2c_{12}). \end{aligned} \qquad (5)$$

The method yields immediately the adiabatic moduli and constants. These are related to the isothermal quantities by the formulae,[4]

$$\begin{aligned} (s_{11})_{\text{ad.}} - (s_{11})_{\text{is.}} &= (s_{12})_{\text{ad.}} - (s_{12})_{\text{is.}} = -T\alpha^2/\rho c_p, \\ (c_{11})_{\text{ad.}} - (c_{11})_{\text{is.}} &= (c_{12})_{\text{ad.}} - (c_{12})_{\text{is.}}, \\ &= T\alpha^2/(\rho c_p)(s_{11}+2s_{12})^2, \end{aligned} \qquad (6)$$

where T is the absolute temperature, α is the coefficient of linear expansion, c_p is the specific heat at constant pressure, and ρ is the density. The adiabatic and isothermal s_{44} and c_{44} are the same.

At temperatures below 273°K the present experimental method is entirely the same as that of Rose, except that the cryostatic bath liquid is petroleum ether cooled by liquid nitrogen.

The initial problem which arises when an attempt is made to extend the method to higher temperatures is the discovery of a satisfactory adhesive with which to cement the quartz to the specimen cylinder. That now in use is a thin paste of sodium silicate solution and talcum powder. The cylinders are cemented together under a pressure of 4.5 kg/cm², and the join is baked under this pressure for 15 minutes in air at a temperature of 150°C. Great care must be exercised to ensure that a minimum amount of cement is left adhering to the sides of the oscillator. The effect of such excess material is to load the oscillator, so that the entire resonance frequency *vs.* temperature curve is depressed parallel to itself by a few tenths of a percent. This shift can be, and is, measured and corrected for by adopting as the correct resonance frequency at 273.1°K that which is observed when

[3] Voigt, *Lehrbuch der Kristallphysik*, p. 739.

[4] Voigt, reference 3, p. 789.

the adhesive is a very thin film of para rubber dissolved in vaseline, and the oscillator is immersed in melting ice.

Numerous tests were made of the satisfactory performance of the talcum-silicate cement. Perhaps the most significant of these is the following: Two cylinders of quartz were chosen whose resonance frequencies for the *torsional* mode of vibration were, respectively, 53 kc and 69 kc. Separate frequency *vs.* temperature observations were made on these up to a temperature of 560°K. The two were then cemented together with their optic axes at right angles (to increase the differential thermal expansion at the interface), and the resonance frequency of the composite oscillator, driven by one of the cylinders, was measured over the same temperature range. The formulae of the method then yielded the resonance frequency of the other cylinder, which was compared with the correct value previously ascertained. The two values agreed to 0.13 percent, without systematic variation. Now Balamuth has pointed out that the effect of the cement is negligible *provided* the lengths of the quartz and specimen cylinders are so adjusted that the fundamental frequencies of free vibration of, respectively, the cylinders separately and the composite oscillator are the same to better than ten percent. Furthermore, Rose observed that the effect of the cement on the resonance frequency is greater for the torsional mode of vibration than for the longitudinal. Hence the foregoing test may be regarded as exceptionally severe.

A further stringent internal check on the measurements made on whatever substance is afforded by calculating s_{12} from measured values of G' and μ' with Eq. (2), and again from measured values of G, μ and μ' with Eq. (3). This test is applied in all cases.

Between 273°K and 373°K the cryostatic bath liquid is a mixture of 75 percent glycerin and 25 percent water; above 373°K it is Socony Super Hecla Mineral Oil. The baths are electrically heated, and the temperature is stabilized to 0.1°K by manual control of the current in an auxiliary heating coil of low heat capacity.

When the thermal expansion coefficient of a fragile specimen is greater than that of quartz, it is not necessary to use at higher temperatures the triple oscillator devised by Rose to prevent splitting of the specimen cylinder caused by differential thermal expansion at the interface. As the oscillator is heated above the temperature at which it was prepared, this differential expansion compresses the specimen instead of rending it.

Results

Sodium chloride

The specimen cylinders of sodium chloride were cut from the same large crystal as were those used by Balamuth and Rose. The elastic moduli and elastic constants of this material over the temperature range 270°K to 480°K are given in Table I. These data fit smoothly onto the observations between 80°K and 270°K which appear in Rose's paper.[2] They represent the mean of measurements of G, μ, and μ', each on four different specimens. The average deviation in the calculated values of s_{11}, s_{44} and s_{44}' is 0.2 percent. The values of s_{12} were calculated with Eq. (3), and are reliable to about two percent. The elastic constants were calculated from the moduli with Eqs. (4), and the isothermal quantities with Eqs. (6).

Between 273°K and 414°K the formula used in computing the density was[5]

$$\rho = 2.1680(1 - 10.6\times10^{-5}t - 0.3\times10^{-6}t^2).$$

Above 414°K the coefficient of cubical expansion is, simply, 14×10^{-5}. Values of c_p were taken from the *International Critical Tables* throughout.

Potassium chloride

The specimen cylinders of this material were cut from a crystal obtained through the courtesy of Dr. Paul F. Kerr of the Department of Mineralogy at Columbia University. According to his records, the source was Kolusz, Silesia. Minute bubbles appeared in this crystal, but otherwise it was clear.

The elastic constants and elastic moduli of potassium chloride over the temperature range 80°K to 280°K are given in Table II. Because of the scarcity of the available material, it was possible to measure G, μ, and μ' each on only two specimens. The values of these quantities

[5] Saini, Helv. Phys. Acta **7**, 494 (1934).

TABLE I. *The elastic moduli and constants of NaCl.*

T°K	Adiabatic Moduli ×10¹² (cm²/dynes)			Adiabatic Constants ×10⁻¹¹ (dyne/cm²)			Isothermal $c_{11}\times10^{-11}$
	s_{11}	$-s_{12}$	s_{44}	C_{11}	C_{12}	C_{44}	
270	22.08	4.49	78.26	5.06	1.30	1.278	4.95
280	22.29	4.58	78.47	5.03	1.30	1.274	4.90
290	22.51	4.67	78.67	4.99	1.31	1.271	4.86
300	22.73	4.76	78.87	4.96	1.31	1.268	4.82
310	22.96	4.85	79.08	4.92	1.32	1.265	4.78
320	23.19	4.94	79.29	4.88	1.32	1.261	4.74
330	23.42	5.03	79.50	4.84	1.32	1.258	4.69
340	23.66	5.13	79.71	4.81	1.33	1.255	4.65
350	23.90	5.23	79.92	4.77	1.33	1.251	4.61
360	24.15	5.33	80.14	4.73	1.34	1.248	4.57
370	24.40	5.43	80.36	4.69	1.34	1.244	4.53
380	24.66	5.54	80.58	4.66	1.35	1.241	4.49
390	24.93	5.65	80.80	4.62	1.35	1.238	4.44
400	25.20	5.76	81.02	4.58	1.36	1.234	4.40
410	25.48	5.87	81.26	4.55	1.36	1.231	4.36
420	25.78	5.99	81.50	4.51	1.36	1.227	4.32
430	26.08	6.11	81.76	4.47	1.37	1.223	4.28
440	26.38	6.23	82.02	4.43	1.37	1.219	4.23
450	26.69	6.36	82.29	4.39	1.38	1.215	4.19
460	27.01	6.49	82.57	4.36	1.38	1.211	4.15
470	27.33	6.62	82.85	4.32	1.39	1.207	4.11
480	27.66	6.75	83.13	4.28	1.39	1.203	4.07

The isothermal c_{12} is 1.17×10^{11} over the entire temperature range.

TABLE II. *The elastic moduli and constants of KCl.*

T°K	Adiabatic Moduli ×10¹² (cm²/dynes)			Adiabatic Constants ×10⁻¹¹ (dyne/cm²)		Isothermal $c_{11}\times10^{-11}$
	s_{11}	$-s_{12}$	s_{44}	C_{11}	C_{44}	
80	21.36	2.3	150.7	4.81	0.664	4.81
90	21.50	2.4	150.9	4.79	.663	4.78
130	22.18	2.6	151.8	4.65	.659	4.64
140	22.37	2.7	152.1	4.62	.658	4.61
150	22.57	2.7	152.4	4.59	.656	4.57
160	22.78	2.7	152.7	4.55	.655	4.53
170	22.99	2.8	153.1	4.52	.653	4.49
180	23.20	2.8	153.5	4.48	.651	4.45
190	23.42	2.8	153.9	4.44	.650	4.41
200	23.64	2.9	154.3	4.40	.648	4.37
210	23.86	2.9	154.7	4.36	.647	4.33
220	24.09	3.0	155.1	4.33	.645	4.29
230	24.31	3.0	155.5	4.29	.643	4.25
240	24.54	3.1	156.0	4.24	.641	4.21
250	24.77	3.2	156.4	4.20	.639	4.17
260	25.00	3.2	156.9	4.16	.637	4.13
270	25.23	3.3	157.3	4.12	.636	4.09
280	25.46	3.3	157.8	4.08	.634	4.05

The adiabatic and isothermal c_{12} are 0.6×10^{11} over the entire temperature range.

differed between specimens by the amounts 0.5 percent, 0.3 percent, and 0.5 percent respectively. Accordingly the value of s_{12} is reliably to only about five percent. The formula used in computing the density was[6]

$$\rho = 1.9920(1 - 10.6t - 0.4\times10^{-7}t^2).$$

Steinebach[7] found the ratios of the value of s_{11} and s_{44} at room temperature to those at 88°K to be 1.195 ± 0.02 and 1.05 ± 0.02, respectively. Those calculated from Table II are 1.205 and 1.044, respectively. Values of the isothermal moduli at 30°C reported by different observers are given in Table III.

Slater[8] found the isothermal compressibility at 30°C to be 56.3×10^{-13}, as compared with the present extrapolated value, 56.7×10^{-13}. It should be noted that the crystals examined by Bridgman and Slater were grown artificially, while those used by Voigt and the writer were natural.

Magnesium oxide

The specimen cylinders of magnesium oxide were cut from large, clear, well formed crystals supplied by the Norton Company, of Worcester, Mass. Because of its hardness this material cannot be turned on a lathe, and these cylinders, like the quartz, were formed by hand grinding in a series of split cylindrical laps. Two part oscillators were used over the entire temperature range.

The elastic constants and elastic moduli of magnesium oxide over the temperature range 80°K to 560°K are given in Table IV. They represent the mean of measurements of G and μ on four specimens, and μ' on three. The average deviations were 0.15 percent, 0.15 percent, and 0.1 percent. Accordingly the value of s_{12} is reliable to about 2 percent.

The density of magnesium oxide at 25°C was measured with a specific gravity bottle. The mean of observations on three sets of specimens was

$$\rho_{25} = 3.5761\pm0.0005.$$

The density at other temperatures was computed from this value, with the coefficient of thermal expansion reported by Durand[9] and Austin.[10]

Madlung and Fuchs[11] found the isothermal

[6] Henglein, Zeits. f. physik. Chemie **115**, 91 (1925).
[7] Steinebach, Zeits. f. Physik **33**, 674 (1925).
[8] Slater, Phys. Rev. **23**, 488 (1924).
[9] Durand, Physics **7**, 297 (1936).
[10] Austin, J. Am. Ceramic Soc. **14**, 795 (1931). The data on MgO are reprinted in reference 9.
[11] Madlung and Fuchs, Ann. d. Physik **65**, 289 (1921).

TABLE III. *Values of isothermal moduli at 30°C reported by different observers.*

Observer	Elastic moduli $\times 10^{13}$ s_{11}	s_{12}	s_{44}
Durand	26.26	−3.7	158.9
Voigt[1]	27.37	−1.4	156.0
Bridgman[2]	29.4	−5.3	127

[1] Voigt, reference 3, p. 741.
[2] Bridgman, Proc. Am. Acad. **64**, 19 (1929).

compressibility of their best specimens of magnesium oxide to be 6.4×10^{-13}. The present value is 6.54×10^{-13}.

It is of interest to note that the behavior of this substance is widely at variance with Cauchy's relation, $c_{12}=c_{44}$, between the isothermal elastic constants.

Calculation of the Debye Characteristic Temperature

The Debye characteristic temperatures of the several substances were calculated from the adiabatic elastic constants at 80°K by an obvious modification of the method of Hopf and Lechner.[12] Thus, for magnesium oxide, $\theta_{80}=946$°K; for sodium chloride, $\theta_{80}=320$°K; and for potassium chloride, $\theta_{80}=246$°K. These values agree with those obtained from specific heat measurements at low temperatures within the limits of error of the latter.

Correlation of the Thermoelastic Properties

The temperature variation of the isothermal c_{11} and c_{44} for NaCl, KCl and MgO can be expressed by the formula

$$(c_{ii})_u=(c_{ii})_0 \exp\,(-A_{ii}F_{ii}(u)), \qquad (7)$$

where $u=T/\theta$, T is the absolute temperature and θ the characteristic temperature, $(c_{ii})_0$ denotes the value at absolute zero, A_{ii} is a constant of the material, and $F_{ii}(u)$ is a function of (u) which assumes the value unity when $u=1$, *and which is the same for all three substances.*

The forms of the functions $F_{11}(u)$ and $F_{44}(u)$ are indicated in Figs. 1 and 2, in which the observed values of $F_{ii}(u)=(1/A_{ii})\ln((c_{ii})_0/(c_{ii})_u)$ for NaCl, KCl and MgO are plotted as ordinates and corresponding values of u as abscissae. Numerical values of $F_{11}(u)$ and $F_{44}(u)$ are given in Table V. It will be seen that the two are nearly the same, but the difference between them is probably real, for, apart from other considerations, there seems to be no way of ascribing it to systematic error of observation.

The isothermal c_{12} for all three substances is constant, within the accuracy of the measurements, over the entire temperature range investigated, and it can be argued that this

TABLE IV. *The elastic moduli and constants of MgO.*

T°K	Adiabatic Moduli $\times10^{12}$ (cm²/dynes) S_{11}	$-S_{12}$	S_{44}	Adiabatic Constants $\times10^{-11}$ (dyne/cm²) C_{11}	C_{12}	C_{44}	Isothermal $c_{11}\times10^{-11}$
80	3.839	0.855	6.380	29.87	8.56	15.673	29.86
90	3.841	.857	6.381	29.87	8.58	15.671	29.86
150	3.872	.872	6.393	29.72	8.64	15.643	29.67
160	3.880	.875	6.396	29.67	8.65	15.635	29.62
170	3.888	.878	6.399	29.63	8.66	15.627	29.56
180	3.897	.882	6.403	29.58	8.67	15.618	29.51
190	3.906	.886	6.407	29.53	8.68	15.609	29.45
200	3.916	.890	6.412	29.48	8.68	15.599	29.39
210	3.926	.894	6.417	29.42	8.69	15.589	29.33
220	3.936	.899	6.421	29.37	8.70	15.578	29.27
230	3.946	.903	6.426	29.32	8.71	15.566	29.21
240	3.957	.908	6.431	29.27	8.72	15.554	29.14
250	3.968	.913	6.436	29.21	8.73	15.542	29.08
260	3.979	.917	6.442	29.16	8.74	15.529	29.02
270	3.991	.922	6.447	29.10	8.74	15.516	28.95
280	4.002	.927	6.452	29.05	8.75	15.503	28.89
290	4.013	.932	6.457	28.99	8.76	15.490	28.82
300	4.025	.937	6.463	28.93	8.77	15.477	28.75
310	4.037	.942	6.468	28.88	8.78	15.464	28.69
320	4.048	.947	6.474	28.82	8.79	15.451	28.62
330	4.060	.952	6.479	28.76	8.80	15.438	28.55
340	4.072	.957	6.485	28.70	8.80	15.424	28.48
350	4.084	.962	6.490	28.64	8.81	15.410	28.41
360	4.096	.967	6.496	28.58	8.82	15.396	28.34
370	4.109	.972	6.502	28.52	8.83	15.382	28.27
380	4.121	.977	6.508	28.46	8.84	15.368	28.20
390	4.134	.983	6.514	28.40	8.85	15.354	28.13
400	4.147	.988	6.520	28.33	8.85	15.339	28.06
410	4.159	.993	6.526	28.27	8.86	15.324	27.99
420	4.173	.999	6.532	28.21	8.87	15.309	27.91
430	4.187	1.004	6.538	28.14	8.88	15.294	27.84
440	4.200	1.010	6.545	28.08	8.88	15.279	27.76
450	4.214	1.015	6.551	28.01	8.89	15.264	27.69
460	4.229	1.021	6.558	27.95	8.90	15.249	27.61
470	4.243	1.027	6.564	27.88	8.91	15.234	27.53
480	4.258	1.033	6.571	27.81	8.91	15.219	27.46
490	4.273	1.038	6.578	27.74	8.92	15.204	27.38
500	4.289	1.044	6.584	27.67	8.93	15.188	27.30
510	4.304	1.050	6.591	27.60	8.93	15.172	27.22
520	4.320	1.057	6.598	27.54	8.94	15.156	27.14
530	4.335	1.063	6.605	27.47	8.94	15.140	27.06
540	4.351	1.070	6.612	27.40	8.95	15.124	26.98
550	4.367	1.077	6.619	27.32	8.96	15.108	26.90
560	4.383	1.085	6.626	27.25	8.96	15.092	26.82

The isothermal c_{12} is $8.57\pm0.04\times10^{11}$ over the entire temperature range.

[12] A description of this method is given by Born, Enc. d. Math. Wiss., Vol. 3, p. 649. The modification consists in identifying $(z+\zeta)^{-3/2}$ with a fifth degree polynomial over the actual range of values assumed by z, instead of over the range $z=0$ to $z=1$.

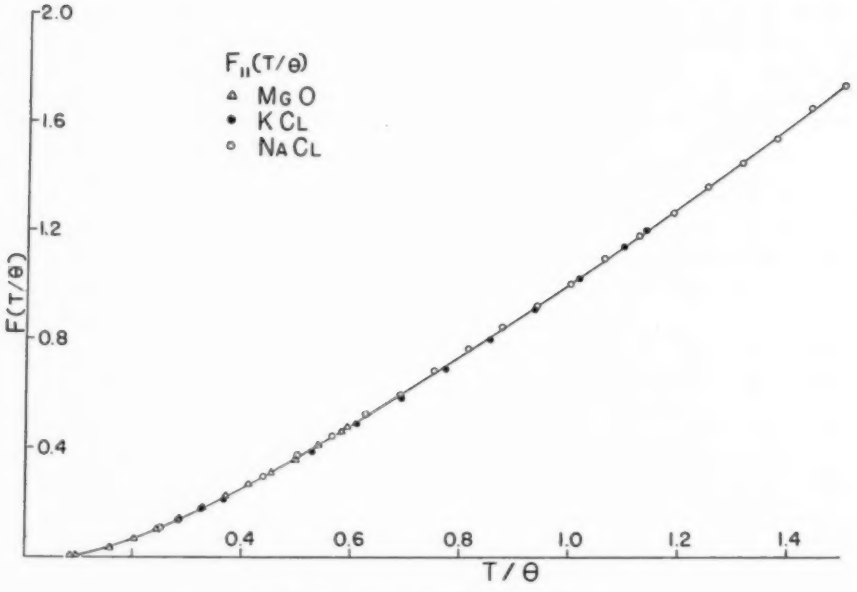

FIG. 1. The characteristic function for c_{11}.

constant value persists clear up to the melting point of the crystal. For at this temperature $c_{11}=c_{12}$, and if the present data are extrapolated, on the assumptions that c_{11} varies linearly with the temperature and c_{12} not at all, to the temperature at which they become equal, one obtains for the melting point of NaCl, 1170°K; of KCl, 1145°K; and of MgO, 2850°K. The observed values are, respectively, 1077°K, 1045°K, and 2800°K to 3100°K.

In order to represent the data as in Figs. 1 and 2 it is necessary to know the values of $(c_{11})_0$ and $(c_{44})_0$ for one of the substances only. Magnesium oxide is chosen, since, as will be evident from a scrutiny of Fig. 3, in this case extremely accurate values can be obtained by extrapolation of the observations above 80°K. The elastic constants of the other substances at absolute zero are calculated from these numbers and the values of the elastic constants which correspond to any two other values of u for which data on magnesium oxide are available. Thus, let $R_1(u', u'')$ denote the quantity $\ln((c_{ii})_{u'}/(c_{ii})_{u''})$ for the substance (1), and $R_2(u', u'')$ the same quantity for the substance (2). Then it follows immediately from Eq. (7) that

$$R_1(0, u'')/R_2(0, u'') = R_1(u', u'')/R_2(u', u'').$$

A_{ii} is calculated with the formula

$$A_{ii} = \ln((c_{ii})_0/(c_{ii})_{u=1})$$

provided $(c_{ii})_{u=1}$ is known, and $F_{ii}(u)$ is then obtained from Eq. (7). Since $(c_{ii})_{u=1}$ for MgO is not known, the A_{ii}'s for this substance are calculated by forcing the single observations at

TABLE V. *Values of the characteristic functions.*

u	$F_{11}(u)$	$F_{44}(u)$	u	$F_{11}(u)$	$F_{44}(u)$
0.1	0.007	0.007	0.9	0.865	0.845
.2	.062	.052	1.0	1.000	1.000
.3	.148	.123	1.1	1.136	1.146
.4	.247	.210	1.2	1.280	1.296
.5	.362	.311	1.3	1.427	1.447
.6	.480	.424	1.4	1.577	1.597
.7	.605	.553	1.5	1.730	1.750
.8	.735	.695			

TABLE VI. *Values of $(c_{ii})_0$ and A_{ii} for the three crystals.*

	$(c_{11})_0\times10^{-11}$	$(c_{44})_0\times10^{-11}$	A_{11}	A_{44}
MgO	29.89	15.679	0.230	0.0920
NaCl	5.85	1.339	.210	.0601
KCl	4.95	.669	.168	.0440

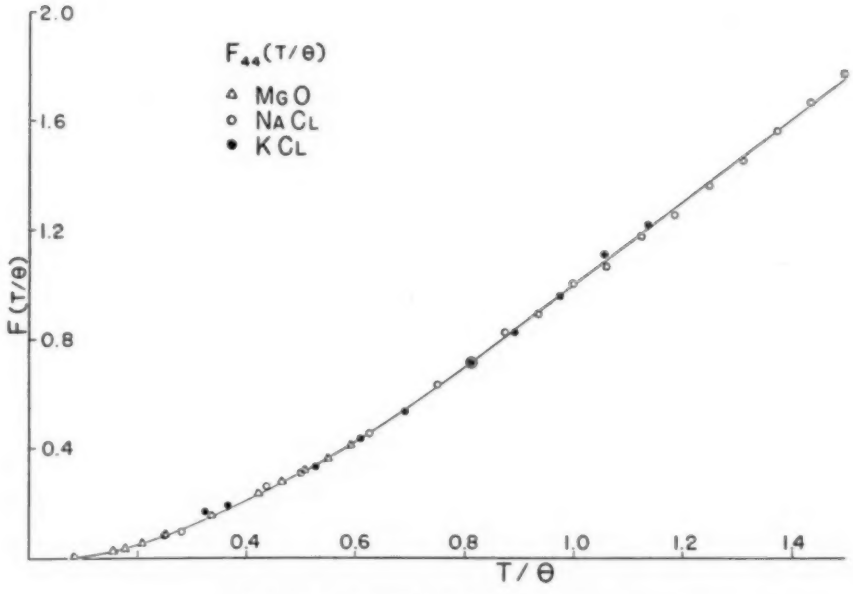

FIG. 2. The characteristic function for c_{44}.

$u=0.592(T=560°\text{K})$ to fit the combined $F_{ii}(u)$ curves of NaCl and KCl. It then appears that the $F_{ii}(u)$ curves of MgO are identical with those of the other two substances. Values of $\frac{1}{4}(c_{ii})_0$ and A_{ii} for the three crystals are given in Table VI.

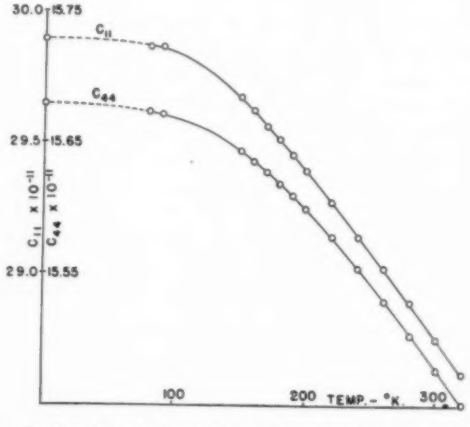

FIG. 3. Showing the method for obtaining the elastic constants of MgO at absolute zero.

It should be noted that a very small variation in the measured value of c_{ii} results in a large departure of the calculated value of $F_{ii}(u)$ from the curves of Figs. 1 and 2. The largest departure there shown indicates a variation of at most 0.2 percent in c_{ii}, and arises from the uncertainty in the terminal digit of the tabulated value. Conversely, the temperature variation of the elastic constants can be calculated from Eq. (7) with greater precision than it can be measured.

In conclusion, the writer desires to acknowledge his indebtedness to Dr. Paul F. Kerr, for the gift of the potassium chloride crystal; to Mr. Raymond R. Ridgway of the Norton Company, who was instrumental in securing the magnesium oxide crystals; and to Dr. S. L. Quimby, at whose suggestion the present research was undertaken, and who followed its progress with helpful counsel and encouragement.

A Mass-Spectrograph Study of Ba, Sr, In, Ga, Li, and Na

MILO B. SAMPSON AND WALKER BLEAKNEY, *Palmer Physical Laboratory, Princeton University*

(Received June 29, 1936)

A mass spectrograph of the 180° type of 22 cm radius has been constructed. The magnetic field of 1400 gauss is supplied by permanent magnets and the accelerating potential by a stabilized rectifier. A mass analysis has been made for a number of elements of the ions obtainable from coated filaments. A peak of Sr at mass 84 comprising 0.5 percent of the total Sr current, and one of Ba at mass 134 comprising 1.8 percent of the total Ba current are concluded to be new isotopes of Sr and Ba, respectively. A search for a third isotope of indium was made but none found. The relative abundances of Ga^{69} and Ga^{71} were determined to be 38.8 percent and 61.2 percent respectively. The existence of Li^5 and Na^{22} recently reported by Brewer was not confirmed. Lower limits were placed on other possible isotopes of these elements.

INTRODUCTION

AT the present time all of the known stable elements have been subjected to analysis by the mass spectrograph. In many cases the spectra were obtained with difficulty and the results are correspondingly inaccurate. Recently Blewett and Jones[1] have succeeded in producing very satisfactory sources of ions from such elements as Ba, Sr, and In and it therefore seemed worth while to investigate the isotopic constitution of these elements in the hope of improving the existing data. Indium is especially interesting since it, like bromine displays three different rates of decay after activation by slow neutrons although only two stable isotopes have been found. A careful search for the stable isotopes Na^{22} and Li^5 was also undertaken with the object of confirming the recent announcement of their discovery by Brewer.[2]

APPARATUS AND PROCEDURE

A mass spectrograph of an unusual type was tried initially but proved unsuccessful. The essential idea was to use crossed electric and magnetic fields over a straight path length of 1 meter. The magnetic field was produced by permanent magnets and the electric field by a potential applied to parallel brass plates. The potentials applied to the condenser plates bore a constant ratio to the field accelerating the ions. The ions followed a trochoidal path, a focus being obtained for ions of a given e/m having the same velocity and entering the analyzer in a nearly parallel beam. Very good resolution was obtained with this arrangement but the peaks were often unsymmetrical or split into several components. The collector current was very unsteady being subject to violent fluctuations. The difficulties were ascribed in part to reflections of the ion beam from the long condenser plates and to wax vapor contaminations causing the surfaces of the plates to charge up to varying potentials. The fluctuation of the current seemed to be related to the intensity of the ion beam striking the deflecting plates. After considerable work with this arrangement it was decided to give it up in favor of the apparatus about to be described.

A mass spectrograph of the 180° focusing type was then constructed with the object of obtaining moderately high resolving power. The magnetic field is supplied by permanent magnets and the accelerating fields are obtained from a stabilized rectifier circuit operating on a.c., and giving up to four thousand volts, constant to a fraction of a volt.

The arrangement of the analyzing chamber is shown in Fig. 1. The positions of the ion source and the collector are indicated in the diagram. The semicircular pole pieces A are pure soft iron, 5 cm wide, 2 cm thick with a mean radius of curvature of 22 cm. The gap between the pole pieces is 9 mm and was made vacuum tight by waxing the two brass strips B which are inset into the two sides of the pole pieces as shown. U-shaped permanent magnets of cobalt steel, made by the Weston Electrical Instrument Corporation, were spaced as closely as possible on the inside of the circle, and the spacing of the outside magnets was arranged to give as nearly

[1] Blewett and Jones, Washington Meeting, Phys. Rev. **49**, 881 (1936).
[2] Brewer, Phys. Rev. **49**, 635, 856 (1936).

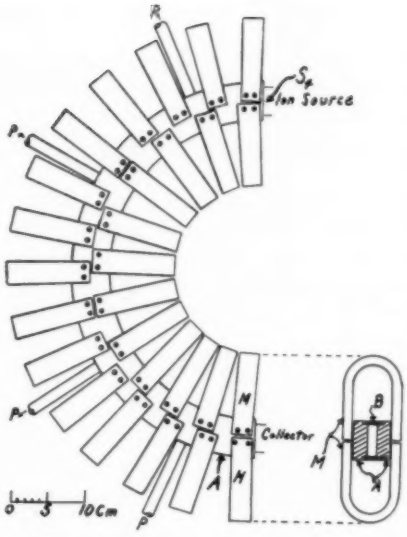

FIG. 1. Magnetic analyzing chamber.

uniform flux density as possible over the pole pieces. The field obtained in the gap was about 1400 gauss and was uniform insofar as could be ascertained by rough measurements with a search coil. In the case of lithium a third of the magnets were removed in order to bring the ions into the voltage range available. Sharp peaks were still observed with the wider spacing of the magnets. Three diaphragms were placed at equal intervals in the analyzing chamber in order to limit the angular spread of the ion beam to 2°. The central diaphragm was made adjustable from the outside and could be used to define the beam still more closely. The chamber was evacuated by two mercury pumps connected to the four pump leads P. The mercury vapor was trapped out with liquid air. A separate pump was connected to the tube containing the filament and accelerating slit assembly. The waxed joints were all made with Apiezon-W wax and the pressure reading on an ionization gauge was always between 1 and 2 times 10^{-6} mm of Hg.

Fig. 2 shows the arrangement of the ion source and the manner in which the output of the voltage regulator circuit is applied to the accelerating slits. The three slits S_1, S_2, S_3, and the two pairs of deflecting plates D_1 and D_2 were fastened to tungsten leads which were sealed into a Pyrex tube, the unshielded parts of which were coated with Aquadag and grounded to S_1. The filament was mounted on a ground glass joint and could be quickly removed for recoating. The filament F was of platinum foil 2 mm wide by 5 mm long, placed across the slit S_1 to make the voltage distribution of the ions as small as possible. G is a guard ring placed in the plane of the filament and connected to one side of it. It was found that the use of this guard ring increased the fraction of the total current that passed through S_1 considerably. The slits S_1, S_2, and S_3 were 1.5 mm by 1 cm. The two pairs of deflecting plates D_1 and D_2 were 1.5 cm apart and had the correct voltage applied to them to counteract the stray magnetic field at the end of the magnets. These two sets of deflecting plates permit the adjustment of both the position and direction of the ion beam striking the slit S_4.

The primary circuit of the transformer supplying the full wave rectifier contained an Acme-Delta voltage regulator to help stabilize line fluctuations. The rectified current from the two R.C.A. 879 tubes was passed through a voltage regulating circuit of the type described by Evans.[3] In this case however a 2A5 tube was used with a plate current of from 1 to 4 milliamperes. This was sufficiently large to prevent the very small fluctuations of the positive ion current (i.e., the load) from producing a perceptible change in the voltage. Large voltage changes

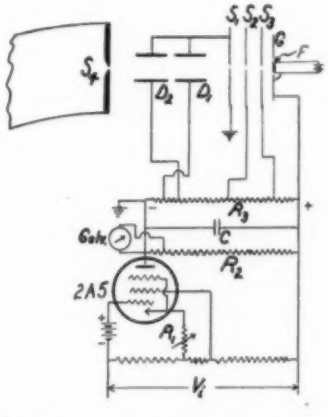

FIG. 2. Diagram showing arrangement of ion gun and connection to the voltage regulator. V_f is the filtered output of the rectifier unit.

[3] R. D. Evans, Rev. Sci. Inst. **5**, 371 (1934).

were obtained by changing the taps on R_3 while continuous changes were made by varying R_1. The changes in the total accelerating voltage were measured with a galvanometer connected across a small section of the ten megohm wire wound resistor R_2. Considerable trouble was experienced with high frequency oscillations in the output of the regulator circuit. Placing a capacity of 2.5 microfarads across the resistor R_3 served to eliminate this difficulty.

The filament source of positive ions was heated by a storage battery and the total emission was generally a few tenths of a microampere. The voltages applied to the accelerating slits, obtained from taps on the resistor R_3, were such as to focus the ions into a parallel beam. The potentials for the deflecting plates were taken from the same voltage divider so that a constant ratio to the accelerating voltage was obtained. This arrangement is desired in order that ions emerging through the final slit shall have traversed the same path regardless of the e/m selected.[4]

The entrance and collector slits were made of phosphor-bronze, a nonmagnetic material, and the edges were beveled to prevent reflections of the ions. The entrance slit S_4 was set at 0.1 mm, and the collector slit at 0.2 mm. The collector was a Faraday cage connected to the grid of a Western Electric D-96475 electrometer tube. The amplifier circuit was that described by Penick,[5] and was used at a sensitivity of 2 times 10^{-17} ampere per millimeter. In the curves shown the positive ion currents to the electrometer tube are plotted against accelerating voltage. The peaks were so sharp that only a few points could be taken on the sides of them. Because of the width of the collector slit with respect to the entrance slit the tops of the peaks were slightly flat and quite accurate readings were obtained for relative abundance measurements as long as the filament emission was low enough to prevent space charge limitation of the positive ion current.

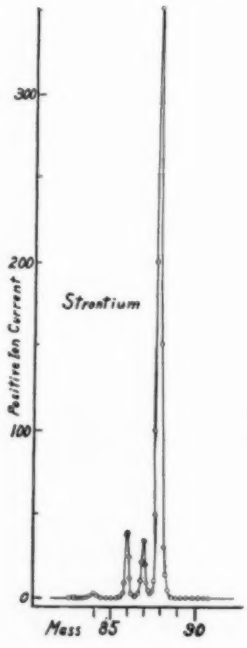

FIG. 3. Mass-spectrum plot of Sr.

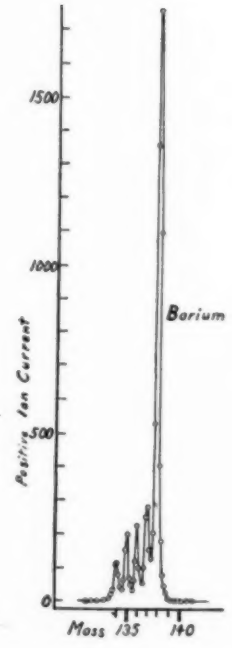

FIG. 4. Mass spectrum of Ba.

RESULTS

Strontium and barium

Figs. 3 and 4 show the mass-spectrograph plots of the strontium and barium isotopes. The ions were produced by the method described by Blewett and Jones.[1] The peaks at mass numbers 84 and 134 for strontium and barium, respectively, are evidence for new isotopes of these elements.[6] The peaks are quite symmetrical and well resolved. The widths of the peaks at the base are probably due to the velocity distribution of the ions and to slight inhomogeneities in the magnetic field due to the gaps in the spacing of the magnets on the pole shoes. These new peaks cannot be attributed to hydrides since they fall on the low mass side of the known isotopes. Neither can they be satisfactorily explained as impurities since the only isotopes in this region belong to krypton and zenon. The heights of the new peaks relative to the element in question were constant under all conditions. It is therefore concluded that they represent true isotopes of strontium and barium respectively. The abundances found for the strontium isotopes are tabulated below together with the upper limits placed on the presence of other possible isotopes.

[4] Bleakney, Am. Phys. Teacher **4**, 12 (1936).
[5] D. B. Penick, Rev. Sci. Inst. **6**, 115 (1935).
[6] Blewett and Sampson, Phys. Rev. **49**, 778 (1936).

Mass number	82	83	84	85	86	87	88	89	90
Percentage	<0.05	<0.1	0.5	<0.05	9.6	7.5	82.4	<0.2	<0.05

Assuming a packing fraction of -8.2 the atomic weight for strontium comes out to be 87.62 which is to be compared with the chemical value 87.63. The peak at mass 134 comprises 1.8 percent of the total barium ion current. Our relative abundance measurements on barium were not very accurate but on combining our results with Aston's and taking a packing fraction of -6.1 we get 137.36 for the atomic weight in exact agreement with the chemical value. The limits placed on other possible barium isotopes are given below.§ The percentages given are the upper limits set on the existence of other possible isotopes.

Mass number	132	133	139	140
Percentage	<0.05	<0.1	<0.25	<0.1

Indium

Fig. 5 shows the curve for indium which has also been previously reported.[6] A very careful search was made for a possible new isotope since its existence is indicated by the observation of three radioactive periods of decay, induced by bombardment with neutrons.[7] Only two of these periods have been definitely shown to be sensitive to slow neutrons. The abundance of the two known isotopes was found to be 21 ± 1 for the ratio of 115 to 113. The limits placed on other possible indium isotopes are as follows.

Mass number	110	111	112	114	116	117	118	119
Percentage	<0.01	<0.01	<0.02	<0.5	<0.02	<0.02	<0.012	<0.003

Gallium

Gallium ions were obtained by coating a platinized tungsten spiral with a water paste of gallium sesqui-oxide.[1] Large peaks of sodium and potassium ions were at first observed but on heating the filament to about 1800°C for some time they disappeared and gallium ion peaks at masses 69 and 71 were observed. The ion intensity however was too small to allow any search for new isotopes. The percentage abundances of the two known isotopes were found to be 38.8 percent and 61.2 percent, respectively, with an error of ±1 percent. These values are in agreement with Aston.[8]

Lithium

Brewer[2] has recently reported evidence for the existence of a lithium isotope of mass 5. An attempt has been made to check his results. Fig. 6 shows the curve obtained for lithium. The peak at mass 7 is 100,000 cm high. The background becomes zero at a small distance from the mass 6 peak as shown in the magnified portion of the curve. A peak 1 cm high should have been observed had it been present so it may be concluded from this experiment that lithium 5 is present to less than 1 part in 100,000 of lithium 7. This is thought to be a conservative estimate. Dr. Blewett of this laboratory has also attempted to find Li^5 with an apparatus very similar in size and arrangement to that used by Brewer. Although his resolving power and background were not as favorable as ours, his total intensity was much greater. He believes one part in 200,000 would have been detectable but could find no trace of Li^5. We are indebted to Dr. Blewett for allowing us to mention his results in this connection.

Sodium

Brewer[2] has also reported the existence of an isotope of sodium of mass 22 present to 1 part in 5000 of sodium 23. The possibility of a stable sodium isotope of mass 22 is particularly interesting since it has generally been thought to be unstable, disintegrating with emission of a positron. Meitner[9] and Frisch[10] have obtained evidence for this positron emission. Laslett[11] has also obtained a positron emitter by a different disintegration process, which he attributes to sodium 22. He has determined the half-life to be about 9 months.

Fig. 7 shows one of the curves obtained in a careful search for Na^{22}. There is a small back-

§ *Note added in proof:* After this paper had gone to press a note by Dempster, Phys. Rev. **49**, 947 (1936) appeared in which he confirmed the existence of Ba^{134} and reported two new isotopes at masses 132 and 130. Using a new type of source we also find these new isotopes and have succeeded in measuring their abundances in the third and fourth orders giving the following results:

Mass number	130	132	134	135	136	137	138
Percentage	0.16	0.015	1.72	5.7	8.5	10.8	73.1

The atomic weight calculated from these abundances comes out to be 136.35.

[7] Szilard and Chalmers, Nature **135**, 98 (1935).

[8] Aston, Proc. Roy. Soc. **A149**, 396 (1935).

[9] Meitner, Naturwiss. **22**, 420 (1934).

[10] Frisch, Nature **136**, 220 (1935).

[11] Laslett, Seattle Meeting, Am. Phys. Soc. June, 1936, paper No. 22.

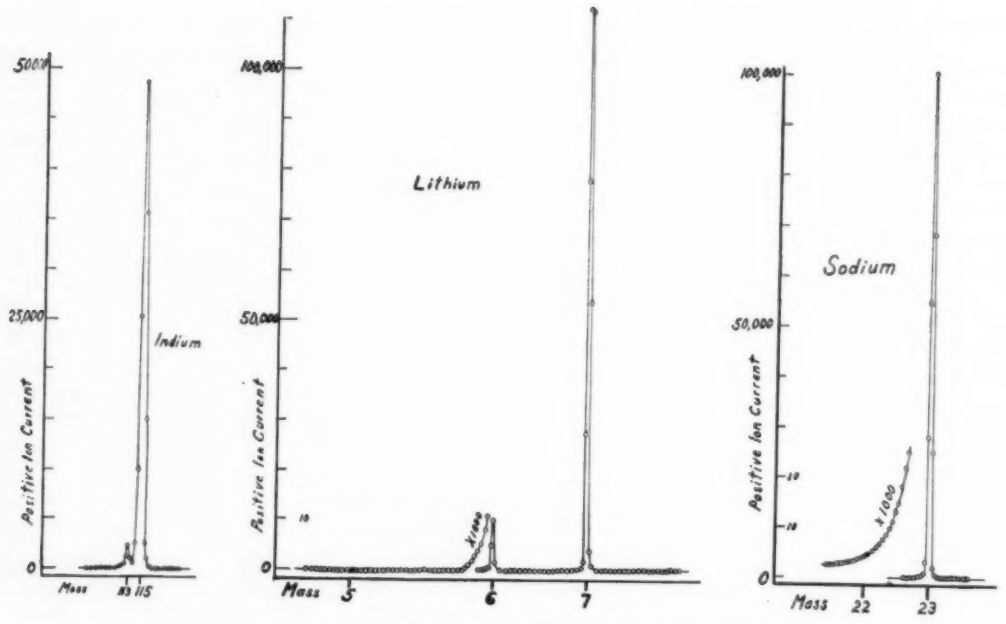

FIG. 5 (left). Mass spectrum of In.
FIG. 6 (center). Mass spectrum of Li. Curve in region of mass 5 is magnified 1000 times.
FIG. 7 (right). Mass spectrum plot of Na. Region of mass 22 magnified 1000 times.

ground of about 2 cm at the mass 22 position. A peak of 2 cm above the background could easily have been detected and it is concluded that Na^{22} is present to less than 1 part in 50,000 of sodium 23. The fact that our apparatus was working properly is indicated by an analysis of potassium which showed the isotope at mass 40, recently reported by Nier,[12] to be clearly resolved and of the right abundance, as measured by Nier[12] and Brewer,[13] in spite of the much higher background than that in the case of either lithium or sodium.

It seems impossible to reconcile our results with those of Brewer unless Li^5 and Na^{22} are present to a much smaller degree than reported, or that the peaks he observes are spurious, possibly due to a reflection of some sort. Spurious peaks have very often been found with our mass spectrograph but careful adjustment, and proper shielding and alignment have served to eliminate them. Moreover while many peaks have been found to be only ghosts, in no case have we been able, by improper adjustment, to make a true isotope disappear from the mass spectrum.

We are indebted to Mr. Briggs E. Napier for his help in constructing the rectifier. It is a pleasure also to acknowledge the many helpful discussions and the assistance of Dr. A. Bramley during part of this work. This research was aided by a grant from the American Philosophical Society for which we express our appr ciation.

[12] A. O. Nier, Phys. Rev. **48**, 283 (1935).
[13] Brewer, Phys. Rev. **48**, 640 (1935).

Diffusion of Slow Neutrons

D. S. Bayley, B. R. Curtis, E. R. Gaerttner and S. Goudsmit, *University of Michigan*

(Received June 29, 1936)

The effect of a few elements on the diffusion of slow neutrons in water is investigated. The interpretation of data on the back scattering of neutrons is discussed.

THE results of most experiments on the absorption and scattering of slow neutrons depend very much on the detectors. In the hope to eliminate this difficulty we performed the following experiments.

A radon beryllium neutron source (200–60 mc) was placed in a cylindrical tank of water (diameter 56 cm, height 80 cm). A detector was placed in a radial position at 6 cm from the axis and its activity observed.[1] Next, the activity of the detector was measured again, but now with a layer of an absorber placed against one side of it. The idea was that the presence of the absorber would lower the density of the diffused neutrons in the neighborhood, without changing the velocity distribution. Therefore the change in activity of the detector would give direct information about the change in density. Unfortunately this ideal situation is not quite realized in the present experiments. The Maxwellian distribution will only be reestablished if the detector is placed at a few mean free path lengths away from the scatterer. The observed change in activity is very large for silver, much smaller for copper, and hardly observable for carbon. These differences show especially well if the thicknesses of the layers are expressed in gram atoms/cm² as is done in the accompanying graphs (Figs. 1, 2, 3 and 4). The graphs also show the intensity of the detector when it is placed between two layers of absorbing or scattering materials.

In order to test further the influence of cadmium on the diffusion of neutrons, we placed a cadmium sphere inside the tank and investigated the intensity of a rhodium detector in its neighborhood. Figs. 5, 6, and 7 show the neutron distribution without and with the cadmium sphere present, along the radius of the cylindrical tank and in a direction perpendicular to this radius.

The results obtained show that the change in intensity of the detectors is not just due to a screening off from one side, but the scatterers and absorbers cause an actual change in the neutron density. This change must also be present in back scattering experiments of the type done by A. C. G. Mitchell and his co-workers.[2] As a result, the coefficient of scattering given by them must be much too large because the presence of the

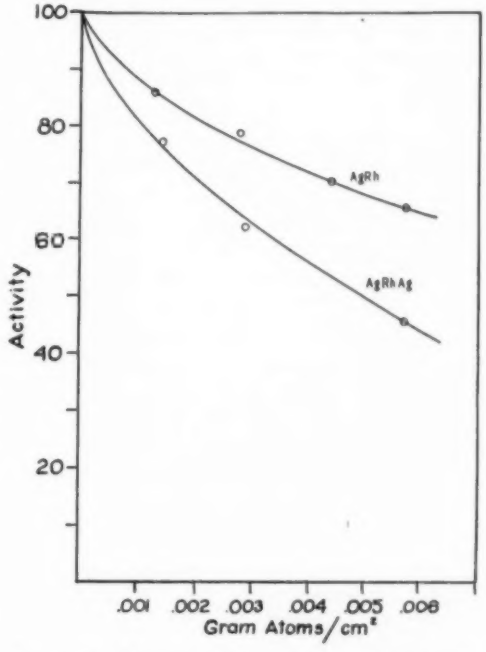

FIG. 1. The decrease of the activity of a rhodium foil (0.30 gram/cm²) against (AgRh) and between layers of silver (AgRhAg) of various thicknesses. The foil and layers were placed radially in a cylindrical tank filled with water, which had the neutron source at its center.

[1] The activity was measured with an ionization chamber placed on an Edelmann electrometer. The drift of the fiber was observed visually and recorded with a chronograph, which facilitated the measurements and increased the accuracy.

[2] A. C. G. Mitchell, E. J. Murphy, L. M. Langer and M. D. Whitaker, Phys. Rev. **48**, 653 (1935); **47**, 881 (1935); **49**, 400 (1936); **49**, 401 (1936).

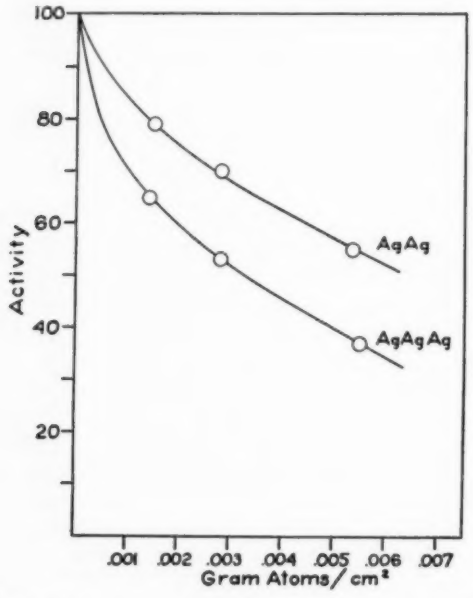

FIG. 2. The decrease of the activity of a silver foil (0.14 gram/cm²) against (AgAg) and between layers of silver (AgAgAg).

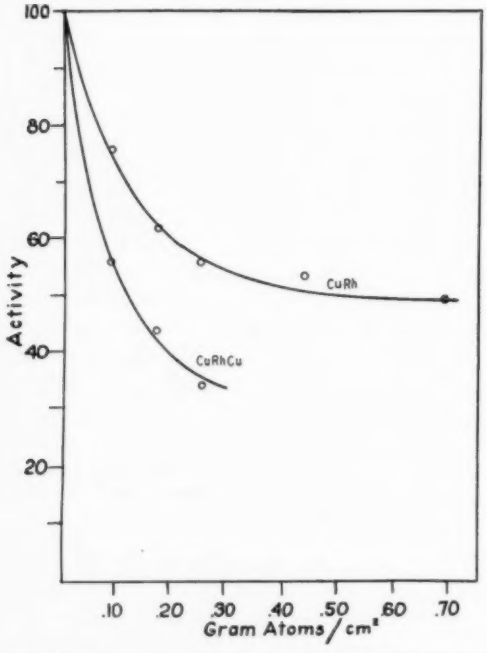

FIG. 3. The decrease of the activity of a rhodium foil (0.30 gram/cm²) against (CuRh) and between layers of copper (CuRhCu).

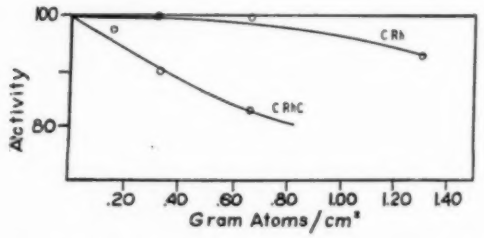

FIG. 4. The decrease of the activity of a rhodium foil (0.30 gram/cm²) against (CRh) and between layers of carbon (CRhC).

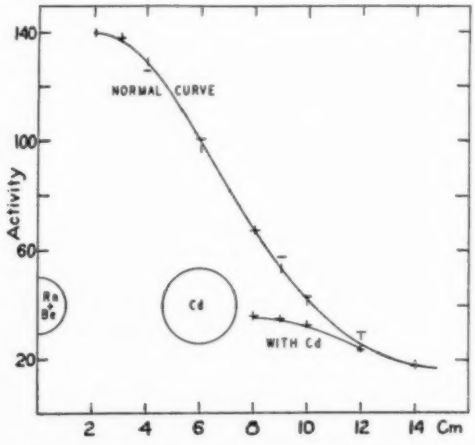

FIG. 5. The activity of a rhodium foil (0.30 gram/cm²) as a function of the distance from the neutron source in a cylindrical water tank (28 cm radius, 80 cm deep) with and without a solid cadmium sphere (1.4 cm radius) at 6 cm from the source. The foil was placed perpendicular to (1) and along the radius (—) of the tank.

scatterer will usually increase the density of the neutrons in the paraffin right behind it. Or differently stated, the neutrons scattered back by the scatterer will again be returned through the detector by the paraffin. The error introduced this way may be 80 percent according to an estimate of this paraffin reflection by Amaldi and Fermi.[3]

If the original number of slow neutrons (for instance of group C of Amaldi and Fermi) is denoted by N, the fractions scattered back from the scatterer and the paraffin by s and S, and the fraction transmitted by the detector by τ, it follows that the number of neutrons traversing the detector from the side of the paraffin is

[3] Amaldi and Fermi, Ric. Scient. **2**, 544 (1935).

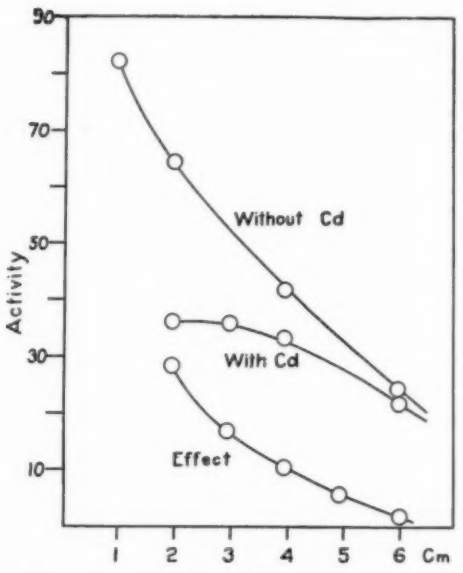

FIG. 6. The effect of a solid cadmium sphere on the activity of the rhodium foil in a cylindrical tank of water as a function of the distance from the center of the sphere measured along the radius of the tank.

$N/(1-\tau^2 sS)$, from the side of the scatterer $N\tau s/(1-\tau^2 sS)$. This expression is, of course, only qualitatively correct. It does not take into account such complications as arise, for instance, from the change of the velocity distribution in the process of scattering. If these corrections could be made with some certainty, the back scattering from thick layers would provide a way to obtain the ratio between absorption (σ_a) and scattering cross section (σ_s). The fraction scattered back is given by

$$(2\sigma_a+\sigma_s)/\sigma_s-\{((2\sigma_a+\sigma_s)/\sigma_s)^2-1\}^{\frac{1}{2}}.$$

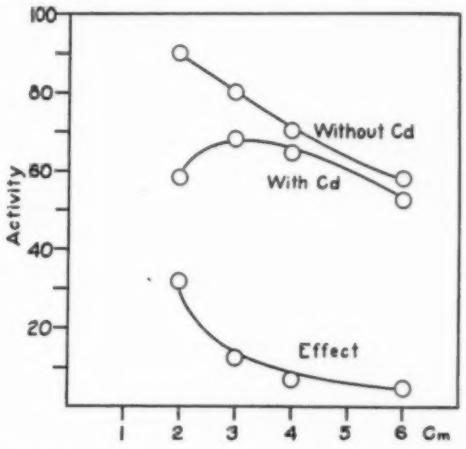

FIG. 7. The same as Fig. 6, but measured in a direction perpendicular to the radius of the tank.

The following experiment showed that the back-scattering from the paraffin is large. The source and a detector foil were both placed on a paraffin cylinder. The intensity of the foil was measured without and with a similar second cylinder covering the first. A large increase in the intensity was observed, but this increase depended upon the size of the gap between the two cylinders and the position of the foil. When the gap was about 2 cm and the foil placed vertically at the edge of the cylinder (to avoid changes due to absorption of the foil itself) the increase was about seven times for Rh. If the foil is placed flat on, and between, the cylinders its absorption causes this increase to be only 3 to 5 times for Rh, depending on the place of the foil. If we ascribe the increase to slow neutrons only, the reflection of paraffin would be about 70 percent.

Filament Sources of Positive Ions

J. P. BLEWETT, *Princeton University, Princeton, New Jersey*
AND
ERNEST J. JONES, *Bureau of Chemistry and Soils, Department of Agriculture, Washington, D. C.*
(Received June 29, 1936)

Efficient filament sources of ions of the alkali metals have been produced by heating synthetic alkali aluminum silicates. Studies of emission of the lithium sources as a function of composition reveal that the silicate 1 Li_2O : 1 Al_2O_3 : 2 SiO_2 is the most satisfactory ion emitter. Similar sources of the other alkalies prove stable and copious. Ions of Mg, Ca, Sr, Ba, Al, Ga, In, Ti, V, Mn, Y, and Ce, are emitted when the oxide of the metal in question is heated to a white heat on a tungsten filament. The O_2^- peak observed by Barton has been checked. In the case of aluminum, negative ions of mass 27—presumably Al^-—were observed.

INTRODUCTION

A NUMBER of methods are known by which ions can be produced in sufficient quantities for mass spectrograph analyses. If the substance to be studied can be used as a vapor, it is a simple matter to produce ions by collisions with slow electrons. For production of ions of solid substances, several gas discharge methods are available, in particular the very fruitful "anode-ray" method used by Aston. However, it has proved difficult in many cases, for instance with the alkaline earths, to obtain ions in large quantities. Still another method for the production of positive ions is the hot filament, and it is with this type of source that the present paper is concerned. The emission of positive ions from hot filaments is a well-known phenomenon, discussed at some length by Richardson[1] as long ago as 1916. It has been studied mainly from the point of view of determining what ions are emitted from various compounds; glass, for example, has been a favorite object of study. But there have been very few attempts to develop filament sources of ions of particular elements. Perhaps this is because the absence of multiply charged ions is a drawback in using such sources for the study of isotopes. Nevertheless some good results have been obtained by this method[2] and in the hope that copious filament ion sources may be valuable both in measurements of relative abundance of isotopes and in the accurate determination of masses, we undertook the work reported in this paper. We have attempted to develop sources that are fairly copious and whose emission is reasonably free from ions of other elements. Except in two or three cases, no claim can be laid to the discovery of new types of emission. Nevertheless, it is hoped that the methods described here may prove useful, not only in mass spectroscopy, but also in other branches of research which deal with phenomena associated with beams of positive ions.

APPARATUS

The substances whose emission was to be studied were coated on filaments which took the form either of platinum strips or mesh, or of tungsten spirals. They were about 15 mm long and 1 to 2 mm in width and were heated directly. The techniques employed in preparing the filaments will be described below in connection with the particular materials investigated.

The ion beams were analyzed in the Dempster type mass spectrograph described by one of us[3] in connection with the analysis of bromine. The ion source described there was removed, and a filament source consisting of the filament under consideration and a drawing out slit was inserted behind the analyzing slit. A constant drawing out voltage of 100 volts was applied between filament

[1] O. W. Richardson, *The Emission of Electricity from Hot Bodies* (Longmans Green and Co., London, 1916), second edition, 1921, Chap. VIII. For a more up-to-date discussion and bibliography of this type of work see Reimann *Thermionic Emission* (Wiley, New York, 1934), Chap. VI, or Jones, *Thermionic Emission* (Methuen, London, 1936), Chap VI.

[2] Cf. Dempster, Phys. Rev. **11**, 316 (1918); Barton, Harnwell and Kunsman, Phys. Rev. **27**, 739 (1926); Kunsman, J. Frank. Inst. **203**, 635 (1927); Cottrell, Kunsman and Nelson, Rev. Sci. Inst. **1**, 654 (1930); Bainbridge, J. Frank. Inst. **212**, 317 (1931); Powell and Brata, Proc. Roy. Soc. **A141**, 463 (1933).

[3] Blewett, Phys. Rev. **49**, 900 (1936).

and first slit, and the analyzing voltage of 300–500 volts was applied between the first slit and the analyzing slit. The filament and drawing out slit were supported on a ground glass joint which was made vacuum tight with stopcock grease. This arrangement made changing the filament a comparatively simple task. As a rule the filament was mounted across the analyzing slit so that only the emission from a short section entered the mass spectrograph. This method was adopted since an appreciable voltage was required to heat the filament, and if ions from the whole filament entered the analyzer, their energy distribution would considerably decrease the resolving power.

Alkali Ion Sources[4]

That alumino-silicates of the alkalies could be used as ion sources has been observed by Hundley[5] and Bainbridge.[2] Preliminary experiments soon proved that these compounds were among the best thermionic sources of ions yet tried. On the basis of these observations it was thought worth while to study the emission of positive alkali ions from the corresponding alumino-silicates in some detail with the object in view of stabilizing and increasing the emission and obtaining some information concerning the mechanism of the process.

Lithium was chosen as the alkali best suited for such a study since the ternary system $Li_2O \cdot Al_2O_3 \cdot SiO_2$ had been studied by several workers,[6] and thus the composition of the various compounds existing in this system are known.

Various compositions were made by melting Li_2CO_3, $Al(NO_3)_3 \cdot 9H_2O$, and pure powdered quartz together at about 1400°C. The melts were then powdered and remelted. The repeated devitrification technique necessary in phase diagram studies was, however, not carried out in this work. After preparation the compounds were examined under the polarizing microscope and were found to consist predominantly (90 percent) of the desired phase. These observations were verified by x-ray photographs.

The compound to be tested thermionically was then powdered and 0.25 g were mounted on a filament of platinum gauze 1 cm² in area. Water was used as a binder. The apparatus used has been described elsewhere.[7] The accelerating potential used was 1500 volts so that the current would be approximately emission limited.

The compounds varied widely in their positive ion characteristics. In general the ternary compounds were considerably better than the binary ones. The most satisfactory one of all was β-eucryptite ($1\ Li_2O \cdot 1\ Al_2O_3 \cdot 2\ SiO_2$) which gave at a particular temperature about twice the current as dids podumene ($1\ Li_2O \cdot 1\ Al_2O_3 \cdot 4\ SiO_2$). Currents as great as 1.0 milliampere were readily obtained from β-eucryptite at a temperature 170° below its melting point. The emission was constant at this value for an hour but of course decreased gradually over longer periods of time. Life tests were made on some of the better sources. One of them, spodumene, gave considerable emission after 72 percent of the lithium had been emitted as positive ions, and the indication is that 90 percent of the lithium could be evolved as positive ions.

Samples of spodumene and eucryptite examined after ten percent and 40 percent of the lithium had been emitted showed the presence of at least two phases. In each case x-ray diffraction patterns showed some of the original compound. From these results it would seem that the filament remains essentially in equilibrium in the ternary system. This is not unexpected since the temperatures are close to the melting points and any unstable phase that might initially appear as a result of the compound losing lithium ions would tend to come to equilibrium during the time of the experiment.

The work function was determined for some of the better sources and gave the value of about 4 volts which within the limit of error was the same for all compounds tested. The work function decreased slowly with time, and Fig. 1 shows a typical curve for β-eucryptite which, when 60 percent of the lithium was emitted, gave a value for the work function of about 2.70 volts.

The ease with which these compounds emitted positive ions indicated that perhaps a clue to the mechanism of the ion emission could be found in

[4] This section is the result of some work done by one of us in collaboration with Dr. S. B. Hendricks, Phys. Rev. **44**, 322 (1933).

[5] Hundley, Phys. Rev. **30**, 864 (1927).

[6] Ballo and Ditler, Zeits. f. anorg. chemie **76**, 39 (1912); Jaeger and Van Klooster, Proc. Am. Acad. **16**, 857 (1914); **17**, 239 (1914); **17**, 251 (1914).

[7] Jones, Phys. Rev. **44**, 707 (1933).

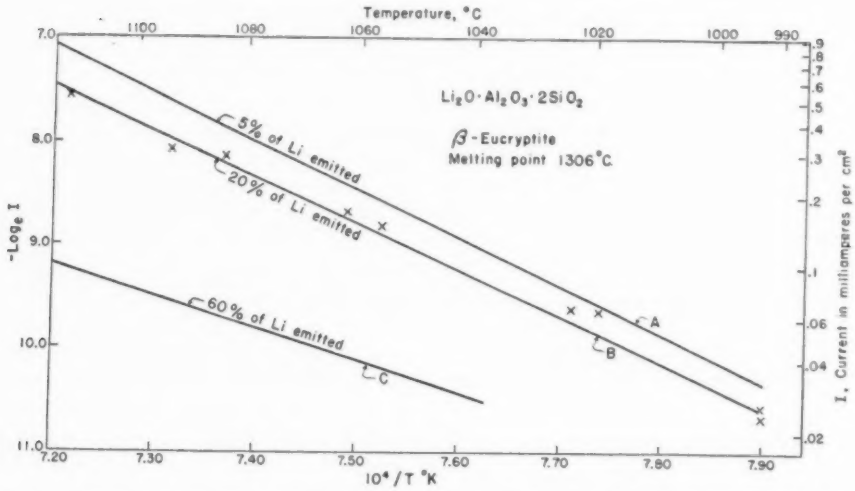

FIG. 1. Thermionic analysis of β-eucryptite. The crosses are the experimental points for curve *B*, showing the typical spread of observed points.

their crystal structures. These structures are not well known but rather probably are three dimensional networks of aluminum-oxygen-silicon ions and possess large "holes" in which the alkali ion is situated; the coordination number of the ion being probably 6 to 8. The alkali ion is therefore comparatively free to migrate within this lattice, and with the aid of small electrolytic potentials which are bound to be present it migrates to the surface and is emitted easily as indicated by the low work function. In order for the lattice to remain neutral, negative charges must leave the lattice also; reversal of potential did not yield any negative current, and the supposition is that the oxygen ions give up their electrons to the platinum strip and escape as neutral molecules. The amount of lithium emitted as positive ions precluded the possibility of any appreciable vaporization of it in any other forms (lithium atoms, LiO molecules, etc.) from the filament.

In preparing any of the other alkali ion sources one is handicapped by the lack of information concerning the ternary systems involved with the exception of the $Na_2O \cdot Al_2O_3 \cdot SiO_2$ system which has been completed. As an empirical rule, however, one can prepare the eucryptite analog of the particular alkali, i.e., 1 R_2O: 1 Al_2O_3: 2 SiO_2 and enrich it with R_2O to the point where the enhancement of the emission ceases. A potassium ion source was prepared with the composition 3 K_2O: 1 Al_2O_3: 3 SiO_2 which proved to be quite satisfactory though no attempt was made to determine the composition having optimum emissivity.

Table I shows the composition of the various compounds prepared and tested, and are given in the order of decreasing emissivity.

Mass-spectrograph analyses were made of the emission from the 1 R_2O: 1 Al_2O_3: 2 SiO_2 sources of all five alkali metals, and the synthetic sources were found to give an emission of ions of the desired element free from more than one or two percent impurity of the other alkalies. They are thus considerably superior to the natural minerals (spodumene. jadeite, leucite, pollucite) which have been widely used as alkali ion sources and whose emissions are frequently found to include ten percent or more of ions of the other alkalies. Presumably the purity of the ion emission is simply a function of the purity of the chemicals employed.

TABLE I. *Emissivity of the various lithium compounds.*

Li_2O	Al_2O_3	SiO_2
1	1	2 Eucryptite
1	1	4 Spodumene
1	1	6
2	1	5
3	1	3
1	0.12	1.6
1	0	1

Sources of Other Ions

For the production of ions of other elements than the alkalies, the oxides of the metals in question were chosen as a rule because of their stability and high melting points. Other compounds which were tried often evaporated or decomposed before temperatures high enough for ion emission were reached.

The oxides were coated on helical spiral filaments of 5-mil tungsten wire, using only water as a binder. Strontium and barium oxides, however, attacked the tungsten at comparatively low temperatures and the filaments burned out below 1500°C. This difficulty was overcome by coating the tungsten filament with a thin layer of platinum. Liquid platinum chloride was painted on the tungsten and then burned off with a Bunsen flame. This technique was used in all subsequent work.

The results obtained for the various elements were as follows:

Magnesium

Magnesium ion currents of the order of 10^{-8} amp. were drawn from a filament coated with MgO when the filament was raised to a white heat. A set of observations of the Mg isotopes is plotted in Fig. 2. Peaks also appeared at masses 23 and 27, the mass 23 peak being due to the sodium impurity which appeared in all filaments, and 27 probably belonging to an aluminum impurity.

Calcium

Fig. 2 also shows the isotopes of calcium observed when CaO was heated to a white heat. The potassium peaks at 39 and 41 always appeared but seemed to become smaller with continued running. However, they never became sufficiently small to make possible a thorough search for Ca^{41}. The ratio of the heights of the potassium to the calcium peaks could be adjusted at will by varying the filament temperature. Andradite and grossularite, natural minerals which contain calcium, were heated to see whether they might serve as copious ion sources, but the potassium impurity peaks were so large as to obscure the whole range.

Strontium

Strontium ion currents of 10^{-8} amp. or more were drawn from a SrO coated filament. A peak was observed at mass 84 which we believe to be due to a new isotope. The evidence supporting this hypothesis has already been presented in the *Physical Review*.[8] A small impurity of rubidium appeared in one sample, but was not present when especially pure strontium oxide was used.

Barium

Barium oxide behaved in much the same manner as strontium oxide, and a peak was observed at mass 134 in addition to the peaks corresponding to the known isotopes. This is believed to be due to a new isotope of barium as reported in the reference above.[8]

A search over the negative ion range was made for both the strontium and barium sources and a small peak was detected in both cases at mass 32. This peak has been observed by Barton,[9] who

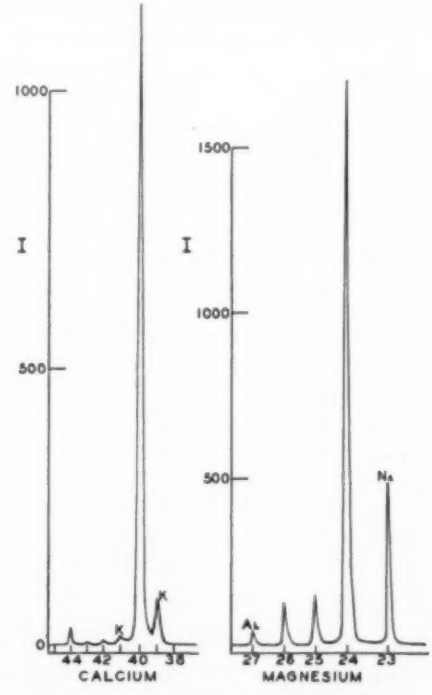

FIG. 2. Mass-spectrograph analysis of emission from magnesium and calcium filament sources.

[8] Blewett and Sampson, Phys. Rev. **49**, 778 (1936).
[9] Barton, Phys. Rev. **26**, 360 (1925).

suggests that it is due to O_2^-. It was of the order of 1/100 of the size of the positive ion peaks and increased very little in height as the filament temperature was raised.

Aluminum

Aluminum ions were obtained in large quantities from Al_2O_3. The emission began to be appreciable for a filament temperature of about 1400°C and increased to almost a microamp. at about 1600°C. A search over the negative ion range revealed only one peak, at mass 27, appearing at the same temperature as did the Al^+ peak. It is difficult to account for this peak unless it is assumed that it is due to Al^-. Its height varied relative to the positive ion peak, but in general it was of the order of 1/100 as high as the Al^+ peak. Attempts at measurements of work function for the two peaks indicated work functions of the same order of magnitude for the two types of emission. It should be noted also that a search for negative ions from the magnesium ion source which had shown a mass 27 impurity revealed only one negative ion peak, which appeared at mass 27.

Gallium[10]

Ga_2O_3 proved a much weaker source of ions, but at temperatures in excess of 1800°C sufficiently high ion currents were obtained to show up the known isotopes of gallium.

Indium

In_2O_3 was the most copious ion emitter observed, with the exception of the alkalies. Indium ions came off in large quantities at very low temperatures, the ion emission becoming appreciable around 900°C and increasing rapidly to be of the order of microamps. An isotopic analysis of indium has been reported[8] and curves are given in a forthcoming paper by Sampson.[11] The negative ion emission due to Al_2O_3 inspired a search for negative indium ions, but none was observed.

Other elements

Ion currents of the order of 10^{-10} amp. were drawn from oxides of Ti, V, Mn, Y, and Ce, but the emission was very unsteady and was thoroughly unsuited to use with mass spectrographs which employ electrical detection.

No ions except those of alkali impurities could be detected from SiO_2, BeO, beryl, Er_2NO_3, ZrO_2 or B_6C although the filaments carrying these salts were heated to about 2500°C. ZnO refused to stay on a filament above about 1400°C. Filaments carrying $Fe_2(NO_3)_3$ and Cr_2O_3 burned out at low temperatures in spite of the platinizing process.

At no time were any ions observed with double or multiple charges.

Discussion

Although no exact mechanism for the emission of positive ions from compounds is indicated in the present work, in general the following requirements seem necessary in order that emission take place: (1) that the lattice be an ionic one; (2) that the forces holding the ion in the lattice be small, as in the alkali alumino-silicates; or if the forces are not small, that the compound be stable thermally so that sufficient energy can be supplied to the lattice to effect a partial breakdown of the structure which will permit singly charged ions to escape with the aid of the drawing-out potential. This seems to be the case with MgO, CaO, BaO, Al_2O_3, In_2O_3, and Ga_2O_3.

Another viewpoint is suggested by the results of a number of workers[12] on thermionic emission of electrons from alkaline earth oxides. These observations seem to indicate that under the influence of the drawing-out potential an electrolysis of the crystalline oxide takes place. The metallic ions would be brought to the surface to evaporate partly as atoms and partly as ions. Studies (see the texts given in reference 1) of ionization of alkali vapors by hot filaments suggest that if the work function of the surface is greater than the ionization potential of the metal, all of the metal will evaporate in the ionized state.

[10] We are indebted to Mr. M. B. Sampson for the observations here reported on gallium.

[11] Sampson and Bleakney, Phys. Rev., this issue.

[12] Cf. Becker, Phys. Rev. **34**, 1323 (1929); Becker and Sears, Phys. Rev. **38**, 2193 (1931).

The Propagation of Potential in Discharge Tubes

L. B. Snoddy, J. W. Beams and J. R. Dietrich, *University of Virginia*

(Received June 22, 1936)

The propagation of potential in a long discharge tube containing air was investigated as a function of pressure (0.017 to 0.24 mm Hg) and applied potential (74 to 171 kv). Impulsive potentials were applied to one end of the tube while the other end was grounded. By means of a high speed cathode-ray oscillograph, it was found that in the case of both positive and negative applied impulses a definite potential wave traversed the tube from the high voltage electrode to ground, immediately followed by a much faster return wave from ground back to the high voltage electrode. The wave velocity, voltage attenuation, wave form and energy carried in the wave front of the initial impulse were investigated and found, in general, to vary with both pressure and applied potential. The similarity of these results to the observations on the propagation of luminosity in long discharge tubes and in the lightning stroke are discussed. With the higher applied voltages the wave shows practically no observable distortion or attenuation so that the long discharge tube provides an excellent transmission line for many purposes.

THE propagation of luminosity produced by the application of an impulsive potential to long discharge tubes was first investigated by J. J. Thomson[1] and has since been studied with an improved method by one of us.[2] Thomson observed that the luminosity did not start simultaneously throughout the length of the tube but traversed it with a finite velocity. Beams found that the luminosity progressed from the high voltage electrode toward the electrode maintained at ground potential regardless of the polarity of the impressed surge. This luminous pulse travels through the tube with a high velocity (10^9 to 10^{10} cm/sec.) which for a given tube is determined chiefly by the pressure of the gas and the magnitude of the applied potential. In addition to this initial impulse found in all discharges he also occasionally observed a second pulse later than the first which started at the ground potential electrode and moved in the opposite direction. This type of propagation is similar to that observed by Schonland[3] and others in lightning discharges, and by Allibone and Schonland[4] for a million-volt spark between point and plane. In the lightning stroke the first luminous pulse or "leader" may travel continuously or in a stepped fashion from cloud to ground with a velocity as high as 5×10^9 cm/sec. This leader is followed by a return stroke of high luminosity starting from the ground and moving in the opposite sense with velocities as high as 1.4×10^{10} cm/sec.

In order to obtain a clearer insight into the mechanism responsible for this "traveling wave of luminosity" the present work was undertaken to determine the nature of the accompanying potential wave. Since a long discharge tube of this kind should constitute a transmission system for potential pulses, a knowledge of the wave velocity, voltage attenuation, wave form and energy carried in the wave front as a function of pressure and applied voltage is desirable.

Apparatus and Method

The apparatus is shown schematically in Fig. 1. The tube T was constructed of Pyrex of internal diameter 5 mm. The terminal electrodes E_1, E_4 were brass rods with hemispherical ends, and the electrodes E_2, E_3 short lengths of brass tubing waxed in place. The pump and drying system were attached at P and the pressure read on a type of Pirani gauge at G. During observations the pump was shut off to avoid any pressure gradient in the tube. The potential was applied to the tube through a spark gap from the three stage Marx circuit C. A high speed cathode-ray oscillograph of the Dufour type was used to determine the potential variations. The oscillograph circuit and the method used to synchronize the oscillograph and supply potential circuits are not shown as they followed the standard practice for such problems. The sweep was used at film speeds of approximately $0.3-1\times10^8$ mm/sec. The electrodes E_2, E_3 were connected to the deflection plates through symmetrical capacity dividers in

[1] J. J. Thomson, Recent Researches 115 (1893).
[2] J. W. Beams, Phys. Rev. **36**, 997 (1930).
[3] Schonland and Collens, Proc. Roy. Soc. **A143**, 654 (1934); Schonland, Malan and Collens, Proc. Roy. Soc. **A152**, 595 (1935).
[4] Allibone and Schonland, Nature **134**, 736 (1934).

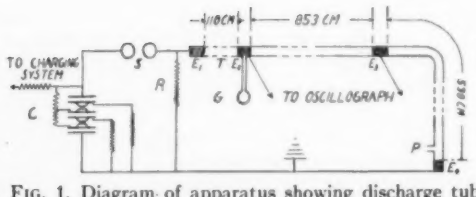

FIG. 1. Diagram of apparatus showing discharge tube and Marx circuit for supplying potential. The oscillograph and synchronizing circuits are not given.

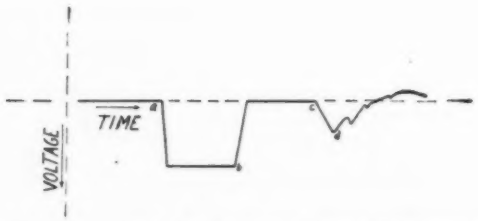

FIG. 2. Diagram giving the main features of the potential variations observed on the oscillograph for both positive and negative impulses.

such a manner that equal potentials at E_2, E_3 would produce no displacement of the electron beam. With this arrangement a potential wave passing down the tube produces a deflection of the beam when it arrives at E_2. This deflection is decreased when the wave arrives at E_3, the amount of decrease depending upon the voltage attenuation between E_2 and E_3. In like manner a return wave from E_4 can be followed from E_3 to E_2. By observing the deflection at each electrode separately a fairly complete picture of the voltage variations can be obtained.

It has been observed[2] that the luminous pulse originating at E_1 started relatively slowly at first and did not reach its final constant speed until it was some 40 cm down the tube. This is probably due to the time lag inherent in the starting of a gaseous discharge and depends for any given potential impulse upon the size of tube, shape of electrodes and initial degree of ionization of the gas. The electrode E_2 was placed at a distance from E_1 such that the rate of potential increase observed was a maximum and did not vary appreciably from one discharge to the next. This minimizes any effect due to a variation in the initial rate of breakdown. Dry air was used for all the observations. The tube was outgassed by continual pumping and repeated discharging with a high applied potential.

RESULTS

A typical diagram of the voltage variations for both positive and negative pulses is shown in Fig. 2, and typical oscillograms in Fig. 3. The arrival of the wave at E_2 is shown at (a), and at (b) the wave has reached E_3. The time b–c represents the time of transit of the initial wave from E_3 to E_4 plus the time taken by the discharge wave to reach E_3 from the grounded end of the line. Since the gas is made highly conducting by the initial pulse, this discharge wave is similar to that obtained by grounding one end of a charged transmission line and travels with a velocity nearly equal to that of light. The time c–d is approximately that required for the discharge wave to travel the distance E_3–C and return to E_3 as a reflected wave. A number of successive reflections can be seen on the oscillograms superimposed upon the potential variation due to the slow damped oscillation of the circuit as a unit.

At relatively high pressures and high potentials the time b–c is variable. This is caused by the practical difficulty of maintaining E_4 at constant potential when the gap S discharges. The potential appearing at E_4 ionizes the gas in that end of the tube and produces variations in the wave velocity near that end. E_3 was placed at such a distance from E_4 that the time of transit over E_3 to E_4 and back to E_3 was always greater than the time length of the initial wave front. When this precaution was observed the time between a–b remained constant for a given pressure and voltage to within five percent. When the electrode E_4 is disconnected from the ground and insulated the initial wave appears the same but the part from (c) on is lacking, showing that the last part is due to the discharge wave.

A number of values of wave velocities, applied voltages and pressures are given in Table I. In general an increase of either pressure or voltage produces an increase in the speed of propagation over the range studied. There seems to be for any given pressure a critical potential necessary for the production of a wave which will travel with a definite velocity without appreciable attenuation. At the higher potentials (127–171 kv) there was no noticeable voltage attenuation or wave distortion in traveling the distance E_2–E_3 (853 cm). However, at 74 kv and the higher pressure (0.24 mm) the voltage variations were analogous to

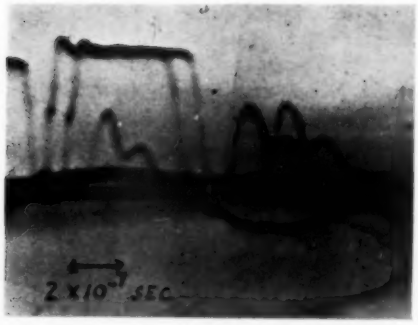

FIG. 3. Oscillogram of negative impulse. Applied potential of 123 kv. Pressure 0.032 mm.

those obtained in charging a cable with a high resistance per unit length. The return wave was not observable in this case.

At 171 kv and 0.17 mm pressure the time length of the wave front is 7.8×10^{-8} sec. and the space length 209 cm. Since the rate of charging observed on the oscillograph for this case is approximately linear, the field in the wave front is about 810 volts/cm. With this value of field and pressure it is probable that the propagation can be explained by the rapid building up of space charge in the front of the wave. It seems possible that the necessary electron supply immediately ahead of the wave is furnished by photoelectric absorption in this region of the gas.

The wave front at E_2 in this case (171 kv, 0.17 mm) is slightly less steep in the initial portion than that at E_2' but reaches its maximum value in about the same time. This indicates that the charging current to the oscillograph deflection plate system does not produce very much wave distortion. Assuming the capacity of this system to be 8 $\mu\mu$fd and the rate of charging linear, the charging current is 17 amp. The current in the initial pulse must consequently be many times this amount. With 74 kv at both 0.017 and 0.24 mm pressure there is pronounced wave distortion increasing greatly with increase of pressure. The ratio between the charging currents to the oscillograph for 171 kv at 0.17 mm and 74 kv at 0.017 mm pressure is 7.4. This gives a current of 2.4 amp. in the 74 kv case. This leads one to expect that a rather high value of current is necessary in the initial wave before the space charge propagation can be maintained without appreciable change throughout the tube.

TABLE I. *Wave velocities for different applied voltages and pressures.*

Applied Voltage (kv)	Pressure (mm Hg)	Speed of Potential Impulse Between E_2–E_3
+127	0.08	9×10^8 cm/sec.
+127	0.18	24
+127	0.24	43
−123	0.032	15
+171	0.17	27
+ 74	0.017	5.4
+ 74	0.24	14

To obtain the maximum currents flowing during the initial wave an electrolytic resistance of 41 ohms was placed in the circuit between S and E_1. E_4 was disconnected from the ground and insulated. The maximum voltage across this resistance was measured by a spark gap irradiated by ultraviolet light. For 170 kv and 74 kv at 0.025 mm pressure the maximum currents were respectively 429 amp. and 146 amp. With E_4 grounded the maximum discharge currents for the same potentials at 0.053 mm pressure were 940 amp. and 480 amp. respectively. With high current values in the initial impulse it is evident that the slope of the wave front at the electrode E_2 is governed to a considerable extent by the impedance of the input circuit and could be made considerably steeper by decreasing this impedance.

This investigation is being continued with the hope that measurements over a wider range of voltages and pressures with tubes of different diameters and with different gases will lead to a quantitative explanation of the mechanism responsible for this propagation of potential. In addition to their close connection with the propagation of luminosity in discharge tubes and in lightning strokes the results already obtained show that for relatively short distances a discharge tube of this kind serves as a transmission line in which the speed of propagation is easily controllable at a value much less than that of light. This is of importance in many problems[5] where it is necessary to obtain time separations between the application of potential at different points.

We wish to acknowledge a grant from the American Philosophical Society which has made it possible for one of us (L. B. S.) to work on this problem.

[5] Beams and Snoddy, Phys. Rev. **44**, 784 (1933).

The Gyromagnetic Properties of the Hydrogens

J. M. B. KELLOGG, I. I. RABI* AND J. R. ZACHARIAS, *Columbia University*

(Received June 25, 1936)

The magnitudes of the nuclear moments of the proton and the deuteron are remeasured by the method of atomic beams. The new experimental arrangement is such that the evaluation of the results does not require any information with regard to the velocity distribution of the atoms in the beam. Detection is made objective by the use of a Stern-Pirani detector. The signs of the magnetic moments of the proton and deuteron are determined by the method of nonadiabatic transitions in a weak magnetic field. The results of the experiment are: $\mu_p = 2.85 \pm 0.15$; $\mu_0 = 0.85 \pm 0.03$ nuclear magnetons. Both moments are positive in sign.

THE discovery by Stern[1] and his collaborators that the magnetic moment of the proton is very much larger than the value predicted by the Dirac theory suggests a number of important problems. These include the development of methods for a more precise determination of the magnitude of the moment and the question of the sign. Because of its much smaller moment the same questions arise in more aggravated form for the deuteron.

The question of the sign of the nuclear moments is particularly interesting since the proton is so anomalous that considerations from the Dirac theory do not suffice for its prediction, while the deuteron is the only nucleus of its type (even atomic weight, odd nuclear charge) for which the moment has been measured,[2] and there is therefore no example from which to draw an analogy. This question arises only when the moment is measured by the deflection of molecular or atomic beams,[3] since it is peculiar to these methods that the sign of the nuclear moments does not affect the deflection pattern.

In the experiments to be described we have developed and applied to hydrogen and deuterium a method of determining the sign of the nuclear moments which is based on the use of nonadiabatic transitions between states of space quantization of the atom in weak magnetic fields. We have also developed a method of measuring the hfs separation of the normal state of the atom, on which the evaluation of the nuclear moment depends, which makes the result in principle independent of any assumption as to the velocity distribution of the atoms in the beam. This eliminates an important source of possible error in measurements of this kind.

General Considerations

A hydrogen or deuterium atom in the normal $^2S_{\frac{1}{2}}$ state may have in a magnetic field one of several values of atomic[4] magnetic moment f.[5] For hydrogen these moments are: (in units of μ_0, the Bohr magneton)

$$\begin{aligned} \pm f_1 &= \pm 1, \\ \pm f_2 &= \pm x/(1+x^2)^{\frac{1}{2}}, \end{aligned} \tag{1}$$

and for deuterium the moments are:

$$\begin{aligned} \pm f_1 &= \pm 1, \\ \pm f_2 &= \pm (x+\tfrac{1}{3})/(1+\tfrac{2}{3}x+x^2)^{\frac{1}{2}}, \\ \pm f_3 &= \pm (x-\tfrac{1}{3})/(1-\tfrac{2}{3}x+x^2)^{\frac{1}{2}}. \end{aligned} \tag{2}$$

The moments are plotted against x in Figs. 1A and B. The parameter x is defined by $x = 2\mu_0 H/hc\Delta\nu$, where H is the value of the magnetic field. The quantity $\Delta\nu$ is the separation in cm^{-1} of the two hfs components in zero field and is related to the nuclear magnetic moment μ_N by

$$\Delta\nu = [(2i+1)/i](8/3hc)\mu_N\mu_0\psi^2(0), \tag{3}$$

where i is the nuclear spin and $\psi(0)$ is the value of the Schrödinger eigenfunction at the nucleus which can be calculated exactly. Both from band spectra determinations[6] and, as will be apparent later, from the experiments here described, it is known that the nuclear spin of hydrogen is

* Ernest Kempton Adams Fellow, Columbia University, 1935–36.

[1] Frisch and Stern, Zeits. f. Physik **85**, 4 (1933); Estermann and Stern, Zeits. f. Physik **85**, 17 (1933).

[2] Estermann and Stern, Phys. Rev. **45**, 761 (1934); Rabi, Kellogg and Zacharias, Phys. Rev. **45**, 769 (1934).

[3] Rabi, Kellogg and Zacharias, Phys. Rev. **46**, 157, 163 (1934).

[4] Atomic magnetic moment is not to be confused with nuclear magnetic moment.

[5] Breit and Rabi, Phys. Rev. **38**, 2082 (1931).

[6] Murphy and Johnson, Phys. Rev. **45**, 761 (1934).

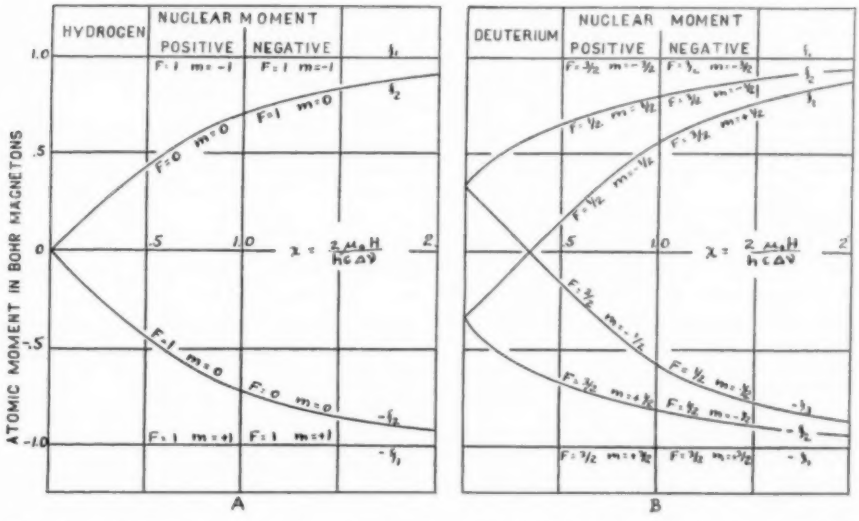

FIGS. 1A and 1B. Diagram to show quantum numbers associated with the magnetic states assuming the nuclear spin positive or negative.

$\frac{1}{2}$ and the nuclear spin of deuterium is 1. For hydrogen, with nuclear moment μ_P expressed in units of $\mu_0/1838$, the above equation reduces to $\Delta\nu=0.0169\mu_P$, and for deuterium with nuclear magnetic moment μ_D expressed in the same units, to $\Delta\nu=0.0127\mu_D$. Thus if an experimental evaluation of one of those atomic moments which depends upon x can be made while the atom is in a known field H, the magnitude of the nuclear moment can be determined.

The results of a deflection experiment may be made to give both of these quantities. Consider a narrow beam of atoms emerging from the collimating slit of Fig. 3 and passing down the apparatus toward the slit of the Stern-Pirani detector. These atoms pass first through a region A of weak inhomogeneous magnetic field and then through a second field B similar to the first but stronger and arranged to give deflections in the opposite direction to those produced by the field A. This latter condition may easily be satisfied since atoms of positive moment are always deflected into regions of stronger field. The deflection of an atom in the direction y perpendicular to the beam is given by

$$s=(1/4E)\mu(\partial H/\partial y)L, \qquad (4)$$

$L=1_1^2+21_11_2$, with E the kinetic energy of the atom, 1_1 the distance the atom moves in the field, and 1_2 the distance the atom traverses from the end of the field to the detector. A suitable choice of H and $\partial H/\partial y$ in the fields A and B will give equality of the deflections produced in these regions, and one can write independently of the value of E and hence of the velocity distribution

$$f'(\partial H/\partial y)'L'=f''(\partial H/\partial y)''L'', \qquad (5)$$

where the primes and double primes refer to the values of the various quantities in the fields A and B, respectively. *If the values of H and $\partial H/\partial y$ in the two fields are known, this equation gives immediately the value of the nuclear moment.* In our apparatus the quantities H and $\partial H/\partial y$ are proportional to and can be immediately calculated from the currents used to produce the magnetic fields. With I' and I'' in amperes approximate values of H and $\partial H/\partial y$ for the two fields may be found from $H'=1.34I'$, $H''=1.16I''$ and $(\partial H/\partial y)'=11.1I'$, $(\partial H/\partial y)''=5.95I''$.

A measurement of the atomic moments according to the theory outlined above is sufficient to determine the magnitude of the nuclear magnetic moments, but because of the symmetry of the deflection patterns cannot yield information as to whether this moment is positive or negative, i.e., whether the nuclear magnetic moment is oriented parallel or antiparallel to the

TABLE I. *Transition probabilities for $F=1$.*

m	-1	0	$+1$
-1	c^4	$2c^2s^2$	s^4
0	$2s^2c^2$	$1-4s^2c^2$	$2s^2c^2$
$+1$	s^4	$2c^2s^2$	c^4

TABLE II. *Transition probabilities for $F=3/2$. $c=\cos(\alpha/2)$ $s=\sin(\alpha/2)$.*

m	$-3/2$	$-1/2$	$+1/2$	$+3/2$
$-3/2$	c^6	$3c^4s^2$	$3c^2s^4$	s^6
$-1/2$	$3c^4s^2$	$c^2(c^2-2s^2)^2$	$s^2(2c^2-s^2)^2$	$3c^2s^4$
$+1/2$	$3c^2s^4$	$s^2(2c^2-s^2)^2$	$c^2(c^2-2s^2)^2$	$3c^4s^2$
$+3/2$	s^6	$3c^2s^4$	$3c^4s^2$	c^6

nuclear angular momentum vector. This question has been discussed by Rabi in a paper "On the Process of Space Quantization,"[7] and he there points out that certain nonadiabatic processes may be used to discover the sign of the nuclear moment.

Consider an atom of the beam moving with constant velocity through a magnetic field varying in strength and direction along its path. The atom is equivalent for these questions to an atom at rest and situated in a field varying in time in the same manner. If the angular velocity of rotation of the field, T, is small compared with the Larmor frequency $\omega=2\pi\mu_0 gH/h$ the atom will remain space quantized with respect to the field with the same component m of its total angular momentum F (adiabatic transformability); if the angular velocity is of the same order of magnitude as the Larmor frequency there will be nonadiabatic transitions to states m' not necessarily equal to m but with the same F. The probabilities of such transitions have been calculated by Majorana[8] and are tabulated in Tables I and II for hydrogen and deuterium. The parameter α which occurs in these expressions is obtained from the dynamical theory of the process. Physically α is the angle between the original direction in which the atom is space quantized (direction of the field H) with quantum number m, and the direction after the process with respect to which the atom is quantized with the same quantum number m. Majorana has shown that this process depends only on the Landé g factor and the nature of the process, and is independent of m. Since the two F states have the same g value, the value of α is the same for both for any dynamical process whatsoever.

Since the form of the field T is not known exactly it is not possible to calculate α as a function of the field and of the velocity. There will also be a different value of α for every atomic velocity. We cannot, therefore, begin by setting the field at some particular value and expect to find nonadiabatic transitions. The procedure which we followed was to find experimentally a value of the current in T for which the transitions occurred.

The effective value of α can be calculated from our knowledge of the fraction of the atoms which do not make the transitions and the value of m for the state which has been selected. Since the atoms in the other states pass through the same field and have the same velocity distribution, they have the same effective α. We are thus at liberty to use a field for which the dynamical problem has not been solved. The type of field which we adopted for reasons of convenience is shown in Fig. 2A. This field is neither the Güttinger[9] nor Majorana type although nearer the former. Data obtained in this manner cannot be used to exhibit the quantitative side of the dynamical theory of these transitions. Our purpose, however, is to recognize a qualitative difference in the behavior of the atoms in the two F states under identical conditions.

Reference to Figs. 1A and 1B shows that the assignment of the quantum numbers m and F to atoms in the several magnetic states depends on the sign of the moment of the nucleus. It is this dependence, together with the nonadiabatic transitions made use of in a method to be described, which enables a decision to be formed as to the sign of the nuclear moments.

APPARATUS

The arrangement of the pumps and the slit system (Fig. 3) is almost the same as that described by R. K. Z.[3] In the present apparatus the beam height is 2 mm, and the widths of the various slits are: source sl0t i.03 mm; fore slit, 0.05 mm; collimating slit, 0.02 mm; selector

[7] Rabi, Phys. Rev. **49**, 324 (1936).
[8] Majorana, Nuovo Cim. **9**, 43 (1932).
[9] Güttinger, Zeits. f. Physik **73**, 169 (1931).

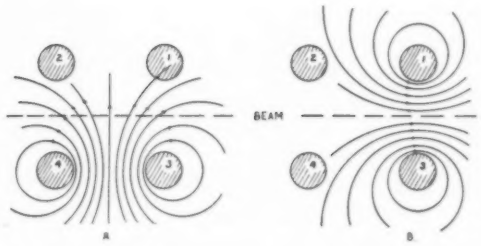

FIG. 2. Diagrams of field near wires T. (A) Nonadiabatic field; (B) Adiabatic field.

slit, 0.5 mm; and detector slit, 0.01 mm. Approximate distances measured from the source slit to the points indicated are: fore slit, 1.0 cm; collimating slit, 17 cm; end of A field, 33 cm; beginning of B field, 38 cm; end of B field, 48 cm; and detector, 50 cm.

The discharge tube: The hydrogen atoms are prepared in a long Wood discharge tube of a design (see Fig. 4) which permits the source slit to be in close proximity to the discharge. The slit is formed by ground edges of thin cover glass held on to the Pyrex tube with picein wax. Water cooling prevents melting of the wax and also seems to keep the temperature of the gas fairly low. With gas pressures of the order of 1 mm the concentration of hydrogen atoms in the beam is between 0.7 and 0.9. In the previous experiment[3] this ratio was only 0.1 to 0.2. The concentration of atoms is taken from measurements of full beam intensity and of the intensity with enough deflecting field on to cast out all atoms.

The ground joint in the threaded collar of Fig. 4 is bored with its axis eccentric and at 5° to the axis of the screw threads. This permits alignment of the source slit parallel to the collimator slit. Motion of the source slit in the horizontal direction is accomplished by moving the brass base plate or by turning the source tube. The canal of the source slit can thus be made to point toward the collimator slit. With the aid of these adjustments it is possible to replace the discharge tube after removing it from the apparatus for cleaning and putting on new slit jaws. This procedure was necessary because Apiezon oil from the diffusion pumps sometimes clogged the source slit.

The magnetic fields: The A and B fields are produced in the manner previously described[3] by current flowing in two horizontal straight tubes parallel to the beam. Great care was exercised both in the construction of the "fields" and in their proper placement with respect to the beam. The B field differs from the A in that it is shorter, capable of carrying more current, and gives a smaller ratio of gradient to field.

Although rheostats, switches, etc., are not worth describing, the leads for the field supply are noteworthy in one regard: in the reduction of stray field. Parallel bus bars of copper placed close together suffice for distances of 20 cm or more from the beam. The insert of Fig. 3 represents a cross section of the leads to the current tubes of the second field in the region near the beam. The cross hatched copper tube is slotted and is soldered to the tube which carries

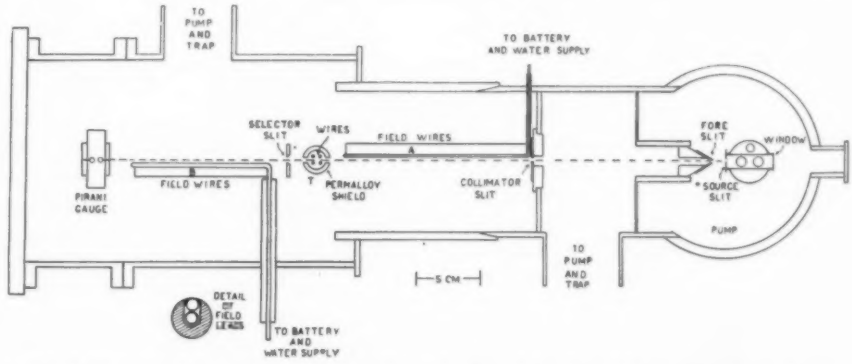

FIG. 3. Diagram of apparatus as used for determination of the sign of the moment for hydrogen and deuterium. The permalloy shield and the wires T were removed from the apparatus for the measurement of the magnitudes of the moments.

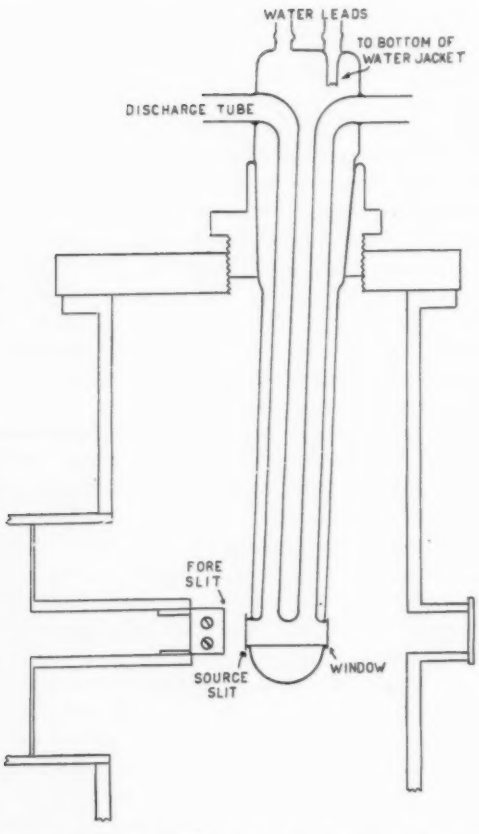

FIG. 4. Section of source chamber to show the construction of discharge tube and of the eccentric brass adjusting collar.

the current in; the central copper tube carries the current out. This arrangement permits simple water connections, simple vacuum seal, good conductivity and small stray field.

A parallel bank of 12 lead storage cells with a capacity of about 1500 amp.-hrs. supplies the first field. For the B field, which requires about 800 amp. continuously, a bank of 6000 amp.-hrs. is maintained. These batteries are charged by a 12-volt, 1200-amp. generator.

The transition field: This field is produced by current flowing in two vertical wires on one side of the beam. It is evident from Fig. 3 that there are four symmetrically disposed copper wires in a region magnetically shielded by permalloy. A system of switches, rheostats, batteries and meters makes it possible to use pairs of wires on either side of the beam as the transition field wires, or to produce an adiabatic field by using one wire on each side of the beam. The forms of these two types of field with respect to the beam direction are shown in Figs. 2A and 2B. Magnetization of the permalloy shield is avoided by running the current in the wires in opposite directions through one hole in the top of the shield.

The detector: The Stern-Pirani detector is of the type designed by Zabel.[10] The detecting gauge and the compensating gauge are enclosed in the same brass block and equipped with slits 2 mm high, 0.01 mm wide, and 4 mm deep. The motions necessary for its proper alignment with the beam are simple screw devices of obvious design. In the early part of the experiment considerable difficulty was encountered in reading the gauge galvanometer while the hydrogen discharge tube was in operation. Unsteadiness of the gauge seemed to be associated with fluctuating pressure in the detecting chamber and with subsidiary electrical effects of the discharge. Therefore the electrical circuit from the gauge wires to the galvanometer was shielded with sheet copper and the backing pressure for the high speed pumps was improved so as to maintain an ion gauge pressure of 10^{-7} mm in the detecting chamber. To avoid electrical and mechanical disturbances by mechanical pumps a three-stage Leybold mercury diffusion pump was inserted in the fore line and the hydrogen gas from the source slit was pumped into an evacuated 30 gal. tank.

METHOD: MAGNITUDE OF THE MOMENTS

The detector slit is set to receive the atoms of the undeflected beam and is left fixed in this position throughout the course of all experiments. The simplest experiment to perform is the determination of the nuclear spin of hydrogen. The current in the B field is turned on and set at such a value as to give an x in the neighborhood of 1.5. With no current in the A field the beam is split in the B field and few atoms enter the gauge. If the A field current, I', is now increased, all atoms in the A field experience a deflecting force proportional to their atomic moments and to

[10] Zabel, Phys. Rev. **46**, 411 (1934).

the current I'. This force is opposite in direction to the force that will act on them when they pass through the B field. At the same time atoms having moments other than $\pm f_1$ are receiving larger deflections in the A field on two counts; first because the larger I' increases H' and hence x and f_2, and second because the force per unit moment is becoming larger due to the increase in $(\partial H/\partial y)'$. These atoms may thus in turn be focused into the detector. Focusing is of course recognized by a maximum of intensity at the detector.

A curve showing the two intensity maxima so obtained for hydrogen is given in Fig. 5. Since four atomic magnetic levels are required to give the two peaks of Fig. 5, and since the number of these levels is given by $(2i+1)(2j+1)$, a nuclear spin of $\frac{1}{2}$ is found for hydrogen.

While the existence of two and only two peaks is sufficient to establish the proton spin, a determination of the position (in current) of the peaks and a more detailed analysis of the operation of the apparatus is necessary before a value can be assigned to the magnitude of the magnetic moment of the proton.

First, the values of H and $\partial H/\partial y$ are neither exactly constant over the height of the beam, nor because of end effects, along the beam. The terms $f(\partial H/\partial y)L$ in Eq. (5) are therefore replaced by a numerical integration over the full path of the beam using values of H and $\partial H/\partial y$ averaged over the height of the beam.

Second, the values of H and $\partial H/\partial y$ are calculated from measured geometry of the apparatus, e.g., the distance between the wires, their diameters, the distance from the wires to the beam, and the lengths of the beam path both in and out of the fields. It is fortunately possible to use the values of the currents required to deflect and focus atoms of constant moment to evaluate directly some of the constants in Eq. (5). If we let $\partial H/\partial y = GI$, then Eq. (5) can be written

$$f'I'/f''I'' = G''L''/G'L' \equiv R. \tag{6}$$

This ratio R can be evaluated in two ways. First it can be calculated directly from the geometry of the apparatus. Second, it can be determined in terms of the currents required to focus hydrogen atoms having $f' = f'' = \mu_0$. A comparison of the values of R obtained in these two ways serves as a check on the geometry used in the calculation of H. The second determination is considered to be more accurate than the first and is used in the evaluation of the ratio f'/f'' for $f' \neq f''$.

Third, consider two atoms emerging from the collimating slit, one with moment $+f$ and the other with moment $-f$. The atom with moment $+f$ is deflected in the A field into regions of stronger field and gradient while that with moment $-f$ is deflected into regions of weaker field and gradient. The result is to give the atom with moment $+f$ a larger deflection than the atom with moment $-f$. The B field which is on the opposite side of the beam from the A field

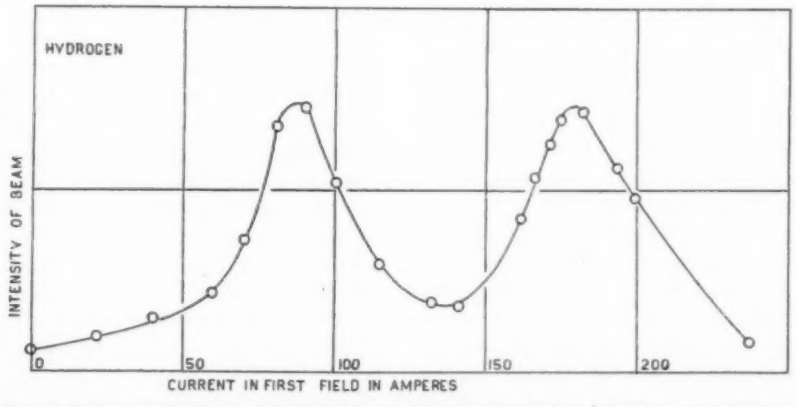

FIG. 5. Intensity at center of beam against field current for hydrogen to show nuclear spin to be $\frac{1}{2}$. The first peak is for $\pm f_1$; the second for $\pm f_2$.

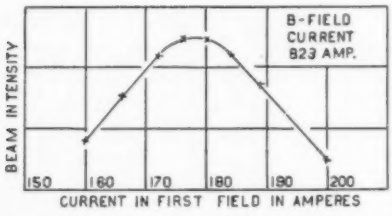

FIG. 6. Intensity of beam against field with selector slit interposed to pass only atoms with negative moments, for hydrogen.

magnifies this effect and $+f$ is underfocused whereas $-f$ is overfocused. Thus instead of a sharp peak a broad maximum is formed by the superposition of the two partially focused beams.

This difficulty is overcome in the following manner. A selector slit is introduced where the beam is split between the two fields. By means of this slit it is possible to cut out of the beam either those atoms with positive or those with negative moments. This slit serves the additional purpose of blocking the undissociated molecules of the direct beam from the detector. Suppose the slit is set to pass only those atoms having positive moment. An intensity-current plot is made for, say, atoms of moment $+f$ (see Fig. 6). The slit is then moved to pass only those atoms having negative moment and an intensity-current plot made for atoms of moment $-f$. If the positive moment peak occurs at current I_+', and the negative moment peak at I_-', then $(I_+'+I_-')/2$ is very closely the current at which the peak would occur in an ideal apparatus, i.e., an apparatus in which the deflecting force on an atom is not a function of the deflection.

Fourth, a method of using the detector is required which will give as accurately as possible the current at which the maximum intensity occurs. A "differential" method of measuring the intensity is adopted. With a given B field current, the current in the A field is set in the neighborhood of the peak. The reading of the detector galvanometer is noted and simultaneously a switch is thrown to vary the A field current by a few percent. After thirty seconds the galvanometer reading is again noted and the switch thrown to give the original A field current. This procedure is continued for six minutes and the readings averaged to eliminate the effect of drift. The difference in the two sets of readings then gives the amount by which the intensity at one current exceeds that at the other. By interrelating two points on the curve so directly one largely eliminates effects of secular changes in the intensity of the beam and changes in the ratio of the number of atoms to molecules. All current-intensity curves were taken in this manner.

METHOD: SIGN OF THE MOMENTS

Hydrogen

The transition field T is fixed in place between fields A and B. The selector slit is set to pass atoms of positive moment and the A and B field currents adjusted to focus the component $+f_2$. According to Fig. 1A this component is either $F=0$, $m=0$, or $F=1$, $m=0$, depending on the sign of the nuclear moment. If the state is $F=1$, $m=0$ (nuclear moment negative), then Table I shows that for a certain value of α, that is, a certain value of the current in the wires of the field T, there will be nonadiabatic transitions to states $F=1$, $m=\pm 1$. If the transition is to $m=+1$, the atom enters the B field region with the sign of its moment changed and is no longer focused. There is therefore a decrease in intensity at the detector. If the transition is to $m=-1$ no decrease in intensity will be observed since the value of x in the second field is so large that all atoms experience approximately the same deflecting force. In any discussion of these experiments, and particularly in the case of deuterium, this equality of atomic moments in the B field must be kept in mind. In the vernacular of the laboratory "only those transitions that cross the diagram (Fig. 1) are counted as 'flop' (nonadiabatic transition)." However, if the state is $F=0$, $m=0$ (positive nuclear moment), no variation in intensity will be observed since changes in F are forbidden. A similar argument may easily be carried out for $-f_2$. The results are summed up in Table III where the expected change in intensity is given for the various possible combinations of nuclear and atomic moment.

While it would seem sufficient to perform an experiment on, say, $+f_2$ and to determine whether this state does or does not make transitions, it is experimentally necessary to show that the result obtained is not due to

extraneous effects of the apparatus. Thus, if it is found that for a particular value of current in the T field wires there *are no* transitions made from the component $+f_2$, it is then necessary to show that for the same value of the T field there *are* transitions made from the component $-f_2$. Furthermore a similar experiment on the components $\pm f_1$ should show that both of these components *do* make transitions. Lastly, to be sure that the asymmetry is not inherent in the position of the beam with respect to the field wires, this whole series of experiments must be performed with the transition wires located on the other side of the beam.

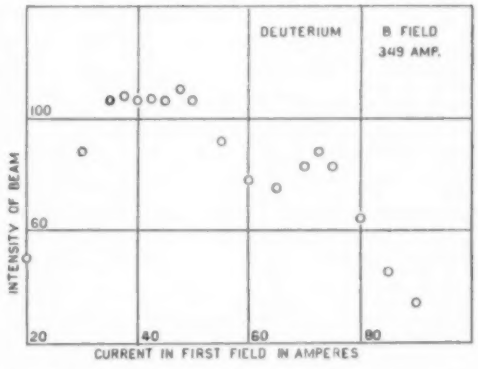

FIG. 7. Intensity of beam against field with selector slit set to pass only atoms with negative moment.

Deuterium

The same apparatus is used as for the sign determination for hydrogen. The selector slit is set to pass atoms of negative moment, and the A and B field currents are adjusted so that only states $-f_2$ and $-f_3$ enter the detector. As is obvious from Fig. 7, when $-f_3$ is focused, the beam is contaminated by $-f_2$. The procedure followed is to focus partially both $-f_3$ and $-f_2$. Suppose the nuclear moment positive. Then transitions are possible to all states with $F=3/2$, and in particular to the state $F=3/2$, $m=-3/2$, i.e., to $+f_1$. Detailed consideration of Table II shows that for an equal mixture of atoms in states $-f_2$ and $-f_3$ this transition probability is a maximum for $\sin^2(\alpha/2)=\frac{1}{2}$. Therefore if the nuclear moment is positive, there will be a value of current in the T field wires which will produce a decrease in the intensity of the beam composed of atoms of moments $-f_2$ and $-f_3$.

On the other hand if the nuclear moment is negative, reference to Fig. 1B shows that the states $-f_2$ and $-f_3$ both have $F=\frac{1}{2}$ and therefore transitions are possible only between these two states. Remembering that the atomic moments in the second field are all practically equal to one Bohr magneton, it follows that the total number of atoms focused into the detector is not changed thereby.

For the atoms with positive moments $+f_2$ and $+f_3$ a similar argument leads to opposite conclusions. The results of this discussion are summed up in Table III.

While current flowing in opposite directions in either wires 1 and 2 or 3 and 4 gives a nonadiabatic field over the region of the beam inside the permalloy shield of the transition field, it is not certain that mere absence of current in these wires gives an adiabatic field in this region. The very existence of the ferromagnetic material of the shield in this space gives rise to the possibility of residual fields which might accidentally fulfill the requirements for a nonadiabatic field. However, with current flowing in opposite directions in wires 1 and 3 the field will be as shown in Fig. 2B and the shield and the region inside the shield will certainly be magnetized in such a manner that there will be no rapid change of direction of the field along the path of the beam. All observations here reported were made by repeatedly switching from configuration B to configuration A of Fig. 2.

If this procedure is not followed, the results are essentially the same. However, there were slight increases of intensity on switching from no current to configuration B which would indicate the presence of this accidental nonadiabatic field.

TABLE III. *The qualitative expected change of focused beam intensity for nuclear moment assumed positive and negative; and the observed change in intensity.*

	Component Focused	Expected Change of Intensity		Observed Change of Intensity
		Positive Nuclear Moment	Negative Nuclear Moment	
Hydrogen	$\pm f_1$	Decrease	Decrease	Decrease
	$+f_2$	None	Decrease	None
	$-f_2$	Decrease	None	Decrease
Deuterium	$\pm f_1$	Decrease	Decrease	Decrease
	$+f_2$ & $+f_3$	None	Decrease	None
	$-f_2$ & $-f_3$	Decrease	None	Decrease

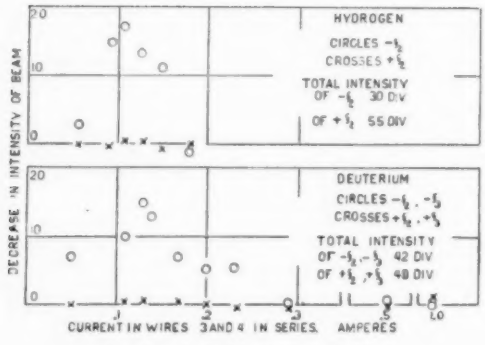

FIG. 8. Nonadiabatic transitions.

RESULTS

The sign of the nuclear moments: Typical experimental results are given in Fig. 8. They show the change in intensity on the introduction of the nonadiabatic field. The striking differences between the behavior of the states with positive atomic moments and those of negative atomic moments is very apparent. This difference is not due to a geometric asymmetry because the same behavior is obtained with either pair of wires 1 and 2 or 3 and 4. Consultation of Table III shows that the experiments establish the signs of the nuclear moments of hydrogen and deuterium to be positive.

The magnitudes of the nuclear moments: Figs. 6 and 7 show typical experimental curves from which the intensity-current maxima were obtained. Table IV gives the results of a series of measurements of the quantity R of Eq. (6) for different values of the B field current and the corresponding values of the A field current for the low current peak. They fall within one percent of constancy and seem to show no trend with current. This table shows the precision of the determination of the maximum of intensity with current. The value of R calculated from the geometrical measurement of field wire distances etc. is 11.05 as compared with 11.09 which is the average of the values of Table IV. This check permits us to place confidence in the values of the moment as calculated from the currents in the A field necessary to focus the atomic moments $\pm f_2$.

Table V gives the results of a series of measurements of these quantities and the proton moments calculated from them. Table VI gives the results of similar measurements with deuterium.

TABLE IV. *Hydrogen.* I_+' is the current to focus $+f_1$, and I_-' is the current to focus $-f_1$. $I_A=(I_+'+I_-')/2$. Currents in amperes.

B Field Current I''	A Field Current I_+'	I_-'	I_A	$R=I''/I_A$
400	32.1	40.1	36.1	11.08
500	39.5	50.3	44.9	11.13
627	50.8	62.5	56.7	11.06
648	52.0	65.5	58.7	11.03
648	50.9	65.5	58.2	11.13

TABLE V. *Hydrogen.* I_+' is the current to focus $+f_2$, and I_-' is the current to focus $-f_2$. $I_A=(I_+'+I_-')/2$. Currents in amperes.

B Field Current I''	A Field Current I_+'	I_-'	I_A	μ_P
601	121.7	142.7	132.2	2.79
732.5	140.0	166.0	153.0	2.87
732.5	141.5	164.5	153.0	2.87
773	145.7	170.0	157.7	2.81
783	148.0	172.0	160.0	2.85
823	150.7	178.0	164.3	2.87

TABLE VI. *Deuterium.* I_+' is the current to focus $+f_3$, and I_-' is the current to focus $-f_3$. $I_A=(I_+'+I_-')/2$. Currents in amperes.

B Field Current I''	A Field Current I_+'	I_-'	I_A	μ_D
349	66.3	73.2	69.7	0.854
400	68.2	78.8	73.5	.841
440	72.4	82.4	77.4	.848

The final results do not have a precision as high as would appear from these tables. First because an error in the determination of the peak current is magnified in the calculation of the moment. Second because of the possibility that the check between the value of R as measured by the ratio of currents and as calculated from the geometry may be partly the result of fortuitous compensation of errors in the very difficult geometrical measurements.

These measurements yield for the proton moment a value of 2.85 ± 0.15 nuclear magnetons; and for the deuteron a value of 0.85 ± 0.03 nuclear magnetons. Our judgment of the precision comes from a discussion of the possible errors in the determination of the geometry.

DISCUSSION

The deuteron value should be somewhat more precise than that of the proton since the geometry

does not enter as importantly. This circumstance arises from the fact that the hfs separation for deuterium is so small that the moment in the B field is practically independent of the field. The ratio of the proton moment to the deuteron moment is 3.35. This value should be somewhat more accurate than that of those for the individual moments since systematic errors should effect both values in the same direction. It is to be noted that this value differs considerably from the value 4 obtained by Farkas and Farkas[11] from the rates of the para-ortho conversion for hydrogen and deuterium.

The value of the proton moment which we previously obtained by the use of atomic beams, 3.25 ± 10 percent is considerably higher than our present results. The cause of this discrepancy is rather obscure but may lie in our previous assumption that the temperature of the beam was the same as the temperature of the source slit.

With the sign of the moments established one can deduce an approximate value of the neutron moment on the naive assumption that the deuteron moment is the algebraic sum of the proton and neutron moments with the additional assumption that the spin of the neutron is $\frac{1}{2}$. The neutron moment is thus -2 nuclear magnetons.

In conclusion we wish to express our appreciation of the aid of a grant from the Carnegie Institution of Washington. Also, we wish to thank Professor H. C. Urey for the generous gift of the heavy water used in these experiments.

[11] Farkas and Farkas, Proc. Roy. Soc. **A152**, 152 (1935).

SEPTEMBER 1, 1936 PHYSICAL REVIEW VOLUME 50

The Photoelectric Properties of Zinc

CHARLES F. DEVOE, *University of Wisconsin*

(Received June 18, 1936)

The work function of a vacuum distilled surface of zinc was found to be 4.24 volts at 1.5×10^{-8} mm pressure; as the pressure of air was increased the work function decreased to a minimum at about 10^{-6} mm pressure and then increased. Helium had no effect to a pressure of 3 mm. Nitrogen had no effect to a pressure of 10^{-3} mm.

EXPERIMENTS on the photoelectric properties of high melting point metals have shown that the metals must be heated at high temperatures for hundreds of hours before reproducible values for the long wave limits are obtained. Since this technique cannot be applied to zinc, several methods have been used to produce a gas-free surface rather than attempt to outgas a contaminated one.[1-9] The values for the long wave limit of zinc obtained in these experiments ranged between 2940A and 4000A.

[1] Richardson and Compton, Phil. Mag. **24**, 575 (1912).
[2] Hennings, Phys. Rev. **4**, 228 (1914).
[3] Küstner, Ann. d. Physik **46**, 893 (1915).
[4] Hennings and Kadesch, Phys. Rev. **8**, 209 (1916).
[5] Welch, Phys. Rev. **32**, 657 (1928).
[6] Werner, Zeits. f. Physik **67**, 207 (1928).
[7] Hughes, Phil. Trans. Roy. Soc. London **212**, 205 (1912).
[8] Dillon, Phys. Rev. **38**, 408 (1931).
[9] Rentschler, Henry and Smith, Rev. Sci. Inst. **3**, 794 (1932).

Hughes[7] measured the long wave limit of a vacuum distilled surface of zinc but the vacuum he used was low compared to that available now. The purpose of this experiment was to study zinc surfaces prepared by Hughes' method under the best possible vacuum conditions.

APPARATUS

The experimental tube is shown in Fig. 1. The thin molybdenum strip A, spotwelded to a tungsten wire yoke and shaft, could be moved into the molybdenum collecting cylinder G, or in front of a tungsten filament E from which the strip could be heated by electron bombardment, or could be placed horizontally over either of the two quartz crucibles Z containing the zinc by means of an electromagnet acting on the soft iron bar C. The collecting cylinder G was sup-

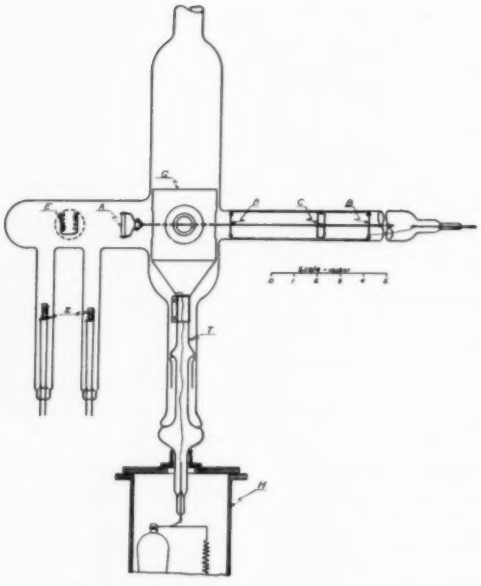

FIG. 1. Diagram of experimental tube.

ported by the skirted tube *T*. This mounting provided a glass path of more than one foot between the cylinder and any other electrode, thus leakage currents were eliminated.

The source of light was a high intensity water cooled quartz capillary mercury arc[10] used with a Leiss double prism quartz monochromator. The monochromator, arc, and auxiliary lenses were mounted on a heavy cast iron base provided with two lateral crossed motions and a rotation around a vertical axis so that the system could be rotated against adjustable stops to send the light either into the photoelectric tube or into a vacuum thermopile. The quartz window on the thermopile was identical with the quartz window on the photoelectric tube, thus the optical paths in the two cases were identical. Thermopile readings were made with a Kipp and Son type ZC galvanometer. The sensitivity of the thermopile was 2.95×10^{-3} erg/sec./mm²/mm deflection of the galvanometer with the scale at three meters. From the current sensitivity of the galvanometer and the resistance of the circuit the absolute sensitivity of the thermopile was 10.91 microvolts/erg/sec./mm². The thermopile was calibrated after each set of observations by radiation from a pyrometer lamp which was calibrated by comparison with a standard lamp. Because of the high intensity of the capillary arcs narrow slit widths of the monochromator ranging from 0.2 mm for 2260A to 0.04 mm for 2805A were used.

The photo-currents were measured by a modification of the Barth[11] circuit using a Western Electric D 96475 tube. The tube and high resistances were mounted in the brass vacuum chamber *H* (Fig. 1) which also enclosed the seal connection to the collecting cylinder, thus the entire photo-current lead was in a vacuum. Three high resistances (6.7×10^{8}, 4.1×10^{9}, 2.2×10^{10} ohms) and a ground lead were mounted on a clear Bakelite block inside the vacuum chamber in such a way that an externally controlled contact arm could shunt the amplifier tube with any one of the resistances or the ground connection. The voltage sensitivity of the amplifier was measured after each set of photo-current readings. The highest sensitivity used was 140,000 mm/volt. Although the high resistances were not calibrated in absolute units (the values given above were the manufacturer's values) the ratios of the resistances were measured several times during the experiment by comparing the deflections produced with the tube shunted by the various resistances and the surface illuminated by light of the same intensity and wave-length. These ratios were found to remain constant during the experiment which indicated that the resistances remained constant.

PROCEDURE

The 99.99 percent pure zinc obtained through Professor Kahlenberg from Evanwall Zinc Company was fractionally distilled four times in a vacuum less than 10^{-7} mm in a series of bulbs. It was then transferred in air to the quartz crucibles which had been outgassed on an auxiliary vacuum system. The gas absorbed during this transfer was removed in the final distillation onto the strip.

The collecting cylinder and the strip mounting were heated to bright red by electron bombardment in separate vacuum systems until pressures less than 5×10^{-7} mm were obtained with the parts heated. The ionization gauge, the filament

[10] Daniels and Heidt, J. Am. Chem. Soc. **54**, 2381 (1932).

[11] Barth, Zeits. f. Physik **87**, 399 (1934).

E, and the crucibles were also outgassed on auxiliary systems. The photoelectric tube, except the side tubes containing the zinc, was baked at 400°C for four weeks while the remainder of the system was heated with a hand torch. During this period the pressure decreased from 8×10^{-8} to 1.5×10^{-8} mm as measured with the ionization gauge. The strip was heated at 1000°C for three weeks after which the tube was again baked for four days.

A small amount of zinc was evaporated to remove the surface layer of gas, then the strip was placed over the crucible and an opaque layer was condensed in about thirty minutes. The pressure during the distillation was less than 3×10^{-8} mm. The strip was then drawn into the collecting cylinder for observations. The long wave limit at absolute zero was obtained by the method of Fowler.[12]

Results

The long wave limits for twenty sets of observations on eight surfaces ranged between 2900 and 2930A; this corresponded to a work function of 4.24 volts. That the surfaces were well outgassed was shown by the facts that (1) the long wave limit did not change during a period of two weeks after the surface was prepared; (2) heating the surface at 100° to 150°C did not change the long wave limit; (3) illumination of the surface by the total radiation from a mercury arc produced no change in the long wave limit.

Although the long wave limits determined by the twenty sets of observations were within one percent of 2915A, the photo-currents per unit incident light intensity for one set of observations were as much as twice the photo-currents at corresponding wave-lengths for another set of observations. Thus the abscissa shifts necessary to put the observed curves into coincidence with the Fowler curve were nearly equal but the ordinate shifts were different. Fig. 2 shows the agreement of the twenty curves plotted with no abscissa shifts but with the ordinate shifts given in Table I. Since these ordinate shifts were not due to changes in the sensitivity of either the thermopile or the amplifier they indicated that the reflecting powers of the surfaces differed by a factor which was constant over the entire spectral range studied, or that there were differences in the electron transmission of the surfaces.

[12] Fowler, Phys. Rev. **38**, 45 (1931).

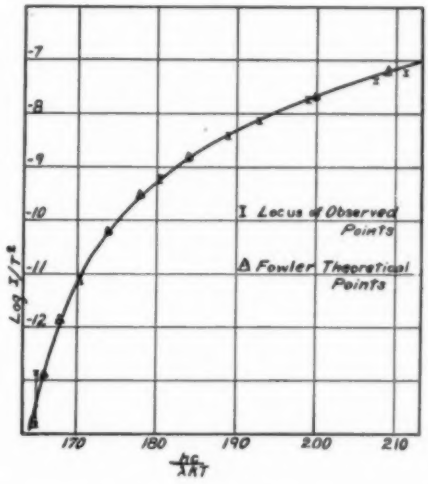

FIG. 2. Plot of the 20 experimental curves. There have been no abscissa shifts but the ordinates have been shifted as given in Table I.

Gas Effects

The fair agreement of the value 2915A with that obtained by Hughes[7] (3016A) for evaporated surfaces in a vacuum less than 5×10^{-4} mm and the discrepancy with Dillon's value[8] (3730A) for a surface in a good vacuum suggested a possible correlation between long wave limit and pressure.

TABLE I. *Values of ordinate shifts used in Fig. 2.*

Curve	Ordinate Shift	Factor	Treatment of the Surface Prior to the Curve
1	Standard curve		New surface
2	0	1	Full arc for 24 hr.
3	+0.3	1.35	Heated quartz window 3 days
4	− .59	0.555	New surface
5	− .165	.85	New surface
6	− .13	.88	New surface
7	− .15	.86	Stood 24 hr. in 1.5×10^{-8} mm
8	− .15	.86	Heating by radiation 6 hr.
9	− .19	.83	Heating by radiation 8 days
10	− .25	.78	Stood 6 days in vacuum
11	− .25	.78	Stood 24 hr. in vacuum
12	− .54	.585	New surface
13	− .39	.675	Stood in vacuum 24 hr.
14	− .26	.77	Stood in vacuum 10 days
15	+ .09	1.095	Heated quartz window 8 hr.
16	+ .07	1.07	Full arc 3 days
17	− .43	0.65	New surface
18	− .43	.65	Stood in vacuum 48 hr.
19	− .43	.65	Full arc 24 hr.
20	− .35	.71	New surface

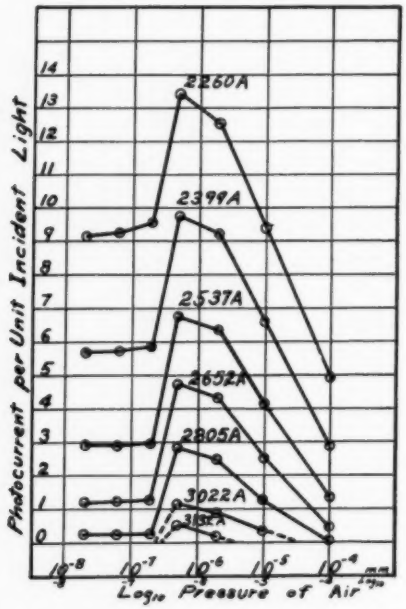

FIG. 3. Photo-currents per unit light intensity as a function of the log of the pressure of air in the tube.

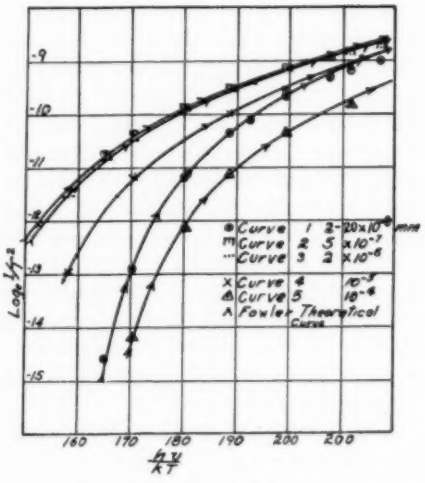

FIG. 4. Photo-currents plotted in Fowler coordinates.

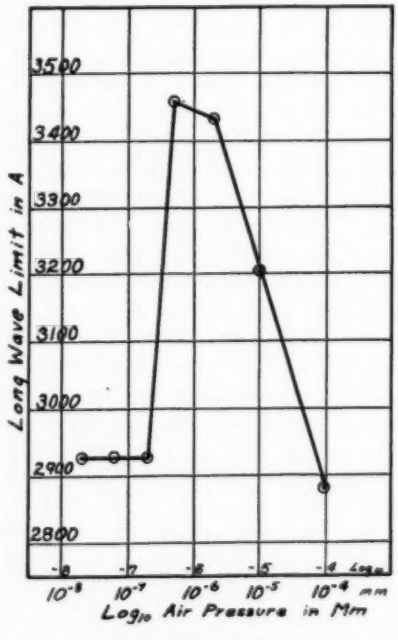

FIG. 5. Long wave-length limits plotted against the log of the pressure of air.

The pressure in the photoelectric tube was therefore varied either by adjusting the temperature of the mercury pump boiler or by introducing small amounts of gas into the vacuum system. The second method was designed especially for introduction of pure gases. Three oblique bore stopcocks were sealed very close together in the form of a T; the volume between the stopcocks was about 1 cc. The other side of one stopcock was connected to a reservoir containing the gas; another was connected to the forepump; and the third was connected through a liquid-air trap containing glass beads to the main system between the liquid-air traps and the mercury cutoff. Thus stopcock grease and water vapor could not enter the vacuum system. The 1 cc volume between the stopcocks was evacuated and filled with the gas to be introduced into the system, it was pumped to 10^{-4} mm by the forepump, and then connected with the main system. The gas contained in the 1 cc at 10^{-4} mm doubled the pressure at 10^{-8} mm.

In Fig. 3 the photo-currents per unit light intensity are plotted against the log of the pressure of air in the tube. Each curve is for one wave-length. The ordinate unit for Figs. 3, 6, and 7 is 3.9×10^{-13} ampere/erg/sec. The photo-currents are plotted in Fowler coordinates in Fig. 4. The curves are theoretical while the points are the experimental values. The agreement between the

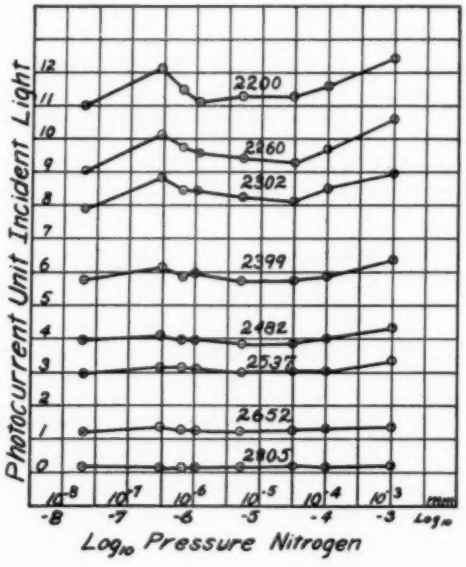

FIG. 6. Effect of pure nitrogen on the photo-currents.

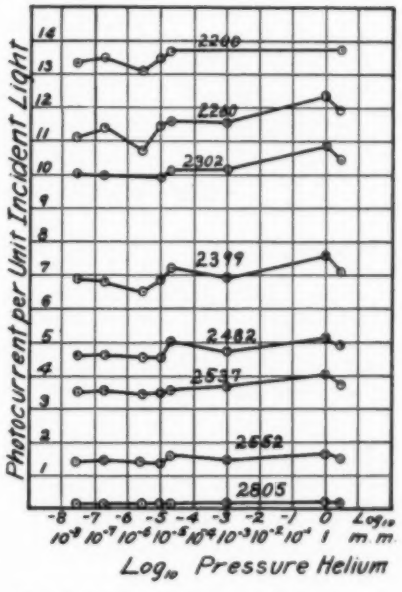

FIG. 7. Effect of helium on photo-currents.

experimental and theoretical curves is very good for all the pressures studied. The long wave limits are plotted against the log of the pressure of air in Fig. 5. This curve shows that the long wave limit was a maximum between 2×10^{-7} and 2×10^{-6} mm. According to this curve Hughes' value is for a surface in equilibrium with a pressure of 5×10^{-8} mm, which probably was the case. Dillon's value is probably for a surface in equilibrium with a pressure of about 10^{-6} mm. The discrepancy between 10^{-6} and the pressure he actually used is probably due to the difficulty of removing the gas absorbed during the transfer of the zinc from the mold to the vacuum system.

The effect of pure nitrogen on the photo-currents is shown in Fig. 6. The nitrogen was purified by passing through hot copper, hot copper oxide, and a liquid-air trap. Although the short wave-length curves show maxima similar to those in Fig. 3, the long wave-length curves do not increase to the high maxima. In fact, the percentage changes in the photo-currents were constant for all wave-lengths at a given pressure, thus there was no shift in the long wave limit.

The effect of helium is shown in Fig. 7. The helium was purified by passing twice through charcoal at liquid air temperature. These curves show that except for small variations in the photo-currents (for which no explanation has been found) the photoelectric properties were not changed by increasing the pressure of helium from 3×10^{-8} to 3 mm. This result explains the agreement of 2915A with that obtained by Rentschler, Henry, and Smith[9] for a surface sputtered in an inert gas atmosphere if the effect of helium is characteristic of the inert gas they used.

The author is indebted to the late Dr. C. E. Mendenhall and to Dr. H. B. Wahlin under whose direction the experiment was performed, to the Wisconsin Alumni Research Foundation for financial assistance and to Mr. R. W. Suchy for his assistance in making observations.

LETTERS TO THE EDITOR

Prompt publication of brief reports of important discoveries in physics may be secured by addressing them to this department. Closing dates for this department are, for the first issue of the month, the eighteenth of the preceding month, for the second issue, the third of the month. The Board of Editors does not hold itself responsible for the opinions expressed by the correspondents.

Communications should not in general exceed 600 words in length.

Christiansen Filters as Polarizers

The Christiansen effect has been used for filters not only in the visible but also in the ultraviolet and infrared. Yet it apparently has not been used with doubly refracting material, as such. Wood has used quartz particles in making filters, but on account of convenience rather than for birefringence.

The dispersion curves for the material of the particles and for the immersion liquid are of course familiar. Suppose however that a doubly refracting material is used. Then the dispersion curves will be as shown in Fig. 1, where the upper solid curve is the dispersion curve for one direction of vibration in the solid, the other is that for the perpendicular direction, T_1 is the dispersion curve for the liquid at a temperature T_1, and T_2 the corresponding curve at a somewhat higher temperature T_2.

Obviously there are two Christiansen wave-lengths, and the beams thus transmitted are polarized at right angles to each other. If the wave-length $\lambda_\perp$ is just below the range of the visible spectrum, the observed transmitted beam is monochromatic and plane polarized. On changing the index of refraction either by changing the composition of the liquid or by changing the temperature, the changes in the transmitted wave-lengths should proceed with each of the two components exactly as in the case of the experiments in which isotropic solids have been used.

The only difficulty then is to obtain doubly refracting material which is sufficiently small in particle size and still remains oriented. The birefringence of Cellophane suggested that fibers of cellulose, such as rayon, might serve the purpose. Accordingly a frame carefully wound with such a material, viscose happened to be available, was immersed in a mixture of carbon disulphide and benzene. In due time the effect was quite clear. The transmitted light was considerably spread out in the direction perpendicular to the fibers, perhaps a diffraction effect due to lack of homogeneity in the fibers, but the light was very nearly plane polarized and of a quite limited spectral region.

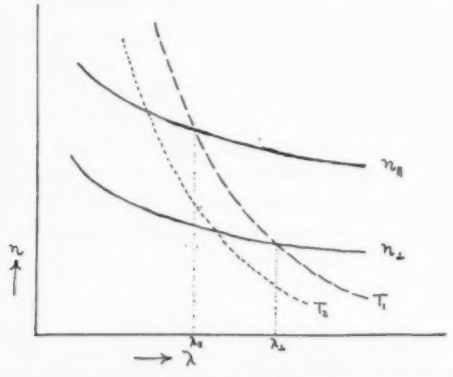

FIG. 1. Dispersion curves for the solid (solid lines) and for the liquid at different temperatures (dotted lines).

The birefringence in this case is such that it is possible, for example, to adjust the filter to transmit green polarized horizontally and blue polarized vertically. The fact that the transmitted light for one direction of polarization follows so definitely the behavior of the light transmitted by the Christiansen cells described by Wood and others[1] indicates that this is a true Christiansen effect.

In the case of the viscose fibers used in the experiments the two indices of refraction were not measured with any accuracy, but it was clearly shown that the index of refraction is greater for a vibration direction along the fiber than for the direction across the fiber. The same result was obtained with silk, the frame being wound with white silk thread.

As is well known, x-ray studies have shown that both rayon and silk possess structure, but it has not been the practice to consider their fibers as doubly refracting crystals for optical work.

H. W. FARWELL

Columbia University,
August 10, 1936.

[1] Wood, *Physical Optics;* Denmark and Cady, J. Opt. Soc. Am. **25**, 330 (1935); Barnes and Bonner, Phys. Rev. **49**, 732 (1936).

Bragg Reflection of Slow Neutrons

The peak of the velocity distribution of thermal neutrons[1] indicates a momentum for which the de Broglie wave-length, h/mv, is approximately 1.6A. If such neutrons suffer Bragg reflection, they will be regularly reflected from a magnesium oxide (MgO) crystal ($2d=4.0$A) when the Bragg angle is about 22°($\eta\lambda=2d\sin\theta_\eta$).

Sixteen well-formed single crystals of MgO, about $8\times25\times44$ mm, were mounted in a ring with the source and detector placed on the axis for a grazing angle of 22°, as shown in Fig. 1.

BACKGROUND, N_{Cd}, OF HIGH SPEED NEUTRONS

The detectors were (1), an ionization chamber filled with BF_3 in the first run, and (2), one lined with B_4C in the second and third runs. The sensitivity of both of these chambers[2] extends to neutrons of such high velocity that it was quite impossible to absorb all detectable neutrons

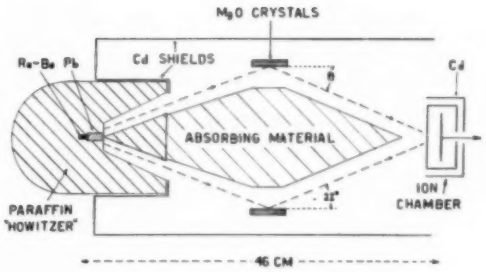

FIG. 1.

emerging in the direction of the chamber. These together with those scattered from the general surroundings account for the number (N_{Cd}) of neutrons counted when the cadmium screening of the chamber is completed by a sheet of Cd across its front.

The entire removal of the crystals made practically no change in the count of these high speed (Cd penetrating) neutrons, and further, the subsequent removal of the Cd from the front of the chamber made no appreciable increase in the count.

Neutrons Scattered by Single Crystals

It thus appears (1), that the crystals do not significantly affect the amount, N_{Cd}, of high speed neutrons counted, and (2), that the slow speed neutrons counted were scattered from the crystals.

When the crystals are in the Bragg positions, the total number N_B of neutrons counted will be the background N_{Cd} plus both those regularly reflected and incoherently scattered by the crystals. The amount of incoherent scattering should be practically independent of crystal orientation, so to observe this without regular reflection the crystals were tilted, alternately clockwise and counterclockwise, about 25° from the Bragg position. In this case of crossed crystals the total count N_X will be N_{Cd} plus the incoherent scattering. Hence $N_B - N_X$ should be a measure of the number of slow neutrons that are regularly reflected. In the first run, $N_B - N_X$ was eight times that accountable on the basis of statistical fluctuations and in the second run, six times. These results at once indicated the Bragg reflection of slow neutrons. As a check, it seemed necessary to determine by actual test whether or not polycrystalline blocks of about the same size and scattering power would, due to the change in geometric disposition, scatter more slow neutrons in the "Bragg" position than in the crossed position.

Scattering by Polycrystalline Blocks

In this, the third run, aluminum metal blocks of rectangular size and thickness equal to the rectangular boundary of the somewhat irregular single crystals, used in the first two runs, were mounted in place of the crystals. Aluminum was used since it has approximately the same effective scattering power per unit volume as MgO. The result

TABLE I. *Observed Numbers.*

Run	Bragg		Crossed		Background	
	Counts $\times 10^{-3}$	Rate N_B/min.	Counts $\times 10^{-3}$	Rate N_X/min.	Counts $\times 10^{-3}$	Rate N_{Cd}/min.
1st	23	$60.5 \pm .4$ $N_B - N_X = 4.9 \pm .6$	21	$55.6 \pm .4$	3.8	$43.3 \pm .7$
2nd	11	$28.8 \pm .3$ $N_B - N_X = 2.3 \pm .4$	8.6	$26.5 \pm .3$	3	$20.9 \pm .4$
3rd	12	$37.6 \pm .3$ $N_B - N_X = .1 \pm .4$	12	$37.7 \pm .3$	6	$28.0 \pm .4$

TABLE II. *Relative Numbers.*

Run	$\frac{N_B - N_X}{N_B - N_{Cd}}$	$\frac{N_X}{N_{Cd}}$	$\frac{N_B}{N_{Cd}}$
	With MgO Crystals		
1st	0.40 ± 0.06	1.28 ± 0.02	1.40 ± 0.02
2nd	$.41 \pm .09$	$1.27 \pm .03$	$1.38 \pm .03$
	With Al Blocks		
3rd	0.01 ± 0.04 corrected	1.34 ± 0.02 1.22	1.34 ± 0.02 1.22

$$N_B - N_X = 0.1 \pm 0.4$$

indicates that the change in geometry could not have changed the incoherent scattering much more than the statistical fluctuations.

Summary of Results

The greatest statistical precision was obtained for N_B and N_X, and hence these two values in Table I are the best evidence for the Bragg type of reflection of neutrons. It is also interesting to note the relative amount of reflection and scattering as shown in Table II.

The correction shown takes account of the fact that the total volume of the aluminum blocks used in the third run was 1.63 times that of the crystals (due to the irregular outline of the crystals, as mentioned above).

On the basis of this evidence it seems reasonable to conclude that we have in these experiments observed the reflection of slow neutrons in accord with the Bragg relation between the de Broglie wave-length of these neutrons and the grating space of these crystals.

It should be noted that the experimental arrangement (see Fig. 1) permits a sufficiently large angular divergence so that the Bragg conditions are satisfied for a large portion of the velocity range in the Maxwellian distribution[1] of the thermal neutrons.

Grateful acknowledgment is made to Mr. Raymond Ridgeway for supplying us with the unusually large single crystals of MgO used in this work.

DANA P. MITCHELL
PHILIP N. POWERS

Pupin Physics Laboratories,
Columbia University,
August 17, 1936.

[1] J. R. Dunning, G. B. Pegram, G. A. Fink, D. P. Whitehall and E. Segrè, Phys. Rev. **48**, 704 (1935).
[2] Dana P. Mitchell, Phys. Rev. **49**, 453 (1936).

The Coulomb Energy of He^3

The assumption[1, 2] that, except for the Coulomb repulsion between protons, the neutron-neutron and proton-proton attractions may be taken as equal leads to the conclusion that the difference in binding energies of H^3 and He^3 should be due entirely to the Coulomb repulsion. This statement is tested here by evaluating the Coulomb energy of He^3 using the variational wave-function

$$\psi = \psi_0 + \lambda H \psi_0, \tag{1}$$

where

$$\psi_0 = N e^{-(\nu/2)(r_{12}^2 + r_{13}^2 + r_{23}^2)}. \tag{2}$$

The Hamiltonian used was the symmetrical form

$$H = -\tfrac{1}{2}(\Delta_1 + \Delta_2 + \Delta_3) - \tfrac{3}{2} A_{II}(e^{-\alpha r_{12}^2} + e^{-\alpha r_{13}^2} + e^{-\alpha r_{23}^2}),$$

the A_{II} being taken from Table I of reference 2. The λ and ν were determined in (1) by varing ν so that the best value of the energy E was obtained using the method described in the appendix of the above reference. Then

$$\lambda = -\frac{(0|H|0) - E}{(0|H^2|0) - E(0|H|0)}.$$

The Coulomb energy is, after normalization of ψ,

$$E_c = \frac{(2\pi)^{\frac{1}{2}}}{8} \int \psi \frac{1}{r_{23}} \psi \, d\tau_1 d\tau_{23},$$

where r_{23} is the distance between the two protons. The integration gives

$$E_c = \frac{1}{8[1 + 2\lambda(0|H|0) + \lambda^2(0|H^2|0)]} \left\{ (12\alpha\rho)^{\frac{1}{2}} + 2\lambda \left[(12\alpha\rho)^{\frac{1}{2}} \frac{63\alpha\rho^2 + 42\alpha\rho - 12A_{II}\rho}{12\rho + 8} - 12A_{II}\left(\frac{6\alpha}{(2\rho+1)}\right)^{\frac{1}{2}} \frac{\rho^2}{3\rho+2} \right] \right.$$
$$+ \lambda^2 \left[(12\alpha\rho)^{\frac{1}{2}} \frac{531\alpha^2(27\rho^5 + 72\rho^4 + 60\rho^3 + 16\rho^2) + 48A_{II}^2(9\rho^3 + 12\rho^2 + 4\rho) - 8A_{II}\alpha(567\rho^4 + 1242\rho^3 + 628\rho^2)}{16(27\rho^3 + 72\rho^2 + 60\rho + 16)} \right.$$
$$+ \left(\frac{6\alpha}{2\rho H}\right)^{\frac{1}{2}} \frac{24A_{II}^2(18\rho^6 + 33\rho^5 + 20\rho^4 + 4\rho^3) - 36A_{II}\alpha(63\rho^7 + 173\rho^6 + 171\rho^5 + 70\rho^5 + 10\rho^3)}{54\rho^5 + 171\rho^4 + 210\rho^3 + 125\rho^2 + 36\rho + 4}$$
$$\left. \left. + 6A_{II}^2\left(\frac{12\alpha}{\rho+1}\right)^{\frac{1}{2}} \frac{6\rho^4 + 8\rho^3 + \rho^2}{9\rho^3 + 24\rho^2 + 19\rho + 4} \right] \right\}$$

in which $\nu = \alpha\rho$. The Coulomb energy E_c^0 given by the wave-function (2) was also calculated, the ν being chosen in this case to make

$$E^0 = \int \psi_0 H \psi_0 \, d\tau_1 d\tau_{23}$$

a minimum. The results are summarized in Table I.

It is seen that E_c and E_c^0 vary much more slowly than $\sqrt{\alpha}$. This is because the wave-functions are forced out of the potential well as the range of forces is decreased. Interpolation gives $E_c = 1.37mc^2$ for $\alpha = 16(1/\sqrt{\alpha} \sim 2.3 \times 10^{-13}$ cm). The experimental difference in the binding energies of H^3 and He^3 is $1.58 \pm 0.18 mc^2$.[3] It should also be mentioned that at $\alpha = 16$, $A_{pp} < (1 - g/2)A_{pn}$ and thus the actual Hamiltonian is not quite completely symmetrical. Unlike particles will on the average be a little closer together than like particles and therefore the Coulomb energy calculated from the correct slightly unsymmetrical Hamiltonian would possibly be slightly smaller. This effect is probably negligible at $\alpha = 16$. There may thus be a slight discrepancy between the calculated Coulomb energy and the experimental difference in the binding energies of H^3 and He^3 which is however very small compared to the Coulomb energy itself. The results, then, support the view that aside from the Coulombian interaction the proton-proton and neutron-neutron forces are equal. Interpolation gives $E = -14.2mc^2$ for the energy of H^3 (experimental value $-16.8mc^2$). The agreement is rather good and the wave-function (1) may be considered as a fairly close approximation to the correct H^3 normal state eigenfunction. The values given in the last column of Table I are taken from Table I of reference 2 and are given for comparison of the variational with the corrected "equivalent two-body" calculations of the H^3 binding energy.

TABLE I. *Calculated Coulomb energies. Energy units* $mc^2 = 0.510$ *MEV, length units* $\hbar/c(Mm)^{\frac{1}{2}} = 8.97 \times 10^{-13}$ *cm.*

Using ψ_0					Using ψ				
α	A_{II}	ν	$-E^0$	E_c^0	ν	λ	$-E$	E_c	$-E'$
10	65	7.9	16.37	1.22	7.0	−0.0145	17.62	1.25	17.9
20	98	10.8	10.08	1.42	9.2	−0.00884	12.72	1.44	14.3
30	129	12.6	5.30	1.54	10.4	−0.00689	9.27	1.55	11.6

Since the wave-functions (1) and (2) give practically the same Coulomb energies it was thought desirable to plot, Fig. 1, the expressions

$$f(r_{23}) = \int \psi^2 d\tau_1,$$
$$f_0(r_{23}) = \int \psi_0^2 d\tau_1.$$

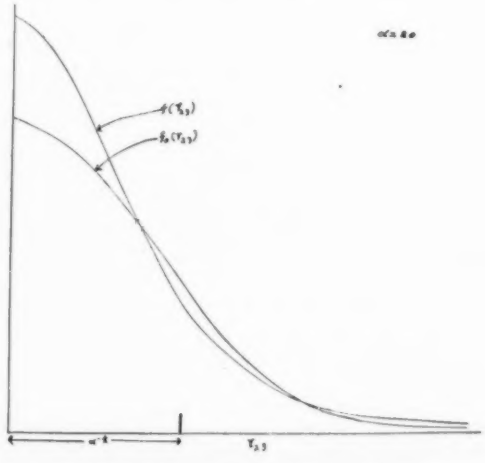

FIG. 1. Functions $f(r_{23})$ and $f_0(r_{23})$ plotted against r_{23}.

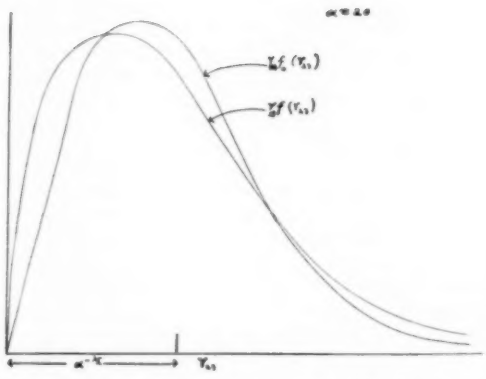

FIG. 2. Functions $r_{23}f_0(r_{23})$ and $r_{23}f(r_{23})$ plotted against r_{23}.

These functions represent the probability of various separations of the two protons in the two cases. Except for the large r_{23}, which contribute only small amounts to the Coulomb energy, the larger region of integration in which $f_0(r_{23}) > f(r_{23})$ is sufficient to practically balance the bigger contribution of f for small r_{23}. In Fig. 2 the quantity $r_{23}f(r_{23})$ is plotted as a function of r_{23}. The areas under the curves are proportional to the Coulomb energies since $E_c = \int 1/r_{23} \times f(r_{23}) dr_{23}$ and the angle integrations merely introduce a factor 4π. (The curves for $\alpha = 10$, 20, and 30 are very similar and only those for $\alpha = 20$ are included.) The writer wishes to express his gratitude to Dr. Eugene Feenberg for suggesting these calculations and for the advice and suggestions which he gave while they were being made.

SIMON S. SHARE

University of Wisconsin,
August 4, 1936.

[1] Feenberg and Knipp, Phys. Rev. **48**, 906 (1935).
[2] Feenberg and Share, Phys. Rev. **50**, 253 (1936).
[3] This value was given by Professor H. Bethe in a private communication to Dr. Feenberg. Bethe and Bacher give the value 0.76 $\pm$0.14 MEV ($1.49 \pm 0.27 mc^2$) in Rev. Mod. Phys. **8**, 147 (1936).

On the Intensity of X-Rays Reflected from Zinc

The senior author has recently investigated theoretically the temperature dependence (usually represented by the factor e^{-2M}) of the intensity of x-rays reflected from anisotropic crystals.[1] He found that in crystals with hexagonal symmetry M has the form

$$M = (a \cos^2 \psi + b \sin^2 \psi) \sin^2 \theta / \lambda^2, \qquad (1)$$

where ψ is the angle between the normal to the reflecting plane and the principal axis. The constants for Zn and Cd were calculated from the known elastic constants, using the simple Debye model of a solid. The constants for Zn are given in the first row of Table I (the original calculations must be corrected by factors of 1.27 and 1.30 for Zn and Cd, respectively).

TABLE I. *Constants at $T = 298°K$.*

	a	b
Simple Debye Model	0.75 A^2	0.42 A^2
Brindley	1.295	0.51
Jauncey and Bruce	2.34	0.68
Modified Debye Model	1.06	0.595

During the publication of this paper an article by Brindley appeared on the intensity of x-rays reflected from Zn.[2] In a second paper[3] he has compared these and further experimental results with formula (1). He finds that a better fit with the experiments is obtained by using the semi-empirical constants in the second row of Table I.

In this laboratory Jauncey and Bruce have investigated Zn by the method of diffuse scattering of x-rays.[4] In the third row of Table I are given the values of a and b which they find best fit their experiments, and which also give an excellent fit with Brindley's experiments. These disagree still more with the theoretical constants of the first row.

One possible source of this discrepancy has been suggested by Brindley. In interpreting the experiments all anisotropy of the atoms has been neglected. A second possible source of error lies in the assumptions of the simple Debye model. In this letter the authors report the modifications introduced by partially taking into account the discrete structure of a solid.

In a linear lattice with atoms of only one mass, the relation between frequency and wave-length is given by[5]

$$\nu = (c/\pi d) \sin (\pi d/\lambda). \qquad (2)$$

Here d is the lattice spacing, and c is the velocity of waves long compared with d. If this relation is used in the three-dimension lattice in place of the usual relation

$$\nu = c/\lambda, \qquad (3)$$

the factor $(2/\pi)\int_0^{\pi/2} (x/\sin x)^2 dx = 1.42$ is introduced into the expression for both a and b when $T > \Theta$. It is interesting to note that a decision between (2) and (3) cannot be made from specific heat data.[6]

The values of the constants obtained by using (2) in place of (3) are given in the last row of Table I. A further improvement was sought by taking the integration in wavé number space over the region appropriate to a hexagonal close packed lattice, in place of over a spherical region. This introduced no appreciable change in either a or b.

Although this change in the theoretical value of the constants is in the right direction, it is not sufficient to obtain agreement with the experiments as interpreted by the assumption of isotropic atoms. The decision as to whether the source of the remaining discrepancy lies in the assumption of atomic isotropy or in the model for a solid used in the theoretical calculations, can only be made by experiments at different temperatures.

CLARENCE ZENER
S. BILINSKY

Wayman Crow Hall of Physics,
St. Louis, Missouri,
June 23, 1936.

[1] C. Zener, Phys. Rev. **40**, 122 (1936).
[2] G. W. Brindley and F. W. Spiers, Phil. Mag. **20**, 865 (1935).
[3] G. W. Brindley, Phil. Mag. **21**, 790 (1936).
[4] Jauncey and Bruce **50**, 408 (1936).
[5] M. Born and Th. v. Kármán, Physik. Zeits. **13**, 297 (1912).
[6] Eucken, *Handbuch der Experimental Physik*, Vol. VIII/1, 256.

The Dependence of Burst Production Upon Atomic Number

In previous communications[1] we have suggested that the rate of occurrence, RdN, of cosmic-ray bursts having a number of ionizing rays between N and $N+dN$, may be represented over a large range of burst sizes by the expression

$$RdN = A/N^s dN, \tag{1}$$

where A and s are parameters and presumably functions of the atomic number, Z, of the burst producing substance. For the bursts from lead, s was found to be about 3.2. To determine the dependence of these parameters upon Z, we have made observations on the numbers of bursts originating in small thicknesses of paraffin, Mg, Fe, Sn and Pb. The bursts were detected in an ionization chamber which consisted of three spherical steel chambers, placed at the corners of a triangle. Each chamber had a diameter of three inches, a wall thickness of a millimeter, and was filled with argon to a pressure of 300 lb. per square inch. A vacuum tube electrometer with photographic recording was employed. The rate of occurrence of bursts greater than 1.6×10^5 ion pairs was determined for each substance. The number of bursts occurring when no material was over the chambers was also measured, and subtracted from the observations taken with the burst producing material present. The rate of occurrence of bursts per atom of the producing material was found to be proportional to the square of the atomic number. The results are illustrated in Fig. 1. Through the point for lead in this figure a line with a slope corresponding to a Z^2 variation has been drawn. It fits the other points satisfactorily with the possible exception of the observations on paraffin. This substance produces so few bursts, however, that it is questionable whether any significance should be attached to this apparent exception.

A similar result has been obtained for bursts of different ranges of sizes by other observers. B. Rossi[2] measured the rates of occurrence of small showers from Pb, Fe and Al by means of Geiger-Müller counters. H. Nie[3] has recently made observations upon very large bursts in an ionization chamber over which were placed these same three substances. Both these sets of observations are as well satisfied by a Z^2 law of variation as the observations reported here upon bursts of an intermediate size. Thus there is good evidence that expression (1) above may be written so as to contain the dependence upon atomic number explicitly as

$$RdN = BZ^2/N^s dN,$$

where B and s are independent of Z.

We may draw two conclusions of significance from this. First, the simple variation with Z^2 suggests that the fields of the nuclei of the burst-producing materials, rather than their particular nuclear structures, are of prime importance, and that it is quite probable that the nuclei remain intact under the impact of the cosmic rays. Second, the picture of a burst being built up by a successive doubling of the number of electrons by the mechanism of pair formation (with or without intermediary photons) is inconsistent with the observed Z^2 variation. Since the probability of each act of pair production, or of the production of intermediary photons, is proportional to Z^2, we should expect the probability of the composite process to vary with a much higher power of Z. We do know that some sort of building up process[4] is involved in the formation of bursts. The experiments here reported, however, seem to show definitely that this building up is not by pair formation, but must involve the simultaneous production of a large number of rays.

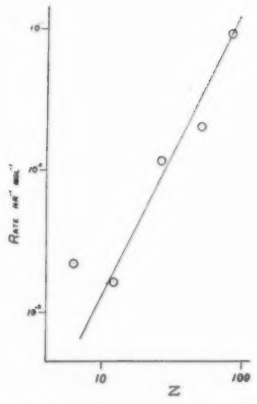

FIG. 1. Rate of production of bursts as a function of atomic number.

The authors are indebted to Professor W. F. G. Swann for much useful advice and helpful encouragement.

C. G. MONTGOMERY
D. D. MONTGOMERY

Bartol Research Foundation of the Franklin Institute,
Swarthmore, Pa.,
August 12, 1936.

[1] C. G. Montgomery and D. D. Montgomery, Phys. Rev. **48**, 786 (1935); **48**, 969 (1935).
[2] B. Rossi, Zeits. f. Physik **82**, 151 (1933).
[3] H. Nie, Zeits. f. Physik **99**, 787 (1936).
[4] C. G. Montgomery, D. D. Montgomery and W. F. G. Swann, Phys. Rev. **47**, 512 (1935).

The Scattering of Neutrons by Protons

We have measured the scattering by protons of neutrons having an energy in the intermediate region by using the homogeneous neutrons from a carbon target bombarded by a monoenergetic deuteron beam, and our results are in satisfactory agreement with the predictions of Wigner's formula, contrary to the results of Goldhaber.[1] The apparent equality of the proton-proton and proton-neutron interactions, deduced by Breit, Condon, and Present on the basis of our measurements on proton-proton scattering, has made it of special interest to test in every possible way the validity of the current theoretical representation of the proton-neutron interaction.

Our first measurements, which gave approximate agreement with Wigner's formula as described at the Johns Hopkins Gibson Island Conference (June 24, 1936) and the Cornell Conference (July 4, 1936), duplicated Goldhaber's geometry and his paraffin-boron detector in order

to measure the scattering of the carbon neutrons as nearly as possible under the same conditions as for his measurement of the scattering of the photo-neutrons (Th C″) from deuterium. The insertion of a paraffin scatterer 1.0 cm thick gave a diminution of the neutron intensity to 0.68 ± 0.05 and 0.59 ± 0.05 in two separate runs, an average of 0.64 ± 0.04. A one-half mm Cd shield was interposed between the scatterer and the Pf-B detector during these runs; measurements without the Cd shield gave no significant change (0.68 ± 0.05). Surrounding the carbon target by paraffin to crudely duplicate the effect of Goldhaber's heavy-water photo-neutron source gave a ratio in agreement with the above average within the experimental error. The value $I/I_0 = 0.64$, without correcting for the appreciable scattering by the carbon in the paraffin, leads to a cross section of 5.7×10^{-24} cm²; estimating the carbon correction, the resulting proton-neutron cross section is 4.7×10^{-24} cm².

The carbon neutrons produced by a 900-kv beam of deuterons have an energy between 600 kv[2] and 1200 kv.[3] If the deuteron level is taken as ± 40 kv, Wigner's formula[4] predicts 5.4, 4.1, and 3.4×10^{-24} cm², respectively, for neutron energies of 600, 900, and 1200 kv. If the deuteron level is ± 130 kv, the values are 4.6, 3.7, and 3.2×10^{-24} cm², respectively.

Rasetti and others pointed out in discussion that these measurements with the paraffin-boron chamber would yield an erroneous cross section if a hitherto unsuspected group of slower neutrons (10 to 20 kv) accompanies the usual carbon neutrons. To eliminate this possibility we have recently made similar measurements (with rather different geometry) using as the detector a small ionization chamber filled with hydrogen to a pressure of three atmospheres and connected with the linear amplifier. This responds only to recoil protons of energies above roughly 300 kv and eliminates any effects due to slow neutrons. A 1.0-cm Pf-scatterer gave a reduction of intensity to 0.69 ± 0.03, in satisfactory agreement with the earlier measurements. To correct for scattering by the carbon in the paraffin the reduction in intensity produced by a 0.50-cm scatterer of Acheson graphite was measured using the hydrogen-pressure chamber; this result was 0.85 ± 0.05. Correcting the paraffin-intensity ratios for the carbon scattering, the cross section for the neutron-proton scattering is 3.7×10^{-24} cm².

These two series of measurements may thus be taken as additional evidence for the correctness of current views regarding the proton-neutron interaction.

We are grateful to our colleagues N. P. Heydenburg and R. C. Meyer for help with these experiments.

M. A. Tuve
L. R. Hafstad

Department of Terrestrial Magnetism,
Carnegie Institution of Washington,
Washington, D. C.,
August 3, 1936.

[1] M. Goldhaber, Nature **137**, 824 (1936).
[2] T. W. Bonner, L. A. Delsasso, W. A. Fowler and C. C. Lauritsen, Phys. Rev. **49**, 203 (1936).
[3] M. A. Tuve and L. R. Hafstad, Phys. Rev. **48**, 106 (1935).
[4] H. A. Bethe and R. F. Bacher, Rev. Mod. Phys. **8**, 82 (1936), see page 117.

The Separation of Isotopes by Centrifuging

Although the separation of isotopes by centrifuging has generally been abandoned as impractical,[1, 2, 3, 4] the development of our new air-driven centrifuge[5] has encouraged us to examine again the feasibility of the method. We first developed a gas[6] or vapor centrifuge in which the gas enters through holes in the periphery and is pumped out at the center of the rotor through a tube which is used both to drive and support the rotor. Two general types of rotors are in use. In the first, which has a horizontal circular cross section, the gas enters the rotor through a channel along the radius. In the second type, which has a triangular cross section, the gas enters the rotor through openings so directed that only those molecules with speeds greater than the peripheral speed can enter. Since in most cases the peripheral speed of the rotor is in excess of the average molecular speed, a "velocity separation" as well as a separation by centrifuging occurs.

In order to check the relative efficiency of the two types of rotors, experiments were carried out upon the separation of a mixture of N_2 and CO_2 at room temperature. Briefly, the results obtained with both rotors were in fair agreement with the simple theory.[1] The rate with which the gas can be centrifuged of course depends upon the design and speed of the rotor, the temperature, viscosity, density of the gas, etc. In our experiments, as high as 1 cc N. T. P. was collected every five minutes, but this probably can be increased by a new rotor design. Since the above results show that the simple theory should serve as a rough guide to the separation, the values in Table I computed for the case of an ideal gas from the formula $K_0/K = e^{(V^2/2RT)(M_2-M_1)}$ may be of interest. The peripheral velocity ($V = 8 \times 10^4$ cm/sec.) used in the computation was the bursting speed of our best rotor. K_0 = ratio of quantities of light to heavy isotopes at the center; K = ratio of the same quantities at the periphery; T = absolute temperature; M_1 = molecular weight of lighter, and M_2 = molecular weight of the heavier isotopes. If the rotors could be made stronger, V and hence the separation, could be much increased as the driving turbine reaches less than half speed when our rotors explode. Although at $T = 20°$ most substances have too low a vapor pressure for gas centrifuging, many can be centrifuged at 80°. For this reason we have developed a rotor that will spin at liquid-air temperatures or even lower. The dependence of the separation factor on $M_2 - M_1$ rather than their absolute values gives the centrifuge method a decided advantage over those methods which do depend upon the absolute values in the case of heavier elements. The naturally lower rate of centrifuging for heavier elements can be partly counterbalanced by improved design. The "velocity

Table I.

M_2-M_1	K_0/K			
	$T=300°$	$T=200°$	$T=80°$	$T=20°$
1	1.13	1.21	1.62	6.8
2	1.29	1.47	2.61	47
3	1.47	1.78	4.23	300
4	1.67	2.16	6.9	2000

separation" increases the tabulated separation factors. For example, for neon at 300° it alone is 1.35. However, this may become a disadvantage in some cases, for it decreases the supply of gas.

We have also tried out a modification of a method first suggested by Professor Mulliken[2] on the separation of CCl_4. The liquid was placed inside a hollow vacuum tight rotor which was spun in an evacuated chamber. The CCl_4 evaporated near the periphery of the rotor and the vapor passed out at the center through the "driving" tube. The lighter fractions distill off first, leaving the heavier ones in the rotor. We obtained a decided change in the density of CCl_4 in the two fractions, but a mass-spectrographic analysis should be made before the theory can be definitely tested. Although the rotors burst at lower speeds with this method, the separation is quite fast, and comparatively large quantities can be centrifuged.

It is a pleasure to acknowledge our indebtedness to Mr. Fritz Linke and Mr. A. V. Masket for much valuable assistance.

J. W. BEAMS
F. B. HAYNES

University of Virginia,
July 30, 1936.

[1] Aston, *Mass Spectra and Isotopes* (Arnold, 1933); Lindemann and Aston, Phil. Mag. **37**, 523 (1919).
[2] Mulliken, J. Am. Chem. Soc. **44**, 1033 (1922); **45**, 1592 (1923).
[3] Joly and Poole, Phil. Mag. **39**, 372 (1920).
[4] Poole, Phil. Mag. **41**, 818 (1921).
[5] Beams and Pickels, Rev. Sci. Inst. **6**, 299 (1935).
[6] Beams and Haynes, Phys. Rev. **49**, 644 (1936).